

ABSTRACT

Title of Dissertation: **MAXIMIZING THE FINANCIAL RETURNS
OF USING LIDAR SYSTEMS IN WIND
FARMS FOR YAW ERROR CORRECTION
APPLICATIONS**

Roozbeh Bakhshi, Doctor of Philosophy, 2019

Dissertation directed by: **Professor Peter Sandborn, Department of
Mechanical Engineering**

Wind energy is an important source of renewable energy with significant untapped potential around the world. However, the cost of wind energy production is high and efforts to lower the cost of energy generation will help enable more widespread use of wind energy. Ideally, wind turbines have to be aligned with wind flow at all times. However, this is not the case and there exists an angle between a wind turbine nacelle's central axis and the wind flow. This angle is called yaw error. Yaw error lowers the efficiency of turbines as well as lowers the reliability of key components in turbines. LIDAR devices can correct the yaw error; however, they are expensive and there is a trade-off between their costs and benefits. In this dissertation, a stochastic discrete-event simulation is developed that models the operation of a wind farm. By maximizing the Net Present Value (NPV) changes associated with using LIDAR devices in a wind farm, the optimum number of LIDAR devices and their associated turbine stay time will be determined. These optimum values are a function of number of turbines in the wind farm for specific turbine sizes. The outcome of this dissertation will help wind farm owners and operators to make informed decisions about purchasing LIDAR devices for their wind farms.

MAXIMIZING THE FINANCIAL RETURNS OF USING LIDAR SYSTEMS IN
WIND FARMS FOR YAW ERROR CORRECTION APPLICATIONS IN WIND
FARMS

by

Roozbeh Bakhshi

Dissertation submitted to the Faculty of the Graduate School of the
University of Maryland, College Park, in partial fulfillment
of the requirements for the degree of
Doctor of Philosophy
2019

Advisory Committee:

Professor Peter Sandborn, Chair

Professor Abhijit Dasgupta

Professor Patrick McCluskey

Professor Laurent Fresard

Professor James Baeder. Dean's Representative

© Copyright by
Roozbeh Bakhshi
2019

Dedication

I would like to first and foremost dedicate this dissertation to my parents and my two sisters, Nooshin and Mahnoosh. I am here today because of their help and sacrifices throughout my entire life and in particular my years in graduate school. Their unconditional love and support helped me to overcome many challenges that I faced these years.

Next, I would like to thank my advisor, Peter Sandborn who believed in me, supported me and never stopped offering a helping hand all the way to the end.

Through ups and downs and hard times, whether related to my research or matters outside of academia, he never hesitated to help.

I would also like to thank my friends who were always there for me. Special thanks to Amir and his lovely wife Christine who were always supportive and helped me all the way to the end specially the last few weeks leading to my dissertation defense. Also, special thanks to my other friends, Ali, Subramani, Jennifa, Kunal, Navid and everyone else who played a role in my success.

Special kudos to Graduate Student Government where I spent 5 years there representing Mechanical Engineering graduate students. I met many amazing people and learned a lot from them. This was one of the most valuable experiences in my life that put me in special situations that I would have never had a chance to experience in the ordinary life of academia.

Lastly, I'd like to thank inspirational figures such as Toni Iommi, Geezer Butler, Ronnie James Dio, James Hetfield, Bruce Dickinson and many more.

Acknowledgements

Funding for this work was provided by Exelon for the advancement of Maryland's offshore wind energy and jointly administered by MEA and MHEC, as part of “Maryland Offshore Wind Farm Integrated Research (MOWFIR): Wind Resources, Turbine Aeromechanics, Prognostics and Sustainability”. I would also like to thank Leosphere for providing data and feedback to this work.

Table of Contents

Dedication	ii
Acknowledgements	iii
Table of Contents	iv
Chapter 1: Introduction	1
1.1. Background	1
1.1.1. Wind Turbines	4
1.1.2. Wind Farm	6
1.1.3. Power Production	7
1.2. Yaw Error	10
1.3. LIDAR	13
1.4. Objective of This Dissertation	16
1.5. Review of Relevant Literature	18
1.5.1. Yaw Error and LIDAR	18
1.5.2. Yaw Error and Reliability	19
1.5.3. O&M Modeling	20
1.6. Research Gaps	24
1.7. Tasks	25
Chapter 2: Stochastic Return on Investment Modeling	27
2.1. Discrete Event Simulation	28
2.2. Return on Investment (ROI) Modeling	30
2.2.1. Monte Carlo Analysis for ROI Calculation	33
2.2.2. Cost Avoidance ROI Calculation	37
2.2.3. Operation and Maintenance (O&M) Modeling	41
2.2.4. Revenue Generation Modeling	43
2.3. Cost of Capital	44
2.4. Net Present Value (NPV)	46
Chapter 3: Performance Model	48
3.1. Wind Speed Generation	50
3.2. Height Conversion of Wind Turbines	52
3.3. Yaw Error Adjustment	53
3.4. Power Calculations	54
3.5. Energy Production	56
Chapter 4: Effects of Yaw Error on Reliability of Turbine’s Blades	59
4.1. Load Analysis	60
4.2. Stress Analysis	66
4.3. Reliability of Blades	68
4.4. Discussion	70
Chapter 5: Modeling Results	73
5.1. Model Assumptions	73
5.2. The Optimization Problem	78
5.3. Analysis Results	79
5.4. Sensitivity Analysis	85
5.4.1. Cost of LIDAR Devices	85
5.4.2. Energy Purchase Price	86

5.4.3.	Discount Rate.....	87
5.4.4.	Yaw Error Regression Profile.....	88
5.4.5.	Turbine Size.....	90
Chapter 6:	Conclusions.....	92
6.1.	Dissertation Contributions.....	94
6.2.	Publications to Date.....	95
Appendices.....		97
Bibliography.....		124

Chapter 1: Introduction

1.1. Background

Due to climate change, the growth in carbon dioxide emission production (Figure 1), geopolitical concerns with fossil fuels and market uncertainties, many nations are looking to alternative sources of energy to reduce their dependence on fossil fuels.

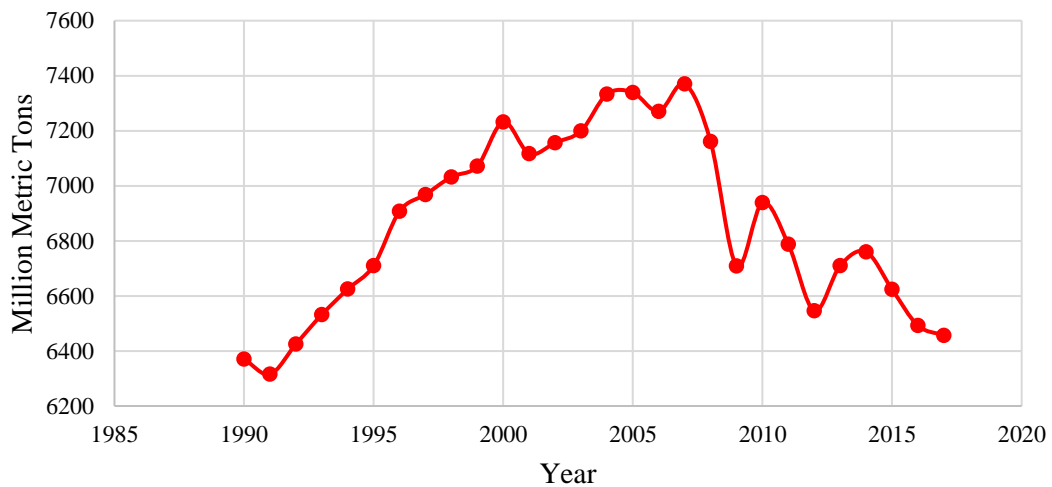


Figure 1- CO2 emissions in the United States between 1980 and 2017 - data from [1]

Wind energy is one of the energy production options. Compared to fossil fuels, wind energy has a very low carbon life-cycle footprint, the fuel (wind) is abundant and free, there is no emission of mercury, nitrous oxide and sulfur oxides, and no consumption of water for cooling purposes (needed by conventional power plants) [2]. The potential wind energy production in the United States is about 32,000 TWh for onshore and 17,000 TWh for offshore installations [3]. According to American Wind Energy Association (AWEA), the United States passed 97 GW of

wind power production the end of second quarter of 2019 [4]. Figure 2 shows the evolution of wind energy production in the United States over time and also the contribution of wind energy as a percentage of the total energy and renewable energy production. Because of the 5-year extension of Production Tax Credits (PTC) in 2016, more onshore and offshore wind projects are expected to be initiated across the US before 2020.

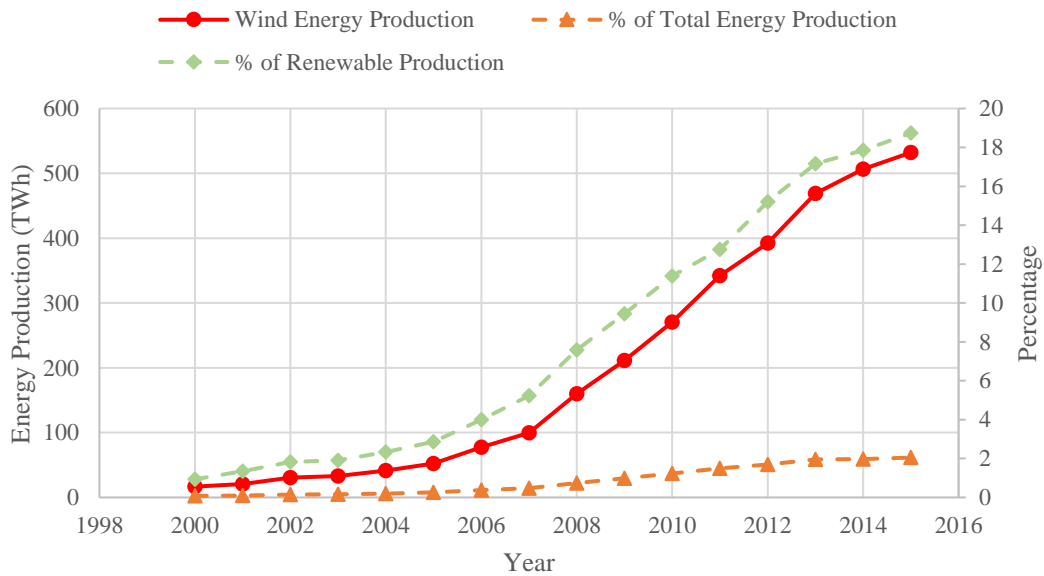


Figure 2- Wind energy production in US over time - data from [5]

All the wind energy production in Figure 2 is onshore production. As of 2019, the only offshore wind farm in the US is the 30 MW Block Island Wind Farm in Rhode Island. However, there are several potential offshore projects ranging from feasibility study and commissioning to construction across the country. Rhode Island's Block Island Wind Farm is the closest offshore project to production. Table 1 shows the state of offshore projects in the United States at the end of 2015.

Table 1- Current state of US offshore wind [6], [7]

Developer	Location	Proposed Capacity (MW)	Status
Cape Wind	Massachusetts	468	Arranging PPAs/Financing
US Wind	New Jersey	500	Conducting Survey
US Wind	Maryland	250	Under Construction
Deep Water One	Maryland	120	Conducting Survey
Dong Energy	New Jersey	1,000	Acquired Lease
Fisherman`s Atlantic City	New Jersey	25	Fully Permitted (Legal Issues)
Deep Water One	Rhode Island	1,000	Arranging PPAs/Financing
Virginia-Dominion	Virginia	2,000	Acquired Lease
Blue Water Wind	Atlantic City	450	Conducting Survey
Virginia Offshore Wind	Virginia	12	Conducting Survey
Wind Float Pacific	Oregon	25	Conducting Survey
Lake Erie	Ohio	18	Arranging PPAs/Financing
New England Aqua Ventus	Maine	12	Arranging PPAs/Financing
Offshore MW/Vineyard Power	Massachusetts	400	Arranging PPAs/Financing

Wind farms are capital intensive projects whose economic viability depends on many factors including: wind resources, the technology, depth of water, price of energy and the long term successful sustainment of the turbines. Sustainment includes: reliability, maintainability, operational logistics, configuration control, technology management and the ability to (and optimum frequency of) system upgrades and refreshes. Sustainment, also referred to as operation and maintenance (O&M) or operation and support (O&S), is projected to be the second largest contributor to the life-cycle cost of offshore wind turbines, representing 17-28% of the total levelized cost of offshore wind farms and more for farms that are more than 12 miles offshore [8].

1.1.1. Wind Turbines

Wind turbines capture and convert the kinetic energy of the wind to electrical power at elevations between 40m to 200m from the installation elevation. Wind turbines can be horizontal axis (HAWT) or vertical axis. This is the axis of rotation relative to ground. Currently most of the installed turbines are HAWTs and in this work we only consider this type of turbine.

Turbine Structure

Wind turbines are complicated structures and consist of many sub-assemblies.

Figure 3 shows a schematic of some of these sub-assemblies in a wind turbine.

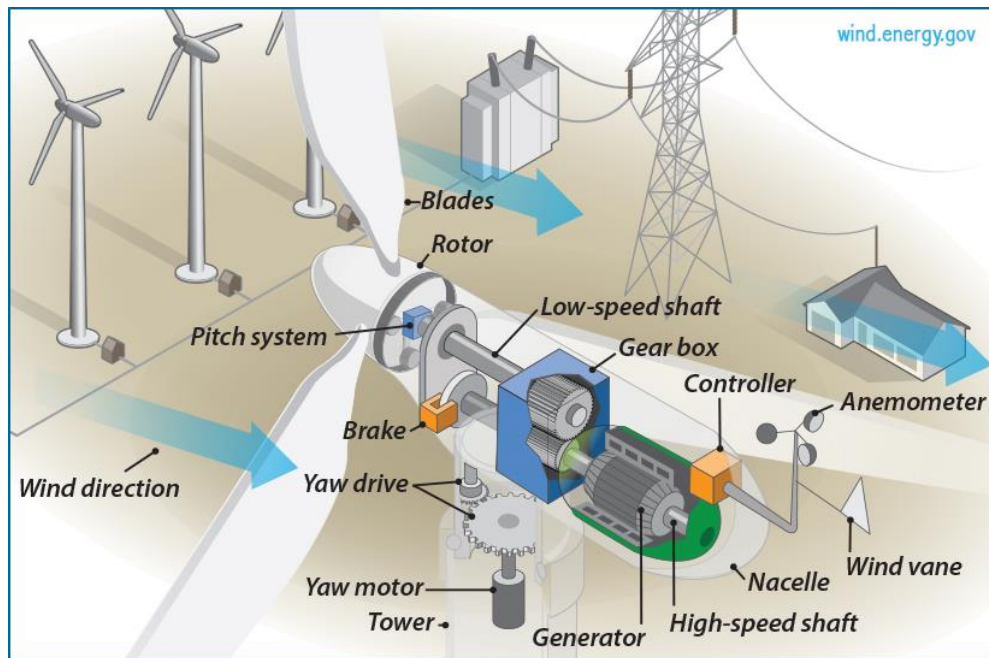


Figure 3- Schematic of a wind turbine sub-assemblies [9]

Rotor and Blades

The rotor, blades and the hub together form the sweeping area of the wind turbine where the kinetic energy in the wind is captured and converted into rotational

mechanical energy. Most of current turbines have only three blades although designs with one or two blades exist.

Gearbox

The low-speed shaft, gearbox and brake in Figure 3 form the drivetrain of the turbine. The gearbox adjusts the speed and torque of the incoming mechanical power from the shaft into the required speed and torque of the generator. Some designs do not have a gearbox. The gearbox could be constant speed or variable speed.

Generator

The generator converts the mechanical power to electrical power. There are several types of generators that can be used in wind turbines. Doubly-Fed Induction Generator (DFIG) and Brushless Doubly-Fed Generator (BDFG) are two common types. Different generator types for wind turbine applications can be found in [10].

Converter

The converter does the conversion of electricity to what is required by the grid. Frequency, voltage current adjustments occur at this stage.

Nacelle

The nacelle is the enclosure for all the components including the gearbox, generator, converter, and pitch control.

Pitch System

Pitch movement is the rotation of blades around their central axis. The purpose of pitch movement is to maximize the wind capture or on the hand lower the rotational speed of the rotor (for cases when the turbine is required to stop or operate at a lower speed). The mechanisms that controls the pitch movement is called the pitch system.

Hydraulic System

The hydraulic systems in wind turbines are one of the mechanisms responsible for braking and lowering the turbine speed in cases of high winds or when the system needs to be shut down.

Yaw System

The yaw system rotates the nacelle around the towers vertical axis in the horizontal plane in order to keep the main shaft in-line with the incoming wind.

Control System

The control system monitors and collects data about the operation of the system. It includes sensors that monitor various parameters on different sub-assemblies of the turbine such as temperature and vibration. The condition monitoring systems (CMS) or prognostic and health management (PHM) systems are a part of the control system.

Tower

The tower is the foundation upon which the turbine nacelle and hub are installed. For offshore turbines, there are several tower designs that are used [11].

1.1.2. Wind Farm

A wind farm consists of several, sometimes hundreds of wind turbines. The most important factor in choosing the location of a wind farm is the wind resource availability. Accessibility to the local grid and transportation for onshore farms are important factors. Onshore wind farms are usually located away from populated areas since seeing and hearing wind turbines causes dissatisfaction among locals. For offshore sites, the site selection becomes more challenging since the farm cannot be in transportation or shipping lanes. In the United States in particular, the farm's

distance from the shore is a significant licensing issue since the location of the farm may fall into either state or federal waters. In the US, all the wind farms in federal waters must receive their permits from the Army Corps of Engineers [2].

Surface roughness affects the wind speed, terrain areas or regions with lots of buildings have high surface roughness which lowers the wind speed. On the other hand, water has a low surface roughness, which increases the wind speeds. In this regard, offshore farms have a significant advantage over onshore sites.

The layout of the wind farm varies depending on the number of turbines. Turbines are set up in rows that are adjacent to each other with a minimum distance of 4 rotor diameters between them. For some farms, there are multiple rows of turbines. The turbines in the back rows (relative to the wind direction) are affected by the wake effect of the turbines in front of them and as a result have a lower energy production.

1.1.3. Power Production

The available power in the wind depends on the air density, wind turbine swept area and the wind speed as it is shown in Equation (1).

$$P = \frac{1}{2}\rho AV^3 \quad (1)$$

where:

P : kinetic energy in the wind

ρ : air density

A : wind turbine rotor sweep area

V : free flow wind speed

This is maximum amount of energy available to be converted into electricity. The actual electricity produced depends on many efficiency factors involved in the conversion of mechanical power into electricity, losses in electricity transport cables from the wind turbine, losses in matching the output power's current, voltage and frequency to the grid, etc. In reality the turbine's power generation is not directly proportional to cube of wind speed. The turbine doesn't start to generate energy until a minimum wind speed called the cut in speed is reached. Then the turbine's power output increases as the wind speeds increase until it reaches the rated speed where the turbine operates at its rated power. Due to limitations in the gearbox and generator, the wind turbine does not produce any power at wind speeds above the rated speed, i.e., the wind turbine stops if the wind speed reaches its cut-off speed. The purpose of cut-off speed is safety and the prevention of damage to turbine and its components. Figure 4 shows the comparison between an actual wind turbine power curve and the available power in the wind flow. The implicit assumption in making this power curve is that the rotor is exactly aligned with the wind speed direction. The difference between the two curves is due to various reasons. One is the drive train efficiency where it is impossible for the turbine drive train to convert all the kinetic energy into mechanical energy. Another reason is the Betz law, which based on conservation of linear momentum indicates that the rotor can capture the maximum of around 60% of the energy in the wind flow. Details of Betz law calculations can be found in [12].

Since the actual production of a wind turbine is less than the available power in the wind, a ratio is defined to measure the fraction of the available power that is

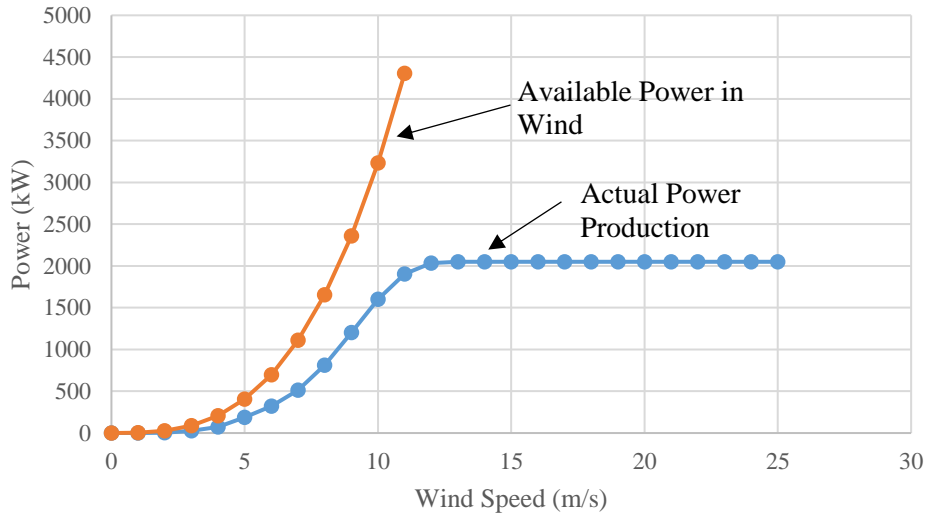


Figure 4- Wind turbine power generation versus available power in the wind converted to electrical power in a given period of time. This ratio is called the capacity factor and is defined as the power production of a turbine divided by available power in wind as shown in Equation (2). The capacity factor of turbines has been increasing over time as technology and designs improve. The rated speed of most turbines is currently around 13 m/s. Turbine manufacturers are focusing on lowering this value so they can capture maximum power at lower wind speeds. Lowering the rated speed is one of the factors that contributes to an increase in capacity factor. Based on the Betz limit, the maximum possible capacity factor for a wind turbine is 0.5926 [12].

$$C_f = \frac{Power}{\frac{1}{2}\rho AV^3} \quad (2)$$

where:

C_f : capacity factor

1.2. Yaw Error

There are a number of efficiency challenges that must be overcome in order to turn the wind potential into actual production. One area that can improve the efficiency of wind turbines is the correction of yaw error. Yaw error (also referred to as yaw angle or yaw misalignment) is the angle between the turbine's rotor axis and the wind direction in the horizontal plane. A yaw error reduces turbine's power production at wind speeds of less than the rated speed. Figure 5 shows the regions of a turbine's power curve where the power production is affected by the yaw error.

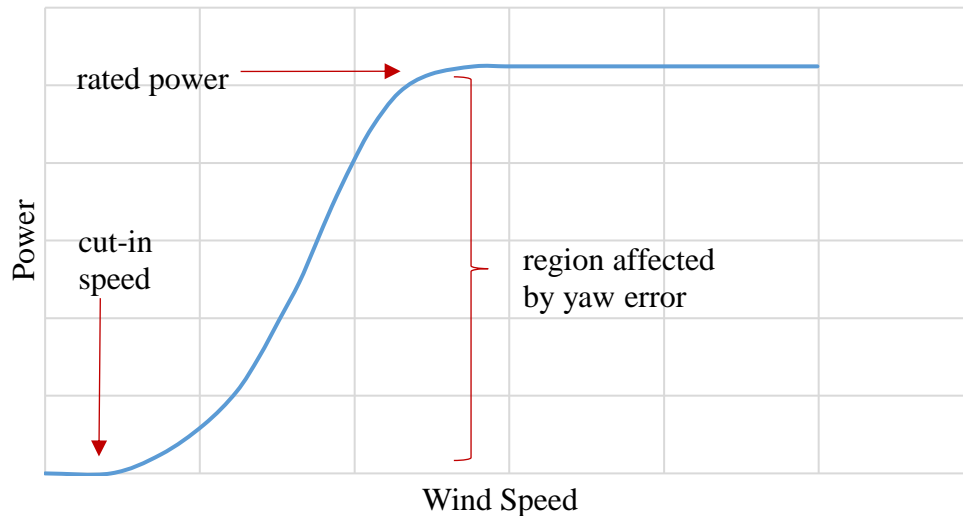


Figure 5- A wind turbine power curve and the regions affected by yaw error

Besides impacting the power producing ability of a turbine, yaw error also affects the reliability of critical subsystems as well. Variation in yaw error (at any wind speed, not just below the rated speed) affects the loads on the components and the subsequent mechanical stresses. These mechanical stresses change the damage accumulation for components and sub-assemblies, which ultimately affects their

reliability. Changes in reliability changes the maintenance events for the turbine and since each maintenance event costs money, a change in reliability will directly affect the operation and maintenance (O&M) costs.

Yaw error consists of dynamic error and static error. Modern turbines use active yaw control, which means there is a yaw mechanism that actively turns the turbine nacelle and aligns it with the incoming wind direction. However, since wind changes direction frequently, it is not feasible to change the nacelle direction as quickly as the wind changes its direction. For example, a common strategy is to change the direction of the turbine only if there was a yaw error of more than 10° during the previous 10 minutes of operation [13]. There is a predefined yaw error threshold at which the yaw system gets activated and turns the nacelle. The uncorrected yaw error (below the threshold) due to this type of yaw control approach is called dynamic yaw error.

The focus of this dissertation is static yaw error. Wind speed and direction are usually measured by a cup and vane mounted on the back of the turbine's nacelle. The data from the cup and vane anemometer are sent to the yaw controller where the data goes through a control algorithm. A yaw error is calculated, and a signal is sent to the yaw system to turn the turbine nacelle. The issue with this system is that the point of measurement for wind speed and direction are located behind the turbine's rotor where flow distortion and rotor blockage will affect the measurements. Inaccurate measurements of wind speed and direction will result in the formation of a bias in the yaw controller that results in inaccurate measurements of yaw error. This error is static called yaw error.

Yaw error values observed in the field range from a few degrees to as much as 35°. Not all the studies distinguish between static and dynamic yaw error. However, as mentioned above, dynamic error is due to a predefined threshold, which is not more than a few degrees, therefore, large values of error are most likely static error. For example, Marin and Pedersen [14] reported values that are as large as 35° with an average of about 7°. A similar range of values was observed by Dai et al. [15] who used SCADA (Supervisory Control And Data Acquisition) data of a wind farm. Marathe et al. [16] studied the data from an utility-size experimental wind turbine and saw a smaller range of yaw error values with the maximum to be around 20° with an average of about 7° similar to other studies. A yaw measurement campaign¹ by Smith et al. [17] showed yaw error values ranging from 12° to 20° with an average of 15°.

Based on the information in the literature, the distribution in Figure 6 has been built to demonstrate the observed values of yaw error on wind turbines in the field. It is important to point out that these values are static and dynamic error together, however, as mentioned earlier, the contribution of dynamic error is as much as the set threshold by the yaw controller. In this dissertation, the negative values are treated the same as positive values.

In the literature, there have been two major approaches to address the issue of yaw error. One focus on using the current technology and equipment that are already available in wind turbines and wind farms. This approach attempts to optimize the

¹ Installing a LIDAR on a turbine for a period of time to collect data is commonly referred to as a 'campaign', i.e., a 'data collection campaign'.

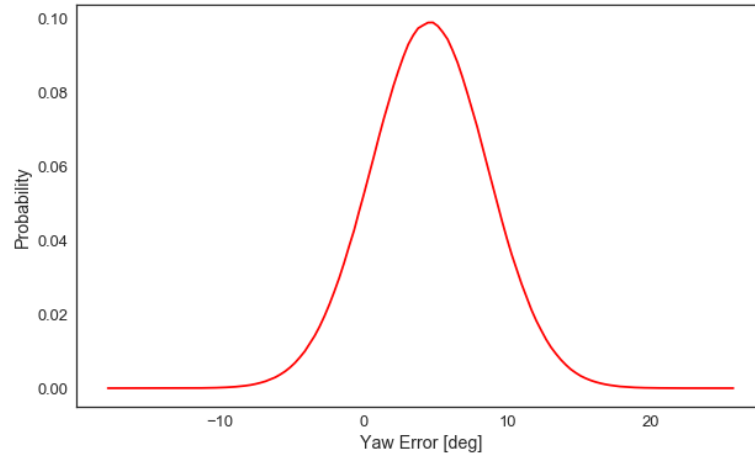


Figure 6- Yaw Error distribution before correction by LIDAR

control algorithm that takes in the wind speed and direction data from cup and vane anemometer (and sometimes a meteorological mast in the wind farm) and processes the data in order to overcome the bias in the yaw system controller that causes the yaw error. This approach is discussed in detail in [18]–[22].

The second approach to address the yaw error issue is using light detection and ranging (LIDAR) systems.

1.3. LIDAR

LIDAR use laser beams to measure the speed and direction of wind in front of the turbine (i.e., before the wind reaches the turbine). A beam of light is emitted by the LIDAR atop the turbine and the light is reflected by airborne particles in the wind. These particles are carried by the wind and have the same speed as the wind flow. LIDAR measures the wind speed by measuring the speed of these particles. LIDAR measures the wind speeds along the laser beam so in order to measure the wind direction, multiple laser beams are needed. Kragh et al. [23] explains how the wind

direction is measured by LIDAR. By using LIDAR, the yaw error in the turbine can be minimized. Unlike conventional vane and cup systems mounted on the turbine nacelle, LIDAR can measure the free wind speed in front of the turbine and as a result, their readings are not affected by the turbine's wake. Also, the LIDAR gives turbine-specific wind speed and direction for each turbine compared to meteorological (met) masts, which only give an overall wind speed and direction for the whole wind farm. The measurements from LIDAR are more accurate than met mast measurements since LIDAR scans a larger area than met masts that represent only point measurements [23]. There are currently two types of LIDAR systems for wind speed measurement applications: constant wave variable focus LIDAR and pulsed LIDAR with a fixed focus [12]. A discussion of the difference of these two types can be found in [24].

Each turbine has a sensor that detects the wind direction and sends a signal to the turbine's yaw system in order to align the turbine with the direction of the wind. However, this sensor loses its calibration over time and as a result, the turbine has a yaw misalignment. There are two types of yaw misalignment: static and dynamic misalignment. Static misalignment is the result of erroneous reading from the wind direction detecting sensor and is the focus of this dissertation. Throughout this dissertation, anytime yaw error is mentioned, it is referring to the static yaw error values. Dynamic misalignments are due to the precision of the yaw control mechanism of the turbine. In other words, if the yaw mechanism on the turbine does not rotate the nacelle (around the tower axis) to the desired angle as it should, the turbine operates under a yawed condition. The error caused by dynamic misalignment

has a different nature than the static yaw error where the cause of error is inaccurate readings of the wind direction.

Using a Supervisory Control and Data Acquisition (SCADA) system, the farm operator detects anomalies in the energy production of individual turbines. A LIDAR will then be mounted on the turbine to measure and fix the yaw error for the turbine if there is a misalignment. The LIDAR is mounted on top of the nacelle and measures the wind directions. The duration that LIDAR collects data on each turbine could vary from several weeks to several months. These measurements are then used to calibrate the direction detection sensor on the turbine. The LIDAR is then be moved to another turbine in the farm to perform the same measurements.

LIDAR can accurately measure the wind direction and reduce the yaw error to values as low as 0° with an uncertainty of approximately 1° .

The behavior of yaw error after the LIDAR is moved to another turbine is not completely clear. Based on conversations with Avent LIDAR Technologies, a leading LIDAR manufacturer at the time of this research, the yaw controller could remain calibrated for a certain period of time, then start losing its calibration, hence formation of yaw error again. Or, it can immediately lose its calibration and signs of yaw error behavior can be detected by SCADA. This gradual formation of yaw error again is referred to as yaw regression in this dissertation. Yaw regression period could be one year or two years after which the yaw error regression stops at some error value and the turbine will continue operating at that value until LIDAR visits again. These scenarios are shown in Figure 7.

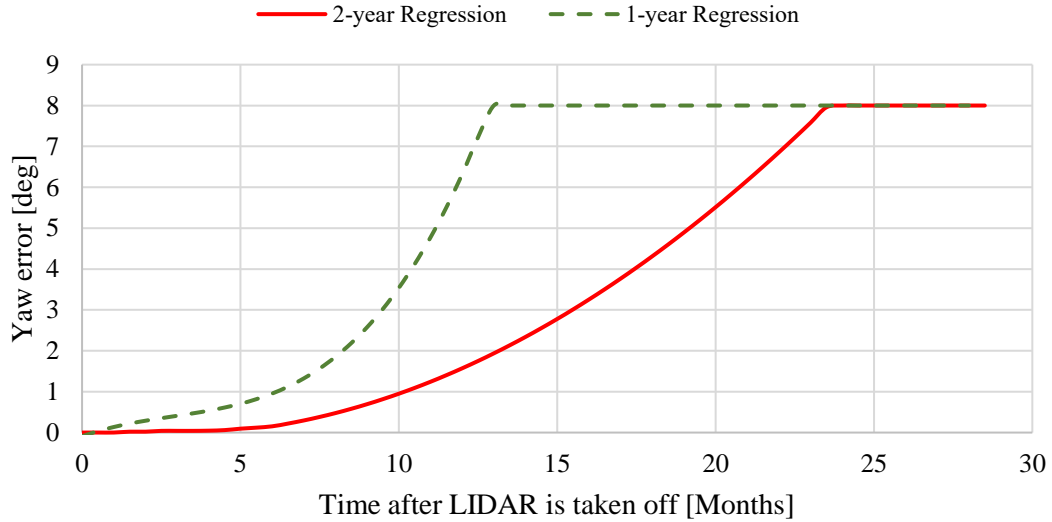


Figure 7- Yaw error regression over time after LIDAR calibration

1.4. Objective of This Dissertation

The objective of this dissertation is to determine how to maximize the return to stakeholders using LIDAR for yaw error correction. This includes determining the number of LIDAR to use within a wind farm and the parameters that should be used to manage the LIDAR, i.e., the stay time on individual turbines in the farm. The goal is to seek a solution to the LIDAR usage problem that minimizes life-cycle cost or conversely maximizes the value of the LIDAR to the farm.

LIDAR systems are capable of accurately measuring the wind direction and fixing the yaw error. This results in extra power production and fewer maintenance events, which increases the revenue and lowers the support cost. However, LIDAR systems are expensive. There is a tradeoff between using the LIDAR systems in a wind farm and leaving the turbines in the farm to operate under yawed conditions. A model is needed to forecast the production and O&M costs of a wind farm and

determining the return on investment (ROI) or net present value (NPV) changes of using LIDAR devices and how they can be optimally used to maximize value.

There's a need for a method that accounts for uncertainties in the wind speeds and incorporates the wind turbine's power curve to calculate how the variations in yaw error affect the revenue generation of wind turbines.

In addition to lowering the power output of a turbine, the yaw error puts extra cyclic loading on the components of the turbine. This extra loading increases the rate of damage accumulation and subsequently shortens the life of critical components. This translates into lower reliability. Component failures result in a maintenance events, which increase the O&M cost of the turbine. This is especially problematic for offshore installations where the maintenance depends on the availability of certain type of vessels (depending the component that has failed), and also the weather and sea conditions, a failure may result in long downtimes and significant production losses.

The model developed in this dissertation must include the two main impacts of LIDAR implementation, the O&M costs and the revenue generation. The reliability improvements due to LIDAR will reduce the number of failures, which lowers the maintenance costs and lowers the number of downtime hours. Minimizing the yaw error, increases the revenue generation and increases the number of operational hours due to fewer maintenance downtime hours. This model also can be used to find the ideal policy of using LIDAR in a wind farm that maximizes the returns.

1.5. Review of Relevant Literature

The current literature associated with the presence of yaw error on turbines, its effects on reliability and energy production, the application of LIDAR in wind direction measurements and the current O&M models for wind turbines are reviewed here.

1.5.1. Yaw Error and LIDAR

Kragh et al. [23] investigated the yaw error measurements using LIDAR. They developed an estimation method that calculates the yaw error based on the measurements of a spinner mounted LIDAR. Their simulation results show that the widest measurement angle is the best one in order to get the most accurate yaw error. Their work also shows that yaw error measurement in complex wind inflows such as vertical shear, horizontal shear and sloped inflow are challenging.

Mikkelsen et al. [13] was one of the first studies in using LIDAR on wind turbines. In their work, they installed the LIDAR on the tip of the rotating spinner of a 2.3 MW turbine to investigate the application of LIDAR in yaw error measurement, collective pitch control and power curve measurements. They compared the yaw error readings from the LIDAR with the readings of a nearby met-mast and turbine's own nacelle mounted vane.

Marin and Pedersen [14] investigated the effects of yaw error on power production of turbines. Their results show that a 10° misalignment results in a 3.02% production loss. Their investigation shows more than 58% of wind turbines have a

yaw misalignment of more than 4° , which is a result of inaccuracy of wind vane and poor yaw control algorithm.

Fleming et al. [25] used a nacelle mounted LIDAR on NREL's research CART2 turbine and investigated the effects of yaw misalignment on the power capture of the wind turbine. Their result show an improvement in power production in the below rated speeds region of the power curve.

Rebeyrat [26] shows the effects of correcting yaw error on the production of a wind turbine. Their study show that fixing a 6° yaw error resulted in 1.8% increase in production, which is higher than the 1.6% theoretical value from Equation 4.

Wagner et al. [27] used nacelle mounted LIDARs to measure the power curve of a wind turbine. They perform a process for calibration of the LIDAR by comparing the LIDAR measurements to a calibrated cup anemometer. After calibration, the LIDAR was mounted on a turbine to measure the wind speed and the results were compared to the readings of a met mast two rotor diameters away. The LIDAR uncertainty in measuring the wind speeds along the horizontal direction was found to be about 0.88 to 1.8%.

1.5.2. Yaw Error and Reliability

There is very little literature that directly connects yaw error and reliability. However, there is literature that discuss the effects of yaw error on turbine loading.

The most relevant literature is a report by the consulting company DNV GL (formerly known as GL Garrad Hassan) [28] where they investigated the effects of yaw error variations on the loads on turbine blades. They performed their analysis on

a generic 3MW turbine, varied the yaw from -20° to 20° in 8° steps for three different wind speeds: 6, 7 and 8m/s. They calculated the value of three loads and three moments at the root and a section of the blade located 18 m from the root.

Damiani et al. [29] performed an analytical and numerical analysis of the effects of yaw error on the rotor loads and confirmed their findings with experimental results. Their work had similar observations as [28]. They also saw that with the vertical wind shear on turbine's rotor, even without yaw error, the azimuth distributions of the angle of attack and relative air velocity are asymmetric and result in more damage accumulation than a symmetric distribution.

Castellani et al. [30] performed numerical and experimental analysis to study the behavior of horizontal wind turbines under yaw error conditions. They ran experiments on an experimental turbine in a wind tunnel with yaw values ranging from -45° to 45° and compared their results to values generated from their in-house blade load analysis model as well as NREL's FAST model. Their work does not directly correlate yaw error and turbine loads however; one interesting finding of their work is the effects of tower blockage that were observed in the experiments that the software models used in the project were not able to account for.

1.5.3. O&M Modeling

Maintenance actions can be divided into three categories: corrective, preventive and predictive maintenance. Corrective maintenance refers to maintenance events where a component has failed and needs a repair or replacement. Preventive maintenance are the scheduled routine maintenance events that occur at fixed

intervals. Such maintenance events could include routine checks, oil and filter change, painting and so on. Predictive maintenance is the type of maintenance that is carried out before the occurrence of a failure while the system is still operational. Predictive maintenance events are carried out based on the information collected from the monitoring methods such as condition monitoring systems (CMS) or the prognostics and health management systems (PHM) on the turbine.

Castro and Diaz [31] investigated the costs of offshore wind farms in all stages of their life cycle from design to dismantling. In their study they dissected the costs of each stage in the life cycle. They concluded that the capital expenditure (CAPEX) of offshore wind farms is not much different than the onshore ones while the operating expenditure (OPEX) is higher. They found that the O&M cost is about 24-31% of the total life-cycle cost of a turbine.

Ding et al. [32] reviewed the maintenance analysis approaches in the literature. The methods are divided into three categories, failure-based, time-based and condition-based. They also investigated the component failures and their subsequent downtimes. Their work shows that the electrical modules, sensors and pitch controls have the highest failure rates but short downtimes. On the other hand, components such as blades and gearboxes that are critical to the whole system availability have a better reliability but longer downtimes.

Tavner et al. [33] investigated the field failure data for the German and Danish wind turbine fleet. Their analysis shows that the main shaft and mechanical break systems have the highest mean time between failures (MTBF), while electrical systems, electrical controls and rotor and blades have the lowest MTBF.

Besnard et al. [34] used an analytical preventive maintenance model on a 5 turbine windfarm to minimize the O&M costs. These maintenance events occur at fixed intervals of time. In this work, the timing of the preventive maintenance was set in a way that they are performed when the power production is lowest or a corrective maintenance is required. Their result showed that by optimizing the timing for the preventive maintenance, the O&M cost could be reduced by 43%.

Zhu et al. [35] investigated the predictive maintenance policy for offshore wind farms through analytical methods. In their study, they investigate the warning time that the monitoring system gives before the occurrence of the failure and when to perform a maintenance. They concluded that for components that are expensive but do not have expensive set-up costs and lengthy downtimes, it is better to perform the maintenance before the failure. For components with expensive set-up costs and downtimes, it is better to delay the maintenance until a closer time to the scheduled time for the preventive maintenance.

Kerres et al. [36] developed a stochastic cost model that simulates the state of a Vestas V44-600 kW turbine as operational, failed or defective. Three maintenance strategies are considered, corrective, preventive and CMS based predictive. Inspections of gearbox and generator during preventive maintenance may result in a component replacement if there is a defect and CMS based predictive maintenance. The components can only be replaced and there is no repair. Electrical system, generator, gearbox, control system and hydraulics were modeled using two parameter Weibull distributions. A Monte Carlo analysis was performed by running the model for 100,000 times. The outputs of the system are O&M cost, opportunity cost due to

lost production and unavailability and their probability distributions were generated for each of the three maintenance strategies.

Nilsson and Bertling [37] evaluated the benefits of implementing CMS systems on wind farms through maintenance cost modeling. Multiple maintenance strategies as a combination of corrective, preventive and predictive scenarios were investigated. The model was run on two wind farms, one onshore and one offshore in Sweden each consisting of 30 wind turbines. Their result show that if the predictive maintenance costs reduce by 4.5% for the whole farm or 47% for a single turbine, the CMS system would be beneficial. Also, a 0.43% increase in the availability of the wind farm would cover the costs of the CMS.

Fischer et al. [38] investigated the reliability of sub components for two Vestas turbines, V44-660 kW and V90-2 MW. Their analysis looks into the most critical sub-assemblies from a reliability point of view, which components have the highest failure rates and failure consequences. They identify the failure cause, mechanisms and the possible solutions for failure prevention.

Besnard et al. [39] developed an analytical model to optimize the maintenance cost for offshore wind farms. The analysis was made on a sample of 100 turbine farm with each turbine having a capacity of 5 MW. They optimized their model based on the logistics of the maintenance such as type of vessels, usage of helicopters, number of technicians, spare parts inventory, etc., and then calculated the sensitivity of their results to price of electricity and turbine reliability. Their result show that for example in an offshore site, having technicians on service 24/7 and using a crew transfer vessel with a motion compensated access system is the optimal case.

Puglia et al. [40] investigated the application of CMS on a 6 MW offshore wind turbine. Different scenarios were investigated with different levels of CMS utilization. Also the failure frequency of the components were modeled in two different approaches. One approach was a constant failure rate over time while the other approach had an increasing failure rate as a function of the system's age. Their result show that CMS has a higher benefit for the cases where the failure rate of the system increases with time. A reduction of 27.5% of a single turbine's corrective maintenance costs is sufficient to justify the use of the CMS system.

1.6. Research Gaps

While there is a significant body of research focused on modeling the maintenance of wind turbines and optimizing their costs, none of the existing models are capable of calculating the cost avoidance ROI (or NPV change) associated with new technology insertion (e.g., LIDAR).

The effects of yaw error and the subsequent extra cyclic loads on the reliability of wind turbines and their components has not been studied. Today the use of LIDAR on wind turbines is only supported by qualitative claims of energy efficiency increases and suggestions of reliability improvement. No quantitative modeling has been done to support the use of LIDAR or to optimize its use (e.g., its circulation within wind farms). The only relevant work in this topic investigates the effect of yaw error variations on the loading of blades, however, no analysis was done on how the yaw error affects the reliability. Furthermore, the effects of yaw error on the maintenance costs of wind turbines has never been explored.

Existing work that investigates the effects of yaw error on energy production uses a wind power formulation to demonstrate the yaw error effects on turbine's energy production. These existing works do not consider:

1. The stochastic nature of wind speeds.
2. That the yaw error power loss is only affecting the region of the turbine's power curve between cut in speed and the rated speed.
3. The turbine design, capacity and power curve. In other words, what range of wind speeds are affected by the yaw error.

Once the relationship between yaw error and reliability is known, it can be used with the effects of yaw error on energy production in an ROI/NPV model. This model will be able to calculate the cost trade-offs of using LIDAR devices in wind farms and by finding the scenarios that maximize the returns.

1.7. Tasks

1. Cost Avoidance ROI/NPV Model – develop a methodology for determining the return on investment from technology insertion. The model will be stochastic discrete-event simulation based and incorporate the cost of money.
 - a) Formulate a stochastic ROI/NPV analysis
 - b) Develop an O&M model for wind turbines
 - c) Extend the model from individual turbines to wind farms
 - d) Incorporate sophisticated maintenance policies, through corrective, preventive and predictive maintenance activities

2. Stochastic Performance Modeling - develop a model that calculates the energy production and subsequently the revenue of the farm. The model has to incorporate the effects of yaw error and yaw variations over time.
 - a) Wind speed modeling
 - b) Energy generation modeling
 - c) Revenue generation modeling
3. Yaw Error Impacts on Reliability - model the reliability changes as a function of yaw error in critical wind turbine components.
 - a. Development of a method to adjust the reliability parameters for components
4. Modeling LIDAR Implementation and Use – calculate the investment costs of LIDAR over time as well as variations of yaw during the support time.
 - a. LIDAR cost and life-cycle modeling
 - b. Yaw error regression after LIDAR removal
5. Evaluating/Optimizing LIDAR Use Policies – investigate the different policies for utilizing LIDAR in a wind farm and determining which policy maximizes the ROI/NPV
 - a. Dedicated LIDAR
 - b. Optimal LIDAR circulation policies

Chapter 2: Stochastic Return on Investment Modeling

This chapter discusses the development of a stochastic model that is capable of quantifying the financial benefits of the implementation of new technologies in systems and systems-of-systems. The metrics used here are return on investment (ROI) and net present value (NPV). The model development initially focuses on ROI, which is then expanded to NPV. The financial terms that make up the two metrics are similar, the difference is in the interpretation of the results.

The particular technology insertion of interest in this dissertation is the use of LIDAR for yaw error management for wind turbines in wind farms. There are two main financial aspects during the operation phase of a wind farm. The costs of operating and maintaining the wind turbines (O&M) and the revenue generation from the wind turbines. A new technology could affect O&M costs or revenue generation or both.

The model developed in this chapter is stochastic as opposed to deterministic. In a deterministic model, the value of all inputs are pre-determined and remain unchanged every time the model is used. In other words, running a deterministic model 100 times results in the exact same answer every time. A stochastic model takes into account the uncertainties associated with the input parameters. For example, for the reliability of turbine blades, the time (or cycles) to failure for each blade is different, even though the operating environment is the same. The difference could come from the materials' micro structural differences and variations in the manufacturing process. In stochastic modeling, many of the inputs have values that

follow probability distributions and by sampling the distributions, a value for the input is generated (later in this chapter, the sampling procedure will be discussed). Running a stochastic model 100 times results in 100 different answers, which themselves form a distribution of answers. This is the basic concept of Monte Carlo analysis, which is used in this analysis.

2.1. Discrete-Event Simulation

The stochastic ROI model is a discrete-event simulator (DES). A DES model simulates the changes in the state of the system due to occurrence of events in discrete periods of time. An event is an occurrence at an instant in time that may change the state of the system. The occurrence time of the events are not predetermined and have a stochastic nature. DES is highly dependent on the timeline, which is the sequence of events and their calendar times.

For example, for modeling the maintenance of wind turbines in a wind farm, the DES simulates the maintenance events of turbines over a period of time by following the state of each component in every turbine in the wind farm. The failures of components are generated stochastically (i.e., probabilistically). Discrete-event simulators are able to capture nonlinear effects, such as combined occurrences of failures and accumulation during inaccessibility with respect to the occupation of crew and equipment. Discrete-event simulation is also able to model many dynamic effects associated with the timing and sequencing of maintenance actions [41], [42]. Figure 8 shows an illustration of a stochastic DES, here we assume the system is a single wind turbine. The system can only have two states, operational and stopped. If

a component in the turbine fails, the system stops and it will be returned to operation after a maintenance event is performed. Figure 8a shows the occurrence of the events while Figure 8b shows the state of the system during the timeline. If each failure results in a maintenance event and its associated costs, the total cost of the maintenance of the wind turbine over the timeline will look like Figure 8c.

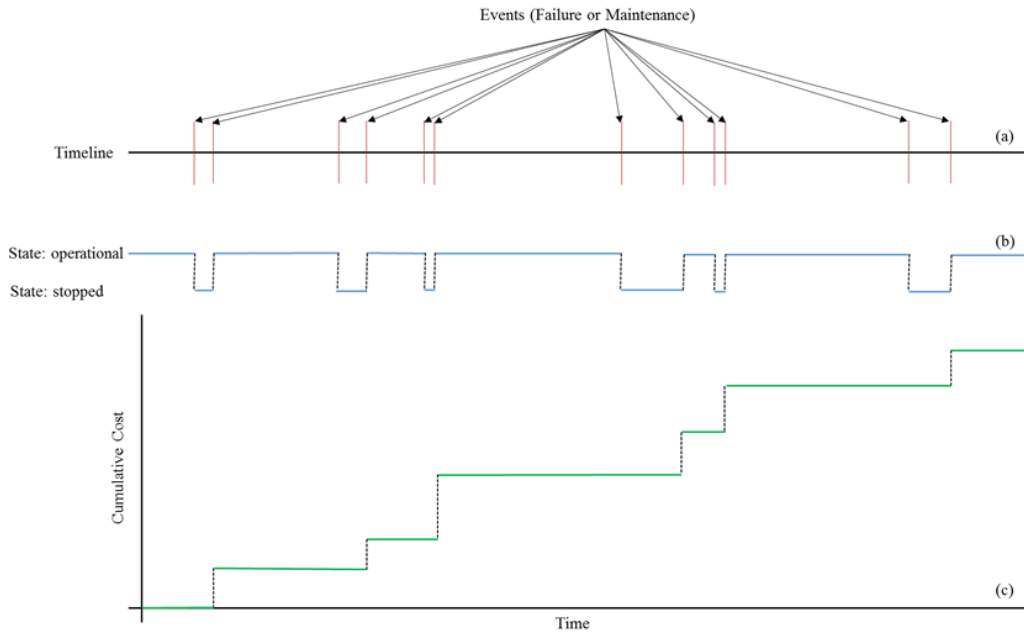


Figure 8- Illustration of a DES, (a): occurrence of events, (b): state of the system, (c): cumulative cost

Modeling the energy production of the wind farm is a DES as well. The difference is the frequency of the events. In maintenance, the events could happen every couple of months and the state of the system remains the same in the periods between the events. For energy production using wind turbines, the state of the system changes every time the wind speed changes. Depending on the wind speed sampling frequency, the state of the system could change every few minutes or hours. During maintenance modeling, the system has a limited number of states (for

example two states in Figure 8, which are either operational or stopped). In energy production modeling, the system has many states, corresponding to different wind speeds. If the wind speeds are assumed to only have discrete values in a particular range, (e.g., wind speed can be between 0 to 30 with values such as 1, 3, 17, etc. or using Natural numbers), the number of states will be limited. However, if it is assumed that the number of possible wind speeds are unlimited in a particular range (e.g., 1.54, 10.6789, etc. or using non-negative Real numbers), the number of possible states becomes unlimited and the DES becomes a continuous system.

2.2. Return on Investment (ROI) Modeling

The classical definition of ROI is the ratio of gain because of an investment over the investment as it is shown in Equation (3) [43].

$$\text{ROI} = \frac{\text{Return} - \text{Investment}}{\text{Investment}} \quad (3)$$

The investment cost consists of the costs of purchasing the technology, maintaining it, keeping an inventory of the technology and any other costs that occur due to the implementation of the technology. For example, for LIDAR, additional costs could include installing and removing LIDAR devices from the turbine. ‘Return’ are the changes that the investment makes to the economics of the system. ‘Return’ is cumulative, which means that at any instant of time, the value of the ‘return’ is the accumulation of all ‘returns’ from time zero to that instant of time. The ‘return’ is calculated using the DES, and since the DES is a function of time, ROI becomes a function of time as well. At the beginning of time, the ‘return’ is zero so

the ROI is -1. As the time progresses, depending on the financial effects of investment, the ROI starts to move away from -1 in either direction. Depending on the expected life of the new technology (it could have a lifespan that is greater than or equal to the turbine or less than that of the turbine in which case the technology has to be purchased again), the recurring maintenance costs, the additional installation/removal costs, and the investment costs become functions of time as well and will change during the timeline.

The return on investment modeling that is performed in this dissertation only focuses on the support period of a wind farm. Total life cycle of a wind farm includes additional stages such as the site study for a wind farm, design, commissioning, land lease, equipment purchase, installation, support time, decommissioning, etc. that are not addressed in this dissertation.

During the support time, a wind farm produces energy, which generates revenue and at the same time the farm requires maintenance that costs money. Any new technology that is implemented on a wind turbine, can either affect the revenue or maintenance costs or both. If the new technology changes the maintenance costs and lowers the O&M costs, these would be avoided costs. Cost avoidance refers to costs that are prevented from happening in the future. Cost avoidance is not the same as cost savings. Cost savings implies lowering the price of an item or activity that results in making extra money available for another item or activity. In the case of cost avoidance, there is no extra money available.

The ‘return’ in Equation (3) can be expanded to include the returns on both O&M cost avoidances and the extra revenue generation (revenue gain) as seen in Equation (4).

$$ROI = \frac{(\text{Avoided Cost} + \text{Revenue Gain}) - \text{Investment}}{\text{Investment}} \quad (4)$$

In order to calculate the ‘avoided cost’ the total life-cycle cost (*LCC*) of the farm during the support time has to be considered. *LCC* includes all the maintenance costs ($C_{O\&M}$), inventory costs (C_{inv}), recurring leasing costs (C_L), insurance costs (C_I), administrative costs (C_A) and other costs (C_{oth}).

$$LCC = C_{O\&M} + C_L + C_I + C_A + C_{oth} + C_{inv} \quad (5)$$

Avoided costs are the difference between the *LCC* for the cases with and without the technology insertion:

$$AC = LCC_{No-tech} - LCC_{tech} \quad (6)$$

where:

AC: avoided costs

Any cost that is not affected by the insertion of the new technology will be the same with and without the new technology and is considered to be a wash. The insertion of LIDAR does not affect any of the cost contributions in Equation (5) other than $C_{O\&M}$. As a result, Equation (6) becomes a function of only the $C_{O\&M}$ terms:

$$AC = C_{O\&M, No-tech} - C_{O\&M, tech} \quad (7)$$

The ‘revenue gain’ calculations are straightforward. The ‘revenue gain’ is simply the difference between the two revenues with and without the new technology.

$$RG = R_{tech} - R_{No-tech} \quad (8)$$

where:

RG: revenue gain

R: revenue

By inserting Equations (7) and (8) into Equation (4), the relation for the ROI becomes:

$$ROI = \frac{(C_{O\&M_{No-tech}} - C_{O\&M_{tech}}) + (R_{tech} - R_{No-tech}) - I}{I} \quad (9)$$

where:

I: investment

It is important to pay attention to the implementation of these two ‘returns’, one is a less money spent while the other is extra money earned. The implementation of Equation (9) is challenging because of the stochastic nature of the problem. In the next section we will discuss these challenges.

2.2.1. Monte Carlo Analysis for ROI Calculation

The calculation of the ROI is performed using a uniquely formulated Monte Carlo analysis approach that requires dependent sampling of parallel life-cycles for cases with and without technology insertion. This section explains the process of sampling, the dependency between the samples with and without insertion of LIDAR and how to use dependent samples to obtain valid ROI calculations.

In this section the definitions necessary to describe the analysis process are provided. Subsequent sections describe how the ROI calculation process proceeds.

O&M costs and revenue in Equation (9) have stochastic natures (and possibly the investment cost too). The inputs that are used to calculate these two parameters have probability distributions that are sampled to determine the occurrence of each event. These probability distributions could be reliability distributions for calculating the time to failure of components, wind speed distributions to calculate the speed of the wind at an instant in time, etc.

Each sample has two characteristics, a value and a probability.

- The value of the sample comes from the probability distribution function (PDF) of the particular input, e.g., the Weibull PDF for the reliability of blades.
- The probability of the sample depends on the cumulative distribution function (CDF) of the particular input. The CDF is the area under PDF between 0 and the value of the sample. The probability is always between 0 and 1.

The O&M costs of a particular turbine over the 20 years of the support time is, in part, the result of failures that occur during the period. Assuming a simple case where the wind turbine has only one component (one input) with a stochastic nature, for which its failure times follow a probability distribution, the first failure time is the value of the first sample from the distribution. The second failure time is the value of second sample plus failure time for the first sample and so on (this simple illustration assumes that the system is instantaneously restored upon failure). This is shown in Equation (10).

$$FT_n = \sum_{i=1}^n (S_V)_i \quad (10)$$

where:

FT : failure time
 S_V : Sample value
 n : n^{th} failure

Three sets can be defined here, a set of values $\{S_V\}$, a set of probabilities $\{S_{Pr}\}$ and a set of failure times $\{S_{FT}\}$. This is shown in Figure 9.

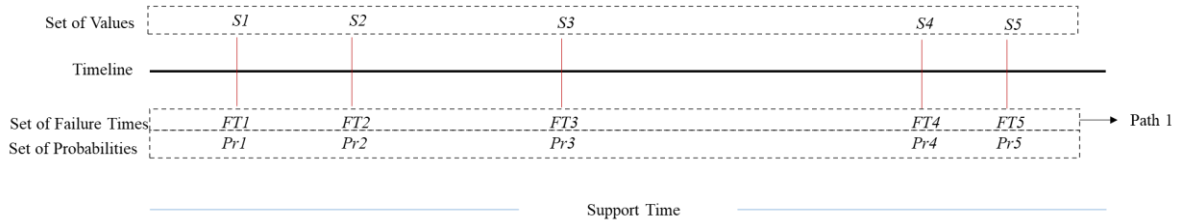


Figure 9- Illustration of different sets

where:

S : value of sample
 FT : failure time
 Pr : probability of the sample

For example, for a case where five failures occur in the support time, these sets could be: $\{S_V\}=\{10, 5, 8, 2, 15\}$, $\{S_{Pr}\}=\{0.6, 0.25, 0.3, 0.1, 0.65\}$, $\{S_{FT}\}=\{10, 15, 23, 25, 40\}$. The $\{S_{FT}\}$ set, which represents the failure times, creates a path. A path is one possible outcome of the O&M cost after the calculations of costs for each failure. The sequence of the samples in every set is important. The sequence cannot change, otherwise the path changes. Since there are infinite possible combinations of the $\{S_{FT}\}$ set, there are infinite number of possible paths.

For a turbine that has multiple components, each with stochastic failure times, the process of sampling and calculating the failure time for each component is the same. The three sets of values, failure times and probabilities can be defined for each component, however they become subsets now. For example, for three components (C1, C2 and C3), a possible subset is:

$$\begin{aligned} \text{Subset of Values} & \begin{cases} \text{C1: } \{S_{11}, S_{12}, S_{13}, S_{14}\} = \{1, 3, 2, 8\} \\ \text{C2: } \{S_{21}, S_{22}, S_{23}, S_{24}\} = \{5, 10, 5, 31\} \\ \text{C3: } \{S_{31}, S_{32}, S_{33}, S_{34}\} = \{18, 4, 9, 2\} \end{cases} \\ \text{Subset of Failure Times} & \begin{cases} \text{C1: } \{FT_{11}, FT_{12}, FT_{13}, FT_{14}\} = \{1, 4, 6, 14\} \\ \text{C2: } \{FT_{21}, FT_{22}, FT_{23}, FT_{24}\} = \{5, 15, 20, 51\} \\ \text{C3: } \{FT_{31}, FT_{32}, FT_{33}, FT_{34}\} = \{18, 22, 31, 33\} \end{cases} \\ \text{Subset of Probabilities} & \begin{cases} \text{C1: } \{Pr_{11}, Pr_{12}, Pr_{13}, Pr_{14}\} = \{0.3, 0.5, 0.4, 0.7\} \\ \text{C2: } \{Pr_{21}, Pr_{22}, Pr_{23}, Pr_{24}\} = \{0.1, 0.25, 0.1, 0.6\} \\ \text{C3: } \{Pr_{31}, Pr_{32}, Pr_{33}, Pr_{34}\} = \{0.75, 0.2, 0.35, 0.15\} \end{cases} \end{aligned}$$

The set of failure times for the whole turbine, is the failure times of components as they occur over time:

$$\begin{aligned} \text{Set of Failure Times } & \{FT_{11}, FT_{12}, FT_{21}, FT_{13}, FT_{14}, FT_{22}, FT_{31}, FT_{23}, FT_{32}, FT_{33}, FT_{34}, FT_{24}\} \\ & = \{1, 4, 5, 6, 14, 15, 18, 20, 22, 31, 33, 51\} \end{aligned}$$

This set of failure times is a new path for the O&M cost. The set of values and probabilities have the same sequence as the set of failure times.

For a wind farm, which consists of many turbines, each turbine having multiple components, a similar method can be followed to create the sets of value, failure time and probability.

2.2.2. Cost Avoidance ROI Calculation

The ROI calculation is the comparison of two cases consisting of a base situation and the new situation. For example, the case of the costs without the investment is the base situation and the case of the costs with the investment is the new situation. In order to make a viable comparison, the two cases have to be evaluated under identical conditions. The way to make the conditions identical for the two cases is to use identical sets (value, probabilities or failure times), but choosing the correct set is crucial to the calculations.

It is challenging to compare the two cases under the same conditions when the system state changes as a result of the stochastic nature of the cases.

In a DES, the sequence of events and their location on the timeline are important. Even for a deterministic DES, where the items in the set of values do not change, if insertion of a technology results in a change of sequence of items in the set of values then the set of values changes.

In a stochastic system, every time the system is simulated from time zero to the end of support, a new set of samples will be generated, which produces completely different sets of values, failure times and probabilities. For the case where a new technology is inserted, if a whole new set of samples is produced, then how can identical conditions for the analysis with and without technology be ensured? As a result, for the cases of technology insertion, the set of samples should be dependent on the set of samples without the technology.

In the LIDAR ROI case, two different groups of samples have to be generated. One group are the wind speed samples and the other group are the component reliability samples.

Wind Speed

Keeping the identical set of samples for wind speed for the cases that use LIDAR and cases that do not use LIDAR is relatively straightforward. LIDAR does not affect the wind speed- it changes the yaw error that affects the energy production. A set of wind speed samples that was produced for the case without LIDAR, will have the same values and sequence for the case with LIDAR. Therefore, the identical condition to use both with and without LIDAR for the wind speed is the set values of the wind speed over time.

Failure Time

As mentioned earlier, the reliability of turbine components comes from reliability distributions. Failure time for each component is calculated by sampling the component's reliability distributions.

LIDAR changes the damage accumulation on a component, this changes the expected life of the components and their reliability. The component will have a new reliability distribution after the implementation of the LIDAR. In this case, using the identical sets of value or sets of failure times for the samples of the two cases is meaningless. Using identical sets of values means failure of a component occurs at the exact same time again. This is in contradiction with the fact the LIDAR has changed the reliability and subsequently the reliability distribution of the component.

Here, using the set of probabilities is the better option. However, the question remains how to use it.

If a turbine has only a single component with a stochastic nature, or only one component that the LIDAR affects the reliability of, then the exact set of probabilities with and without LIDAR can be used. Figure 10 shows how the probabilities of samples can remain the same while the value of samples (time to failure or TTF) changes.

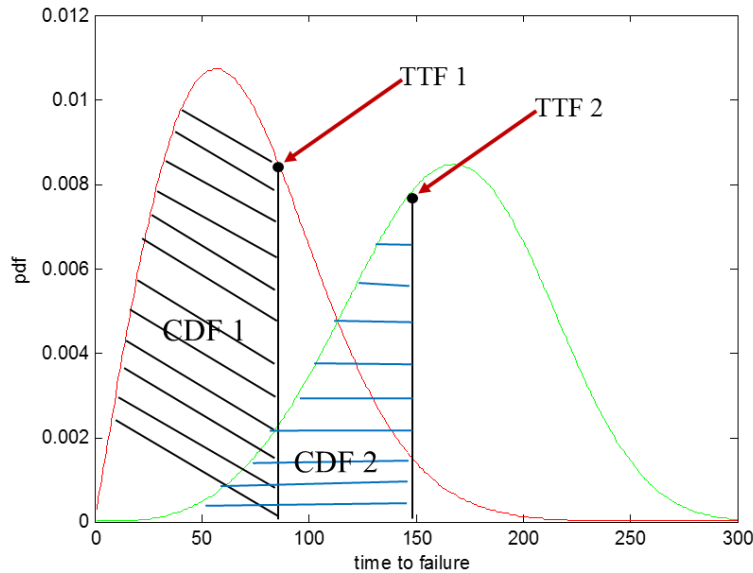


Figure 10- Schematic of sampling the reliability distributions for LIDAR and no LIDAR cases. In this case $CDF 1 = CDF 2$, but $TTF 1 \neq TTF 2$.

When a turbine has multiple components and the reliability of all the components changes when the LIDAR is used, the sequence of items in the subsets of probabilities remains the same for each components, e.g., for component one, failures 1 to 5 have the same probability of occurrence with and without LIDAR, but the value of the sample (TTF) changes since the distribution changes. Since the value of

the samples changes, the failure times change as well so the subsets of value and failure time change while the subset of probabilities stays the same.

The failure time subsets change (subsets are for a single component), this affects the failure time set (the compilation of all the subsets, which is for the whole turbine). Not only have the items in the failure time set changed but also their sequence may change as well. For example, the second failure of component 1 in the case without LIDAR was the second failure in the turbine, but after implementation of the LIDAR, the reliability of this component improves enough that the second failure of the component 1 becomes the tenth failure of the turbine, this is an example of the change of sequence in the failure time set. As a result, the sequence of the items in the set of probabilities for the turbine changes while the probability of each event remains the same. The conclusion is, after the implementation of LIDAR, none of the three sets (a set is a combination of component subsets) stays the same, so there will be no identical condition.

In this case, in order ensure that identical conditions are used, the same probabilities for identical events have to be used. The probability subsets for each component stay the same for cases with and without the LIDAR. For example, five failures of component 1 will always have the same probability of occurrence for LIDAR and no LIDAR even though the subsequent failure times are different and this may relocate the position of failure time in the failure time set.

Generating the sets for the cases without LIDAR will create a path for the O&M costs and another path for the revenue, which together are assumed to be a new single path. Performing the analysis for the case with LIDAR and considering the

appropriate sets for the samples will provide another path. This pair of paths will then be used in the ROI formulation to calculate a single value of ROI. Repeating the analysis process, e.g., 100 times, results in 100 different pairs of paths, which will give 100 different ROI values, which generate a distribution of ROIs.

2.2.3. Operation and Maintenance (O&M) Modeling

In order to model the maintenance of the turbines, reliability distributions for the components are used. The reliability of the components can be modeled using different types of distributions, normal, exponential, lognormal, and so on. The most common distribution for reliability purposes is the Weibull distributions. This reliability distributions are calculated using historical failure data.

Each component in the turbine has its own unique distribution, which will be sampled to generate its TTF. The TTF could be a complete shut down of a system or just operation at a limited capacity. The maintenance event corresponding to a TTF could be a repair or replacement of the component. When using reliability data in the O&M model to generate a TTF, it is important to know how 'failure' was defined in the original database and whether it means a complete loss of functionality or just not working properly or both. Also, some data could be reported based on the maintenance action performed (repair or replacement) and not the type of failure that occurred. As a result, the distributions generated from the data represent what maintenance action is required rather than what happened to the component.

In the current model, based on the failure database used, failure of a component means a complete loss of functionality and the subsequent maintenance

action is a replacement of the component. The type of maintenance is predictive, which means that the farm operator will be notified in advanced before the occurrence of the failure and performs the required replacement in a timely manner while the component is still operational.

Here, the assumption is that the reliability of the turbine as a whole follows a series system reliability model. Failure (complete loss of functionality) of a single component will result in the shut-down of the whole turbine. In parallel reliability systems, failure of a component leads to a limited performance of the turbine but not a complete shut-down. It is important to mention that the parallel reliability does not mean parallel components or redundancy. For example, in the event of failure of the yaw system, the nacelle won't be aligned with the wind flow direction and the turbine produces less energy but the failure of yaw system theoretically won't lead to a shutdown of the turbine.

O&M costs are called life-cycle costs or LCC. As discussed in the previous chapter, maintenance of the turbines in a farm could be corrective, preventive or predictive. The most practical maintenance strategies are a combination of all three as was extensively discussed in the literature review section. As a result, the LCC of a wind farm will consist of multiple terms. These terms are shown in Equations (11).

$$LCC = C_C + C_P + C_{PR} \quad (11)$$

where:

C_C : corrective maintenance
 C_P : preventive maintenance
 C_{PR} : predictive maintenance

Each of the maintenance costs consists of a component cost, labor cost, transportation cost and a production loss due to downtime as it is shown in Equation (12).

$$C_M = C_{Comp} + C_L + C_T + C_{PL} \quad (12)$$

where:

C_M : maintenance cost (corrective, preventative or predictive)

C_{Comp} : component cost

C_L : labor cost

C_T : transportation cost

C_{PL} : production loss

Transportation costs include all the costs of transporting the component from the inventory location to the wind turbine and mounting it on the turbine. This could be costs of using trucks for onshore sites or various vessels depending on the component for offshore sites along the required cranes for the purpose of mounting.

The production loss includes the revenue that could have been generated during the maintenance period and may involve other penalties in the cases where downtimes are long. The production losses for preventive and predictive maintenance have less uncertainties than the production losses for corrective maintenance since the former can be planned ahead while for the corrective maintenance, the maintenance timing depends on the availability of spare parts, labor, transportation and weather conditions.

2.2.4. Revenue Generation Modeling

The revenue generation model calculates the energy production of the wind farm and by using the price of energy it calculates the revenue. The revenue generation model is stochastic since probability distributions are used for calculating the energy production. The revenue generation model takes into account the downtimes from the O&M model when the turbines were not operational due to

maintenance. The energy loss due to downtimes for each year are deducted from the total energy production of that year to calculate the net annual energy production. The development of the revenue generation model is thoroughly explained in Chapter 3.

2.3. Cost of Capital

The costs of operating a wind farm along with the revenue that is generated by it create a cash flow. This cash flow has to be discounted to account for the cost of money. Cost of money means that the money that is invested in a project is not free and the entities that provide the money expect a return.

Each maintenance event has a cost, the cost of maintenance events for each year produces a cash flow in that year. This is the same case for energy production. The revenue for each year provides a cash flow in that year. Each cash flow should be discounted depending on when the money is received or spent to calculate the present value (in year 0 dollars) of that cash flow using Equation (13)

$$PV = \frac{CF}{(1 + WACC)^n} \quad (13)$$

where:

WACC: weighted average cost of capital per year

CF: cash flow in year n

Each term in Equation (99) is the present value of a set of future cash flows. The total O&M cost is the sum of the discounted costs of all the maintenance events, this is the cash out (14). The revenue is the cash in and is calculated similarly (15).

$$C_{O\&M_{tech}} = \sum_{n=1}^y (PV_{O\&M_{tech}})_n \quad (14)$$

$$R_{tech} = \sum_{n=1}^y (PV_{R_{tech}})_n \quad (15)$$

The money required to finance a project can be raised from different sources. These sources can broadly be categorized as equity and debt [44]. Investors (whether debt or equity) expect a return on their investment. As a result, each capital component has a required rate of return or capital cost. The total expected return for the whole capital is a weighted average of capital components called weighted average cost of capital or WACC. There are several methods for calculating WACC [45] with the most common one being the Miles and Ezzell's [46] equation:

$$WACC = R_e \frac{E}{V} + R_d (1 - T_c) \frac{D}{V} \quad (16)$$

where:

R_e : cost of equity

R_d : cost of debt

T_c : corporate tax rate

E : the portion of project that is equity financed

D : the portion of project that is debt financed

V : total project value (E + D)

WACC is highly project dependent and for wind projects, values between 5 to 10% have been reported [11], [47]–[50]. These values are assumed to be constant over the lifetime of the project. WACC is also referred to as discount rate. These two terms will be interchangeably used throughout this dissertation.

2.4. Net Present Value (NPV)

ROI has several caveats that can make it a misleading metric. ROI standardizes the cash flows in order to create a unitless metric. This doesn't always demonstrate the true value of returns. For example, a \$1M investment that returns \$4M will have an ROI of 3 with a \$3M net return. A \$2M investment that returns \$6M will have an ROI of 2, but a \$4M net return. Comparing these two investments from an ROI standpoint one would conclude that the first investment is better (higher ROI). However, from a net return perspective, the second investment is better (assuming the money was available to invest). From an accounting prospective where the goal is to generate the highest returns, ROI can be misleading. In order to address this shortcoming, a Net Present Value (NPV) metric is selected to perform the analysis in the remainder of this dissertation. NPV is defined as [44]:

$$NPV = -Inv + \sum_{n=1}^y \frac{CF_n}{(1+WACC)^n} \quad (17)$$

'*Inv*' is the initial investment in the project at time zero. Each CF_n represents a possible cash flow through the life cycle of the wind project. These cash flows could be cash in or cash out. The appropriate sign for either case has to be included in Equation (17).

An NPV of zero means that the project's cash flows are exactly equal to the invested capital for financing a project. As a result, a project is worth pursuing if the NPV of the project is positive.

The goal here is to calculate the NPV changes due to implementation of a new technology.

$$\Delta NPV = NPV_{tech} - NPV_{no-tech} \quad (18)$$

In the case of LIDAR devices, similar to ROI, only performance, O&M and LIDAR life-cycle cost cash flows will be affected by the new technology while the rest of cash flows will be a wash (subtracts out).

The relation between ROI and ΔNPV can be generated by rearranging the cash flows in Equation (9) to form the NPV values from Equation (17) and then substituting them into Equation (18).

From Equation (9), with rearrangement of the terms:

$$ROI = \frac{(R_{tech} - C_{O\&M_{tech}}) - (R_{no-tech} - C_{O\&M_{no-tech}}) - I}{I} \quad (19)$$

Technology revenue and O&M along with the investment term in the numerator of Equation (19) represent the cash flows for NPV_{tech} in Equation (18) while the remaining term in the numerator represents the cash flows for $NPV_{no-tech}$. As a result, the relation between ROI and ΔNPV becomes:

$$\Delta NPV = ROI(I) \quad (20)$$

This addresses the issue of ROI where the cash flows are standardized with regards to the investment value and may not demonstrate the true returns of an investment. Unlike ROI, which was unitless, ΔNPV has the same unit as the currencies used in the cash flow calculations.

Chapter 3: Performance Model

In order to measure the effects of yaw error on the power generation of a turbine, a performance model is required, which calculates the power generation of the wind farm.

The power produced by a wind farm depends on the performance characteristics of its turbines and the properties of the wind at the location of each turbine. Wind characteristics are a function of time and location and they fluctuate depending on the time of the day and the seasons. A feasibility analysis is needed before commissioning a wind project to estimate the annual energy production of the potential wind farm. The estimation can be achieved using analytical methods or by developing simulation models where the wind characteristics and the performance metrics of the turbines are the inputs.

Multiple previous studies have looked at modeling a wind farm's power output as well as the parameters and conditions that affect the output. For example, Jin et al. [51] used analytical and simulation methods to generate a distribution of possible power outputs of a 20 kW wind turbine. Lydia et al. [52] reviewed the methods used to model wind turbine's power curves. Existing methods can be divided into two categories, parametric and non-parametric. The first category uses analytical methods that employ the power curve equations (exponential, cubic, up to 9th degree polynomial, etc.) to model power curves. The second category investigates methods such as neural networks and fuzzy logic to establish a relationship between input wind speed and output power. Wagner et al. [53] considered how to calculate an

equivalent wind speed in the presence of shear on the rotor. They used LIDAR to measure wind speed at 9 different heights on the rotor and then fit a shear exponent by using hub height as the reference height. Wagner et al. [53] took more than 900 sets of measurements and the resulting shear exponent values range from 0.0 to 0.6. Then, by calculating the kinetic energy on the rotor, they calculate equivalent speed on rotor for operations under shear conditions. Elliot et al. [54] investigated the effects of turbulence on power output of a 2.5 MW wind turbine. Wind speeds were measured at the hub height of the wind turbine while the power output of the turbines were recorded. Their results show that there is a large sensitivity of power curves to turbulence. Sumner et al. [55] investigated the effects of atmospheric conditions on wind turbine's power output by using wind speeds measured by meteorological masts and recorded power production of 0.4 MW turbines in England. The wind speeds were measured at different heights of below, equal and higher than the hub height. Their results show that using hub height wind speeds yields 5% higher energy production than using the average rotor wind speed that considers the effects of wind shear. Chang et al. [56] used time series and Weibull distribution of wind speeds to evaluate power production of a 660 kW wind turbine. Wind speeds were measured using an anemometer mounted on the turbine's nacelle, behind the turbine hub and as a result the measurements were affected by the wake effect. By integrating time series and Weibull distribution of the wind speeds, the authors calculated the estimated power production of the turbine and compared their results with its actual production. Nemes et al. [57] developed Weibull distributions for wind speeds of a site in Romania and calculated the power output of a 1.5 MW wind turbine using analytical

methods. Then, they verified their results with a Monte Carlo simulation and used the results to calculate the capacity factor of the turbine for variable cut in, cut off and rated speeds.

The approach used in this dissertation is to calculate the power generation through modeling rather than analytical methods. The key elements of the model are:

- Generating wind speeds
- Converting the wind speed from measurement height to rotor height
- Incorporating yaw error in the wind speed
- Calculating the power using the wind speed
- Calculating the energy production

In the following sections, each of these considerations will be discussed.

3.1. Wind Speed Generation

Wind speed measurements are performed using several methods such as readings at several heights of meteorological masts, LIDAR, or floating buoys (for offshore installations). These measurements are at heights that are not necessarily the same height as turbine's hub. In all of these cases, the data collection has a predefined frequency where several measurements can be collected per second. The common practice in the literature, is to average these readings and use the 10-minute average values. These values are in a time series format. In order to use them, either the time series values themselves can be used, or the data can be converted into probability distributions (Weibull distributions in particular).

Time series is deterministic modeling where all the turbines in a wind farm experience the exact same wind speed. At the same time, data collections were performed for a particular length of time (e.g., few months, or years). This provides only information for the specific period of data collection. In cases where the model is predicting the power production for several years, time series does not provide enough data points to build the model. In order to overcome this shortcoming, the data has to be reused and duplicated to cover the entire time period of the model.

Using probability distributions (in this case Weibull distributions) for wind speeds can address the issues associated with time series and the lack of sufficient data. Historical time series data can be used to produce the probability distribution, which then can be sampled as many times as needed for each wind turbine in the wind farm. The probability density function (pdf) of a two-parameter Weibull distribution is shown in Equation (21):

$$f(V) = \frac{\beta}{\eta} \left(\frac{V}{\eta}\right)^{\beta-1} e^{-\left(\frac{V}{\eta}\right)^\beta} \quad (21)$$

where:

- V : Wind speed
- β : Weibull shape parameter
- η : Weibull scale parameter

By sampling the Weibull wind speed distribution, wind speed values for 10-minute time intervals will be generated. These values correspond to the height where the measurement was performed.

3.2. Height Conversion of Wind Turbines

Wind speed changes with elevation, meaning the speed at the point of measurement is not the same as the speed on the rotor. The wind speed changes with elevation can be calculated using the power law in Equation (22):

$$\frac{V(h)}{V(h_r)} = \left(\frac{h}{h_r}\right)^\theta \quad (22)$$

where:

$V(h)$: Wind speeds at the desired height
 $V(h_r)$: Wind speeds at the reference height
 h : Desired height
 h_r : Reference height
 θ : Shear exponent

Many researchers consider the shear exponent to be constant, with the most common values being 0.1, 0.14 and 0.3 [12]. θ can also be considered as a variable. In the literature there exists formulas for θ as a function of either wind speed or surface roughness. For example, the formula proposed by Justus [58] is shown in Equation (23), which calculates θ as a function of wind speed at a particular reference height:

$$\theta = \frac{0.37 - 0.088 \ln(V(h_r))}{1 - 0.088 \ln\left(\frac{h_r}{10}\right)} \quad (23)$$

In this dissertation, the wind shear exponent is assumed to be constant with value of 0.14. This value converts the wind speed from the measurement height to the hub height of wind turbine.

It is also important to point out that due to size of the wind turbine rotor, which is twice the length of a single blade, there is wind shear on the rotor area as

well. This means in practice, the distribution of the wind speed over the rotor area is not uniform and top of the rotor experiences higher wind speeds than the bottom of the rotor. In this dissertation, a uniform distribution of wind speeds over the rotor is assumed. This uniform distribution is the equivalent to the sheared flow on the rotor. The equivalent value of the wind speed is the wind speed at the hub height.

3.3. Yaw Error Adjustment

Yaw error affects the wind turbine with a cosine relation.

$$V = V_{flow} \cos(\alpha) \quad (24)$$

where:

V : wind speed on rotor

V_{flow} : speed of free wind flow

α : yaw error

As mentioned earlier in Chapter 1, Equation (1), power in a wind flow is a function of V^3 . Therefore, from a theoretical point of view, the power under yawed condition has to be affected by $\cos^3(\alpha)$. A considerable body of literature that investigated this relation using field observations exists.

Fleming et al. [25] used a nacelle mounted LIDAR on NREL's research CART2 turbine and investigated the effects of yaw misalignment on the power capture of the wind turbine. Their result show an improvement in power production in the below rated speeds region of the power curve. Although they use Equation (24) and $\cos^3(\alpha)$ to relate yaw error and power production, they mention that the relation could follow $\cos^2(\alpha)$.

Wan et al. [59] simulated the power production of a turbine as a function of yaw error, rotor speed and blade pitch angle. Their model shows that the effects of yaw error on power loss is varied at different wind speeds. They believe that neither $\cos^2(\alpha)$ nor $\cos^3(\alpha)$ give an accurate estimation of the effects of yaw error on power production while their model yields more accurate results.

Johnson et al. [60] investigated methods to increase the power capture of wind turbines. They developed a model that used $\cos^3(\alpha)$ for the relation between yaw error and power production. They cited an earlier set of experiments by NREL (earlier than [25]) for the use of this relation. Their study showed that for yaw error values less than 20° , this relation is a good approximation to the experimental data.

Cortina et al. [61] investigated the application of LIDAR in measuring wind speed and direction and tried to calculate the optimal upstream scanning distance for LIDAR through simulation. They also use $\cos^3(\alpha)$ in modeling the power loss due to yaw error. Their numerical simulation shows that there could be up to 22% difference between LIDAR measurements and turbine vane for wind direction measurements, which was validated by experimental results of [13] as well.

As it can be seen, there is no conclusive agreement on whether the relation should be $\cos^3(\alpha)$ or $\cos^2(\alpha)$. In this dissertation, it is assumed that yaw error affects the wind speed with $\cos^3(\alpha)$ relation.

3.4. Power Calculations

Now that the wind speed is adjusted for height of the turbine and yaw error, it can be used to calculate the power production. There are two ways to calculate the

power using the wind speed. First way is to use Equation (25), which calculates power by using turbine's power coefficient.

$$P = \frac{1}{2} \rho A V^3 C_p \quad (25)$$

where:

C_p : turbine's power coefficient

V : wind speed on rotor

The issue with this approach is that the power coefficient is a function of blades' tip speed ratio, which itself is a function of wind speed. Power coefficients are different from turbine-to-turbines and are provided by the turbine manufacturer. Accessing the information on the power coefficient of a particular design is a challenging task since this information is not provided by the manufacturers to the public domain.

The second approach is to use the adjusted wind speed in a turbine's power curve (Figure 11). Like the power coefficient, turbine power curves are different from manufacturer-to-manufacturer, however, they are easier to find in public domain than power coefficients. It is also important to point out that the power curve shown in Figure 11 is a deterministic power curve. In practice, there are uncertainties associated with this curve where the actual production could be higher or lower than the average values shown in the figure.

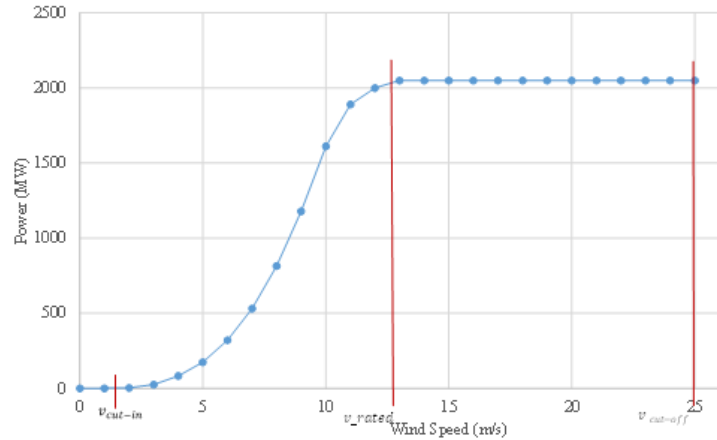


Figure 11- Deterministic power curve for Enercon E-82 2 MW wind turbine, data from [62]

3.5. Energy Production

The process explained so far describes the power generation for a single sample of wind speed. The frequency of the sampling depends on the frequency of the original data used to generate the distributions. For example, in the case of wind speeds, if the original wind speed dataset reported wind speeds for every hour, then the sampling of the probability distribution has to be every hour. Overall, during the data collection period, several readings are done per second. The common practice in the wind industry is to average these readings for 10-minute time intervals and this time interval will be the basis of generating the wind speed distributions. The 10-minute sampling frequency is the assumption of this dissertation as well. Each wind speed samples represents the power generation for 10 minutes. By sampling the wind speed distribution over time, the *energy* production of the wind turbine over specific periods of time can be calculated (i.e., a year). However, there will be times where the turbine is shut down due to maintenance or LIDAR circulation. These downtimes

energy loss values have to be deducted from the total energy production in order to calculate the actual production. Equation (26) shows the total energy production of a wind turbine for a specific period (e.g., 1 year). Downtime calculations due to maintenance will be explained in Chapter 4 while LIDAR related downtime will be discussed in Chapter 5.

$$E = \sum_{m=1}^M P_m(t - d_t)_m \quad (26)$$

where:

E: total energy production for a period (e.g., 1 year)

m: time interval (e.g. 10 minutes)

M: total number of time intervals in the period

P_m: power generation in a time interval

t: value of the time interval (e.g., 10 minutes)

d_t: downtime

After calculating the energy production, the revenue has to be calculated. The price of energy depends on the power purchase agreement (PPA) between the wind farm owner and the customer (which could be a utility company). Depending on the PPA, the price of energy could vary based on the time of day, month of year and from year to year. There could be penalties in the PPA in cases where the farm does not produce a required amount of energy in a particular time. These factors all affect the revenue generation of the wind farm. In this dissertation, PPA requirements and price fluctuations are not considered. A fixed value of energy purchase price is assumed and later in Chapter 5, the sensitivity of results to this value will be investigated.

Figure 12 shows a summary of the process of calculating turbine's power production under yawed condition that was explained in this chapter.

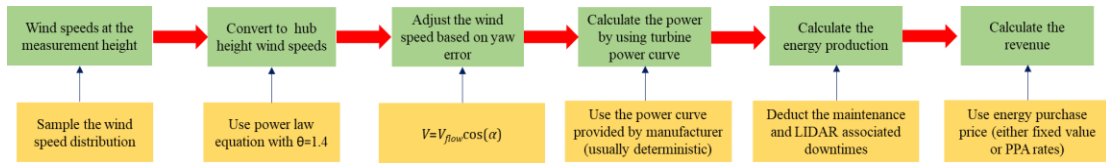


Figure 12- Summary of calculating the power generation of a turbine described in this chapter

Chapter 4: Effects of Yaw Error on Reliability of Turbine's Blades

Besides impacting the power producing ability of a turbine, yaw error also affects the reliability of critical subsystems in wind turbines. Variation in yaw error (at any wind speed, not only below the rated speed) affects the loads on the components and the subsequent mechanical stresses. These mechanical stresses change the damage accumulation for components and sub-assemblies, which ultimately affects their reliability. Approximately 17 to 28% of wind project costs are attribute to O&M costs, which are directly affected by the reliability [8].

In this chapter, the effects of yaw error on the reliability of blades are investigated by performing load and stress analysis for various yaw errors. The results of these analyses will be used to determine the Weibull parameters used for predicting the failure time of blades. Figure 13 shows the flowchart of the approach of the reliability analysis of a blades in this chapter.



Figure 13- Flowchart of the approach for reliability analysis of blades

Several existing papers address fatigue modeling of blades. Sorensen et al. [63] performed a series of experiments to understand the damage evolution in turbine blades. Blades were run to failure under static and cyclic loads. Damage types observed were compression failure and crack growth along adhesive joints. Loadings were in the flapwise direction. Delamination was the most common failure mechanism observed. Ronold et al. [64] investigated the fatigue life of blades under

flapwise bending loads. The flapwise loads have a range and cycle number at a 10-minute wind speed value. They used a linear relation to translate the loads into stresses. Jang et al. [65] performed a comprehensive study on fatigue life prediction of blades. They chose a small 1.5 kW turbine as a case study, calculated flapwise and edgewise moments, then used the loads in an FEA model to calculate the stresses.

4.1. Load Analysis

Load analysis in wind turbines, includes the forces and moments applied to components and sub-assemblies. These loads are either extreme loads or cyclic loads. Extreme loads are due to extreme conditions such as high or unusual winds speeds. Cyclic loads come from attributes such as the rotation of the rotor, yaw movement, uneven wind profiles on the rotor (shear wind), etc. Extreme loads result in overstress failure mechanisms whereas cyclic loads result in wearout failure mechanisms. A single occurrence of an extreme load at a very high wind speed may result in an immediate failure whereas occurrences of lower wind speeds do not result in any immediate failures but they introduce damage to the component and over time, this damage accumulates and results in a failure. Cyclic loads are the primary cause of fatigue (which is a wearout failure mechanism) in turbine sub-assemblies, [66], [67]; in this analysis the focus is on wearout. In order to study cyclic loads, an understanding of the wind speeds distributions is required. Figure 14 shows the wind speed Weibull distribution of the Delaware Bay at hub heights of 65 m. As it can be seen, the most probable wind speeds are 6, 7 and 8 m/s.

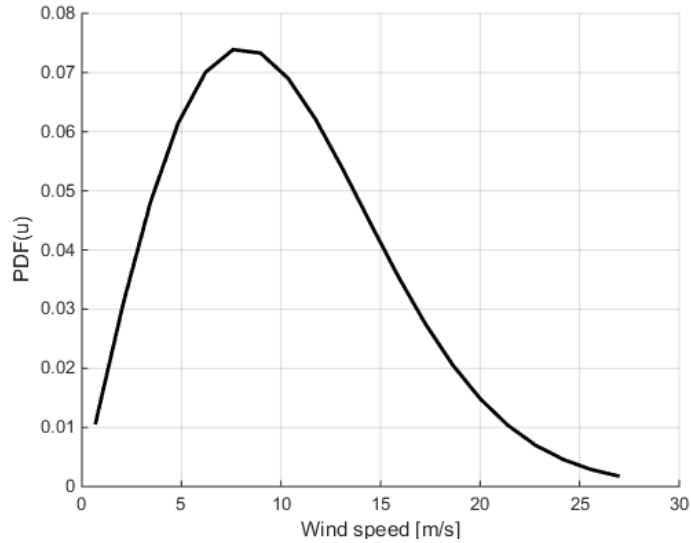


Figure 14- Wind speed pdf for year 2011 at Delaware Bay, using data from [68]

Load analysis can be applied at any location on the blades; however, the most susceptible site for failure is the blade root, where the blade is attached to rotor. Research shows that most fatigue related failure of turbine blades occur at the junction where blade attaches to the rotor [69]. Wind turbines constantly operate under vertical shear flow, which means that the wind speed at the top of the blade is different from the bottom. Shear flow causes flapwise and edgewise loads, which are shown in Figure 15. As it is mentioned by Shen et al. [70], blade root flapwise moments on the all the blades together cause yawing and tilting forces, which through the drive train effect the yaw system and the tower as well as the blades.

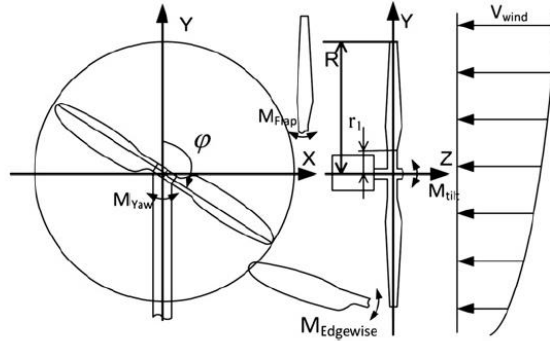
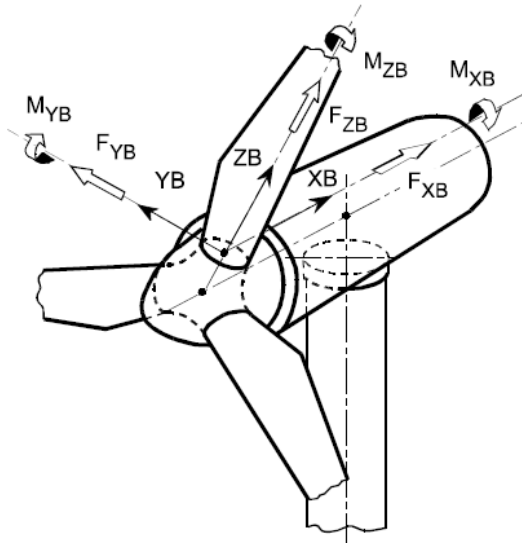


Figure 15- Schematic of edgewise and flapwise moments [70]

As mentioned in Chapter 1, there is very limited literature on the topic of yaw error effects on reliability of turbine sub-assemblies. The most relevant work in this subject is a report by the consulting company DNV GL [28], which is used as the basis of the load analysis in this dissertation.

The report in [28] covers a yaw dependent load analysis. 6 loads (3 forces and 3 moments) were calculated as a function of yaw errors ranging from -20 to 20° in 4° increments at two locations on a turbine blade: the blade root and a segment of the blade at 18.2 m from the root. These loads are force along the z-axis of blade, flapwise force and edgewise force. The moments are moments around the z-axis, flapwise bending moment and edgewise bending moment. The coordinate system for this analysis is shown in Figure 16. The analysis is performed on a generic 2 MW wind turbine with rotor diameter of 75 m and hub height of 65 m. The analysis is performed at three wind speeds: 6, 7 and 8 m/s.



ZB-Radially along blade axis

XB-Perpendicular to ZB and pointing toward the tower for an upwind

YB-Perpendicular to blade axis and shaft axis

Origin-At each blade station

Figure 16-- Coordinate system for the blade [28]

Variation of the six main loads, flapwise bending moment (Flap BM), edgewise bending moment (Edge BM), moment around z axis (M_z), flapwise shear force (Flap SF) and edgewise shear force (Edge SF) and forces along z axis (F_z) as a function of yaw error are plotted in Figure 17-19. Assuming a yaw error of 0° as a point of reference, the vertical axis shows how much loads at each yaw error change relative to the loads at 0° . These plots represent the loads at the blade root since it is the most susceptible site to failure.

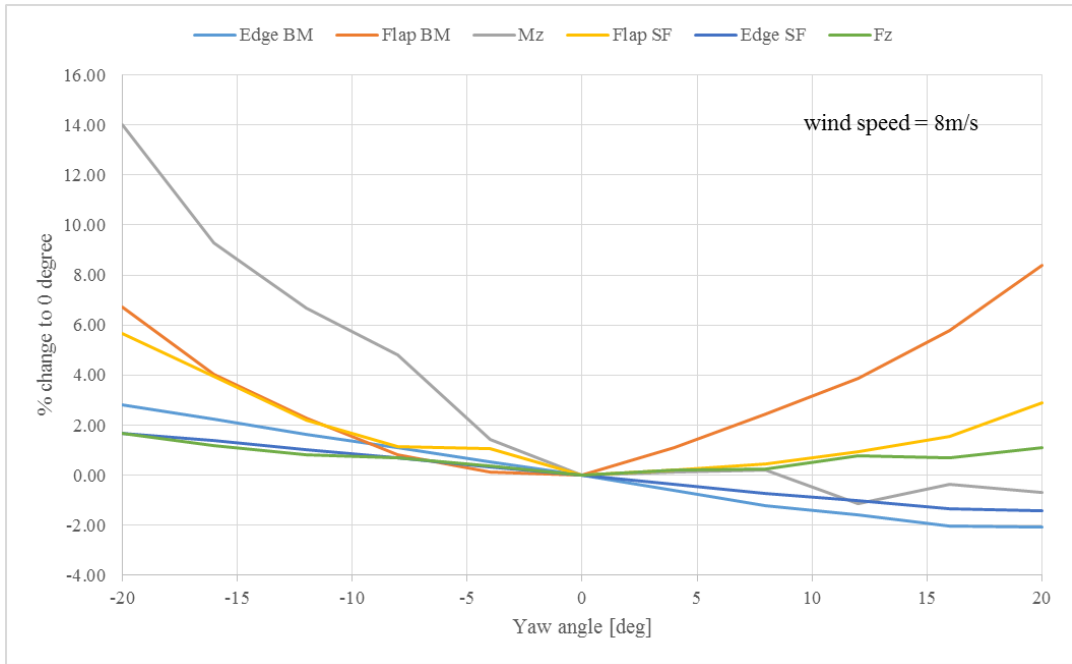


Figure 17- Variation of loads with yaw error at the blade root for wind speeds of 8 m/s, data from [28]

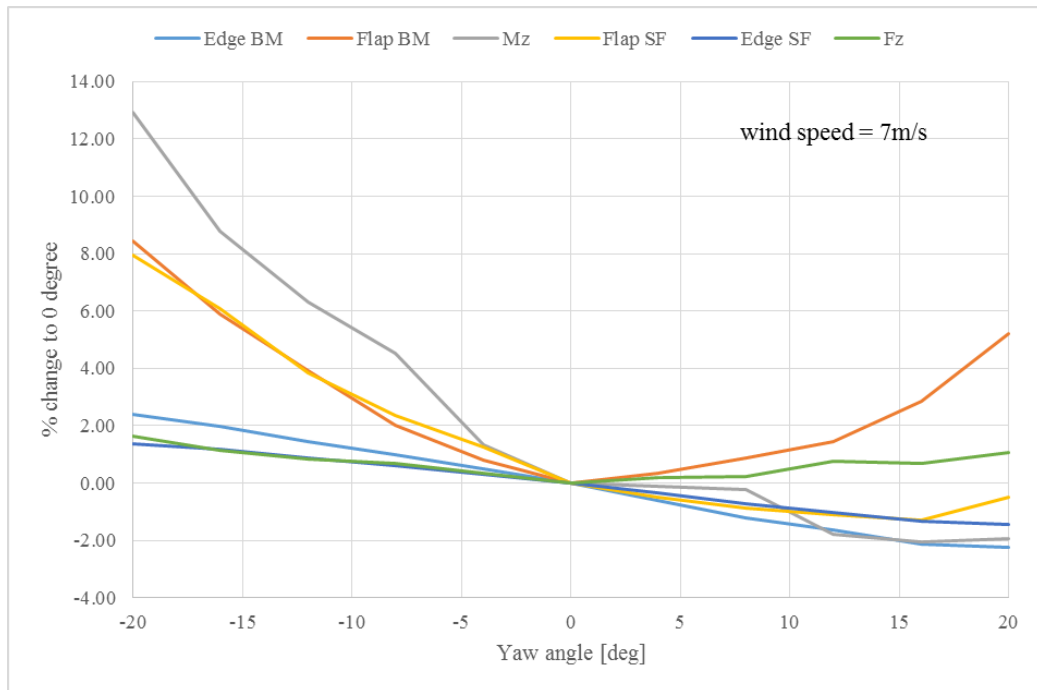


Figure 18- Variation of loads with yaw error at the blade root for wind speeds of 7 m/s, data from [28]

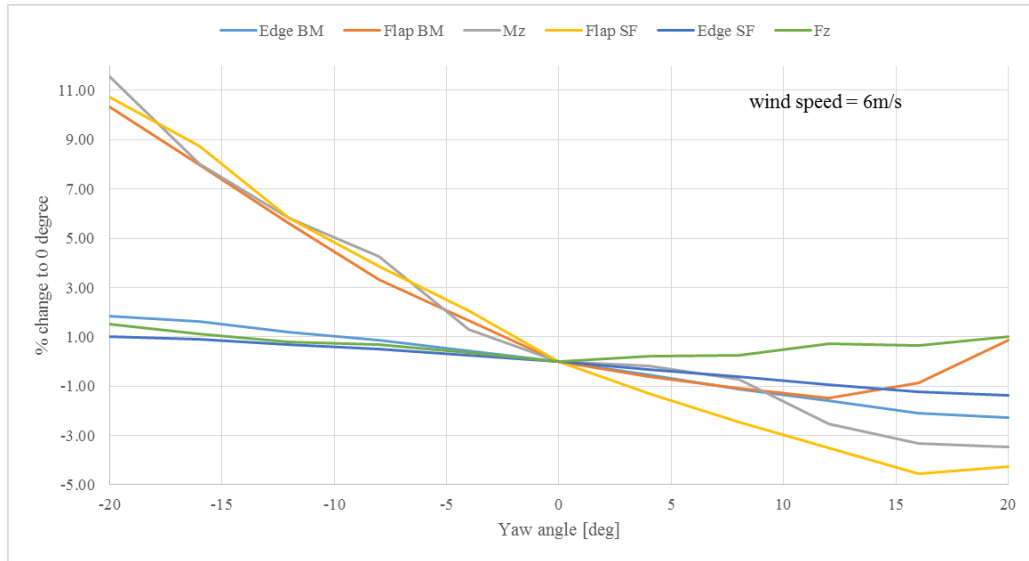


Figure 19- Variation of loads with yaw error at the blade root for wind speeds of 6 m/s, data from [28]

In all the scenarios shown in Figure 17-19, the changes in edgewise bending moment and edgewise shear force have a direct reverse relation with changes in yaw error, i.e., they decline as the yaw increases and they never reach a minimum.

The flapwise bending moment and flapwise shear force show a different behavior. They have a deflection point where the load reaches a minimum. The deflation point is different at different wind speeds. For the flapwise bending moment, the minimum occurs at 0° of yaw error for wind speeds of 7 and 8 m/s, whereas at 6 m/s it doesn't reach the minimum until a much larger yaw error.

Another important observation is the sensitivity of loads to yaw error variations. The most sensitive load is flapwise bending moment where a drop of 8% to 11% at different wind speeds is observed when yaw error changes from -20 to 0 degrees.

4.2. Stress Analysis

The six different loads shown in the previous section cause stresses at the blade root of the turbine. There are several fatigue life models that can be used to calculate the equivalent fatigue life based on the equivalent stresses. The most common model is the Basquin model [64], which is used here. The Basquin model or S-N curve is a stress based model for high cycle fatigue (number of cycles more than 10⁴) where it is expected that the material remain in the elastic region of their stress-strain curve at each cycle and all the strains are reversible. Through the use of S-N curves, the equivalent stress can be transformed to the fatigue life (number of cycles to failure). S-N curves depend on the components' material properties. Equation (27) shows the mathematical form of an S-N curve.

$$\sigma = BN_f^m \quad (27)$$

where:

σ : Equivalent stress

B : Reduction factor (depends on material properties)

N_f : Fatigue life (number of cycles to failure)

m : fatigue strength exponent (depends on material properties)

The number of cycles to failure calculated through this method corresponds to the point where 63.2% of the population have failed. Equation (27) can also be written as a ratio as shown in Equation (28) in order to compare the number of cycles to failure for cases where stress changes.

$$\frac{N_2}{N_1} = \left(\frac{\sigma_2}{\sigma_1}\right)^{m^{-1}} \quad (28)$$

The equivalent stress (σ) in Equation (28) is the stress at a specific point on a structure caused by all the loads at that particular point. In the cases where there is a dominant load, which contributes the most to the variation of stress, it can replace the stress in Equation (28). In this study, the flapwise bending moment, as discussed in the previous section, is the load that reacts the most to variations of yaw error and therefore can replace the stress. A linear relation between load and stress can be assumed here. This is similar to the approach taken by Ronold et al. [64] where they developed a fatigue failure model for turbine blades as a function of flapwise bending moment.

The blade material is glass reinforced plastic (GRP) and the value of m is - 0.01. Using the flapwise bending moments in Equation (28) in place of the stresses and assuming state 1 is zero yaw error and state 2 is any of the yaw errors from -20° to 20° with 4° steps, Table 2 can be derived by calculating the ratio for changes in fatigue life.

Table 2- Changes in fatigue life with yaw angle relative to no yaw error

Yaw Angle [deg]	8 m/s		7 m/s		6 m/s	
	N2/N1	Change (%)	N2/N1	Change (%)	N2/N1	Change (%)
-20	1.9134	91	2.2505	125	2.6737	167
-16	1.4844	48	1.7752	78	2.1523	115
-12	1.2519	25	1.4687	47	1.7259	73
-8	1.0826	8	1.2234	22	1.3863	39
-4	1.0128	1	1.0852	9	1.1772	18
0	1.0000	0	1.0000	0	1.0000	0
4	1.1151	12	1.0356	4	0.9418	-6
8	1.2755	28	1.0918	9	0.8956	-10
12	1.4640	46	1.1548	15	0.8623	-14
16	1.7526	75	1.3254	33	0.9183	-8
20	2.2359	124	1.6615	66	1.0908	9

For example, for a case where wind speed is 8 m/s (the most probable wind speed from Figure 14), for a yaw error change from 8° to 0°, the fatigue life improves 28%. The changes in fatigue life from -20° to 20° are not symmetric. For example, for the case of wind speeds of 8 m/s, for 20° yaw error changes, there is 91% improvement in the fatigue life for the negative yaw and 125% improvement for the positive yaw. Here, for the wind speed of 8 m/s, the side that shows the most variation (positive yaw errors) was considered and by curve fitting a parametric formula was developed that relates the fatigue life to the yaw error:

$$N = 0.0139(\alpha)^3 - 0.1553(\alpha)^2 + 3.7151(\alpha) + 0.0733 \quad (29)$$

The formula calculates the fatigue life when the corrected yaw is 0°. In order to use it for corrected yaw values other than 0°, a ΔN value has to be calculated where N_1 and N_2 represent the fatigue life at yaw errors before and after correction. Similar equations can be developed for other wind speeds as well.

4.3. Reliability of Blades

The reliability of the wind turbine and its sub-assemblies can be modeled using two or three parameter Weibull distribution. Equation (30) shows the probability density function (pdf) of 3-parameter Weibull distribution

$$f(t) = \frac{\beta}{\eta} \left(\frac{t-\gamma}{\eta} \right)^{\beta-1} e^{-\left(\frac{t-\gamma}{\eta} \right)^\beta} \quad (30)$$

where:

t : failure time

β : shape parameter

η : scale parameter

γ : location parameter

The location parameter refers to failure free operating time.

Spinato et al. [71] studied failure of turbine sub-assemblies for wind farms in Germany. They performed statistical analysis on field failure data of 10 years for populations in the order of 1000s of turbines and generated 2-parameter Weibull distributions for each of the turbine sub-assemblies in their populations. They investigated cases where a failure of the blade occurred and the subsequent maintenance was a blade replacement. The data provided does not specify the yaw errors, however, since the population is large (on the order of 1000s), and the data goes back as far as 1994 where LIDAR yaw correction was not common, it is assumed that the yaw error was around the 7° average that is shown in Figure 6 of Chapter 1. The result of their analysis for blades is a scale parameter $\eta=10.323$ years and shape parameter of $\beta=1.042$. In a Weibull distribution, the scale parameter represent 63.2% unreliability, which is the same concept as the number of cycle to failure from S-N curve. By using Equation (3429), for a 7° to 1° yaw improvement, the reliability of blades improves 19.8%. The subsequent improved Weibull scale parameter will be 12.366 years. These parameters (shape and the new scale) form a new Weibull distribution, which represent the time to failure of blades in the case where the yaw error is 1° . Figure 20 shows the Weibull distribution for blade time to failure before and after the yaw error correction for a total support time of 20 years.

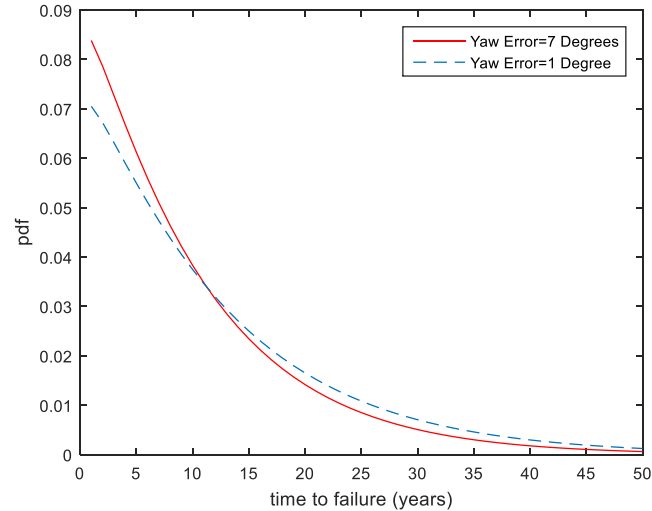


Figure 20- Weibull distribution for blades failure before and after yaw error correction

The new shape parameter, which represents a different distribution of failure times then can be used in the ROI model. By using Equation (2929), the shape parameter can be adjusted based on the yaw error that the turbine is experiencing.

4.4. Discussion

It is important to point out the simplifying assumptions of this analysis and what could be done in the future to improve it. Starting from the load analysis, the loads were only calculated at three wind speeds and a range of yaw errors with 4° increments. The load calculations could be done at wider range of wind speeds and at yaw errors with smaller increments for example, e.g., every 1°.

The stress analysis performed is simplified. The assumptions here is that only one load affects the stress (flapwise bending moment), and this load has a linear relation with stress. Therefore, the ratio of load changes for different yaw errors is the same for stress too and it can replace the stress term in Equation (28). A more

complex stress model where several loads are considered at the same time could result in a more accurate analysis.

Equation (29) is only generated for wind speeds of 8 m/s and in the application of these analysis in the NPV model, this equation is used for different yaw errors at all times. However, in reality the fatigue life is a function of both the yaw error and wind speeds. An more detailed version of Equation (29) would have terms that incorporate the effects of both yaw error and wind speed.

The implementation of the current version of Equation (29) in the NPV model is challenging, since the yaw error of the turbine changes over time and Equation (29) assumes a constant yaw error. At this point in the NPV model, an average of yaw error over a period of time is assumed as the input in Equation (29) to predict the next failure time. However, a damage accumulation model such as Miner's rule is needed to calculate the incremental damage on the blades at each yaw error over time (and possibly each yaw error and wind speed) to calculate a more accurate fatigue life.

It is important to note that wind turbines' design and the material used in turbines depend on the location of the wind farm. Wind turbine manufacturers tweak their designs based on the environmental requirements of the site so no matter what design is chosen in the analysis and how accurate it is, the answers only represent a particular site and particular turbine. On the other hand, using the results of the analysis on the field failure reliability distributions is challenging. There is no information about the yaw error of the turbines in the reported data. The reports usually represent a turbine population in a whole nation, which means various locations (different working environments), different turbine manufacturers and

designs, different turbine capacities and different turbine ages. Most of this information is also not reported². As a result, there is a limit to the accuracy of the conversion of the reliability parameters (that are calculated based on field failure data) based on variations of yaw error. The level of uncertainty in the reliability conversion is a topic that could be investigated in the future work.

Finally, it is necessary to point out that this analysis was only done for turbine blades. There are other sub-assemblies that are affected by the yaw error such as the drive train, main shaft, hydraulic systems, pitch control, yaw system and the turbine's tower, which need their own analyses.

² The databases that provide the field failure data along with the literature that analyzed these data are discussed in Appendix I.

Chapter 5: Modeling Results

The model requirements described in the previous chapters are designed to optimize the utilization of LIDAR devices for yaw error correction applications. The metric to optimize, as described in Chapter 2, is the change in NPV before and after adding LIDAR systems to the wind farm, i.e., Δ NPV. Details of the model development as well as its verification and validation can be found in Appendix II.

To reiterate the problem at hand, LIDAR devices improve the efficiency of wind turbines while lowering their O&M costs. However, LIDAR systems are expensive and therefore there is a cost trade-off in using them for yaw error correction applications. In practice, there are one or more LIDAR systems circulating between wind turbines in a farm.

The process of yaw controller calibration and the behavior of yaw error after LIDAR is moved to another turbine was explained in Chapter 1. Finding the LIDAR stay time on each turbine, as well as the number of LIDAR devices in a wind farm that yield the maximum returns for the wind farm owners is the goal of this chapter.

In this chapter, first the model assumptions are discussed, then the results will be shown and lastly a sensitivity analysis will be performed to show how sensitive the results are to the most important input assumptions.

5.1. Model Assumptions

For the base model, a wind farm with generic 4 MW wind turbines is considered. The number of turbines in the wind farm is a variable but all the turbines

are identical. Figure 21 shows the power curve of this wind turbine. Turbine rotor diameter is assumed to be 125 m and the hub height is 137 m.

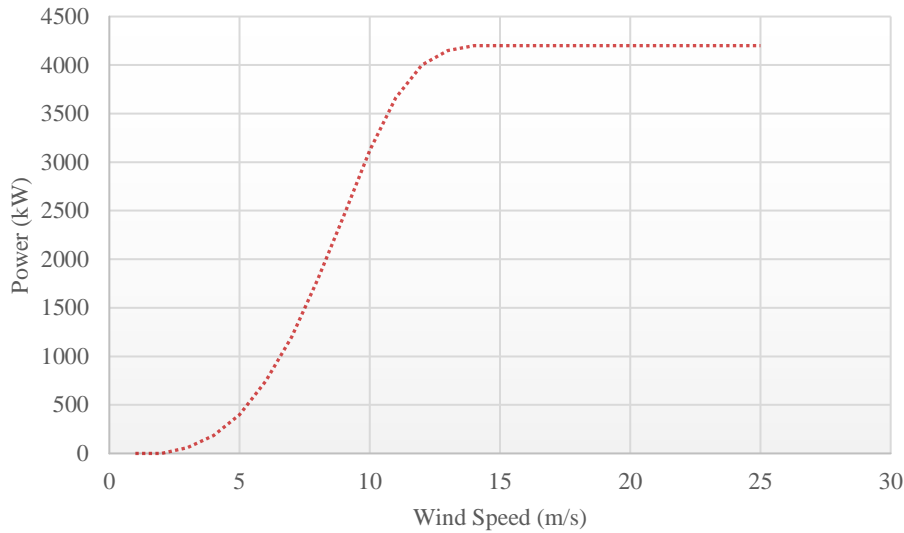


Figure 21- Power curve of a generic 4 MW turbine.

To model the maintenance of the wind turbines, the focus will be on four primary components that are affected by the presence of the yaw error: blades, generator, gearbox and the pitch control system.

Several studies discuss the reliability of wind turbine components using field failure data. These studies along with the databases that provide the failure data are thoroughly discussed in Appendix II. In this dissertation, the results from Spinato et al. [71] are used where they provide 2-parameter Weibull time-to-failure distribution information for the four components under consideration here. There is no information provided about the yaw error on [71] or any other study discussed in Appendix I. Here, it is assumed that these values correspond to the average yaw error value observed in the field (mean of Figure 6 from Chapter 1). The Weibull distributions are used to generate the time-to-failure values for each of the

components. The parameters of the distributions are given in Table 3. Table 3 also includes the expected downtime for maintenance events associated with the component.

Table 3- Maintenance parameters for the case study

Component	Scale Parameter (years) [71]	Shape Parameter [71]	Downtime (days) [72]
Blade	10.32	1.04	7
Generator	27.43	1.2	3
Gearbox	45.72	1.83	5
Pitch Control	4.72	1.57	2

The maintenance strategy is assumed to be a combination of corrective and predictive maintenance where condition monitoring systems are actively monitoring the operation of wind turbines and alert the operators when there is an anomaly. Upon receiving an alert, the plant manager will deploy a maintenance crew to perform the necessary maintenance action. It is assumed that replacement parts (spares) are as good as new. Each maintenance event leads to a downtime of the turbine. The downtime assumed for each component is shown in Table 3.

The effects of yaw error on the reliability of these components are assumed to follow Equation 29 developed for blades in Chapter 4. In this model, the first time to failure (TTF) is generated based on the yaw error that the turbine has for the 1st year of operation. After the replacement, the new TTF is calculated based on the average yaw error of the turbine for the 1st year after the maintenance event. The yaw errors are dependent on the presence of LIDAR-based correction. The scale parameters of the components will be updated to reflect the reliability improvements due to yaw error correction (as explained in Chapter 4).

Maintenance costs consist of the replacement component costs, transportation, labor, installation, etc., which are combined together for each maintenance event of a component. These costs remain the same over the support time of the turbine. The costs of components are calculated using a cost model developed by U.S. National Renewable Energy Lab [73], which is dependent on the size of turbine and whether it is onshore or offshore

For revenue generation, the energy production model used is based on the discussion in Chapter 3. Buoy data at height of 10 m are used [68]. The data are converted to the turbine's hub height using a shear factor of 1.4. Then the wind speeds are used in the turbine's power curve (Figure 21) to calculate the power. Turbine's power curve equations (in kW) are shown in Equations 31-35 as a function of wind speed in (m/s).

$$P = \begin{cases} 0 & v < 3 \\ P(v) & 3 < v < 14 \\ 4200 & 14 < v < 25 \\ 0 & 25 < v \end{cases} \quad \begin{matrix} (31) \\ (32) \\ (33) \\ (34) \end{matrix}$$

$$P(v) = -8.3895v^3 + 213.53v^2 - 1187.8v + 1988.3 \quad (35)$$

The total energy production for the year is calculated assuming there is no downtime, then the downtime of the systems, which were calculated from the O&M section are deducted from the revenue. Once the amount of generated energy is defined, by using an energy sales price of \$0.144/kWh, the revenue generation of the wind farm will be calculated. The value of energy sales price is assumed to be constant throughout the life of the wind farm.

The LIDAR devices used in this study are expected to last 10 years. After this period, a new set of LIDAR devices must be purchased. The LIDAR price is assumed to be \$120,000. It is expected that LIDAR devices have to go through maintenance every two years, with the cost of approximately \$12,000 per event. LIDAR cost information was obtained through communication with Avent LIDAR Technologies [74]. It is expected that installation and uninstallation of LIDAR take one day each, during which the turbine is not generating energy. These downtimes and their corresponding energy loss due to LIDAR circulation are considered in the model as well. In order to install/uninstall a LIDAR device, two maintenance personnel are required. Each event takes about 8 hours. The costs of purchasing LIDAR, maintaining it and circulating it makes up the LIDAR cash flow, which is the investment costs in this work.

All the cash flows generated in the model (performance, O&M and investment) will then be discounted using a discount rate value of 7%/year. Table 4 summarizes the model cost assumptions.

Table 4-Cost Assumptions

Model Input	Value	Unit
Discount Rate	7%	per year
Energy Price	0.144	\$/kWh
LIDAR Price	120,000	\$/unit
LIDAR Maintenance	12,000	\$/unit-event
Turbine Downtime Due to LIDAR Circulation	1	day (Installation/Uninstallation)
Transportation Cost	2000-5000	\$/day
Number of Personnel Required	2-10	per event
Number of Hours	6-12	per day-personnel
Number of Days	1-4	per event
Hourly Wages	100	\$/hour
Yaw Error Regression Profile	2	years

5.2. The Optimization Problem

Depending on the number of turbines in a wind farm, there may be a need for one or several LIDAR devices. If there is only a single LIDAR for a large farm, it may take a long time for the LIDAR device to arrive at a wind turbine that is operating with a large yaw error value (i.e., other turbines with larger yaw error values are visited by the LIDAR sooner). At the same time, having too many LIDAR devices in a wind farm, may result in idling a significant investment in LIDAR devices. The LIDAR stay time on a turbine is variable as well. The stay time can depend on how much data is required for yaw error correction, and applications of LIDAR other than yaw error correction (discussed in Section 1.5). Therefore, depending on the number of turbines in the wind farm and the turbine size, there is an optimal number of LIDAR devices with an optimal stay time. Figure 22 shows the methodology flowchart for the case study. In this process, ΔNPV is calculated as a function of LIDAR stay time, number of LIDAR devices and number of turbines. In the first step, number of LIDAR devices (NL) and number of wind turbines (NT) are assumed to be constant, then optimum stay time (ST) is calculated through a grid search optimization. Once the optimum stay time is found, NL becomes a variable and for each case, the optimum ST will be calculated. In the last step, NT becomes a variable and all the optimum NL and ST values will be calculated.

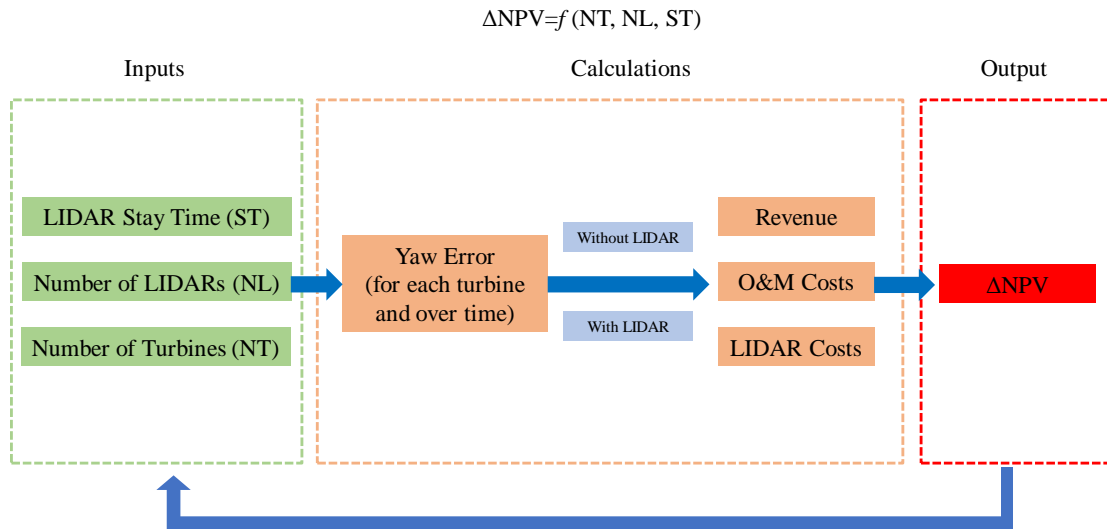


Figure 22- Flowchart of the methodology used in the case study

5.3. Analysis Results

In the case presented in this section, the number of turbines in the wind farm can vary from 20 to 100. One or multiple LIDAR devices will be used in this farm, circulating between turbines. For example, Figure 23 shows the changes of NPV for one example scenario where the wind farm has 50 turbines and there are 4 LIDAR devices circulating between them with the stay time of a LIDAR device on a turbine set at 8 weeks. This case has a positive ΔNPV meaning that it is potentially a good investment for the wind farm owners. In this particular case, the mean increase in the NPV of the wind farm is approximately \$6.5 million over the wind farm's 20 years operation.

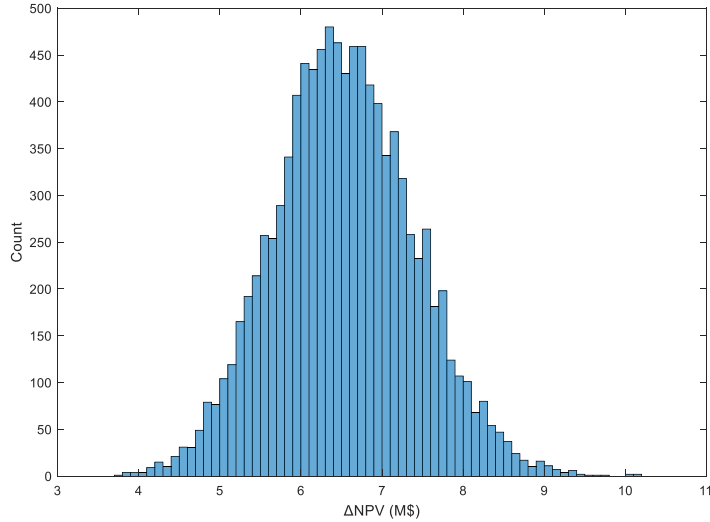


Figure 23- Turbines (4 MW), 4 LIDARs and 8 Weeks of stay time (20 year wind farm life)

Next, the stay time of LIDAR devices on the turbines are varied. This will allow us to understand how long a LIDAR should stay on a turbine to maximize the returns for a particular number of LIDAR devices in the wind farm. Figure 24 shows the results for the case of 50 turbines and 4 LIDAR devices in the farm. The solid point is the mean of all the Monte Carlo runs for each scenario. For the remainder of this section, wherever the ΔNPV is mentioned, it is referring to the mean of Monte Carlo runs.

From Figure 24 it can be seen that for a wind farm that has 50 turbines (4 MW) for which the owners decided to purchase 4 LIDAR devices, an 8-week stay time is optimal – this is the case shown in Figure 23). However, for example, if the LIDAR devices are circulated quickly between the turbines (e.g., every 2 weeks), the costs of using LIDAR will overcome the benefits and result in a net loss (a negative ΔNPV).

The process of finding the optimal stay time can be repeated for different numbers of LIDAR devices in the farm to calculate the optimum stay time for each case (an 8-week stay time was optimal only for the case of 4 LIDAR devices in the farm, what if there were more or less LIDAR devices?). By doing so, it makes it possible to determine the combination of LIDAR devices and stay time that yield the maximum returns for the wind farm.

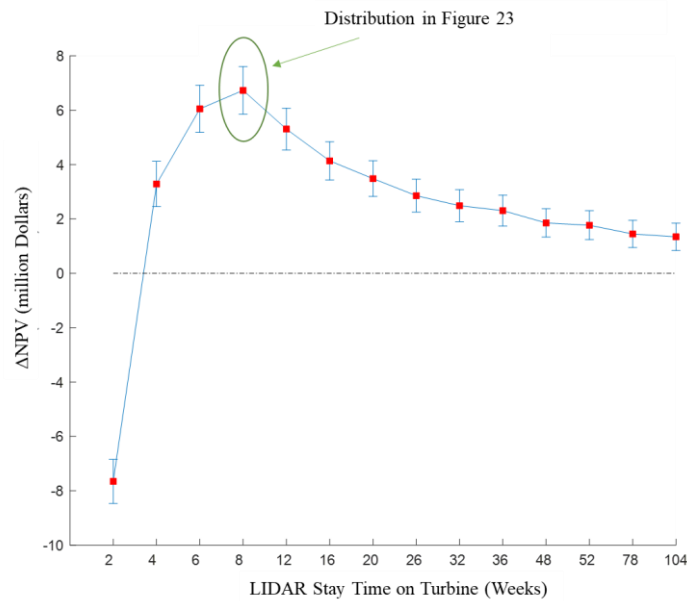


Figure 24- 50 Turbines, 4 LIDAR devices and variable stay times

Plots similar to Figure 24 can be generated for various number of LIDAR devices in the wind farm with 50 turbines, then the maximum value of each of these analyses can be put on a single plot. Figure 25 shows an example of such plot for the 50-turbine wind farm where ΔNPV is maximized for each case.

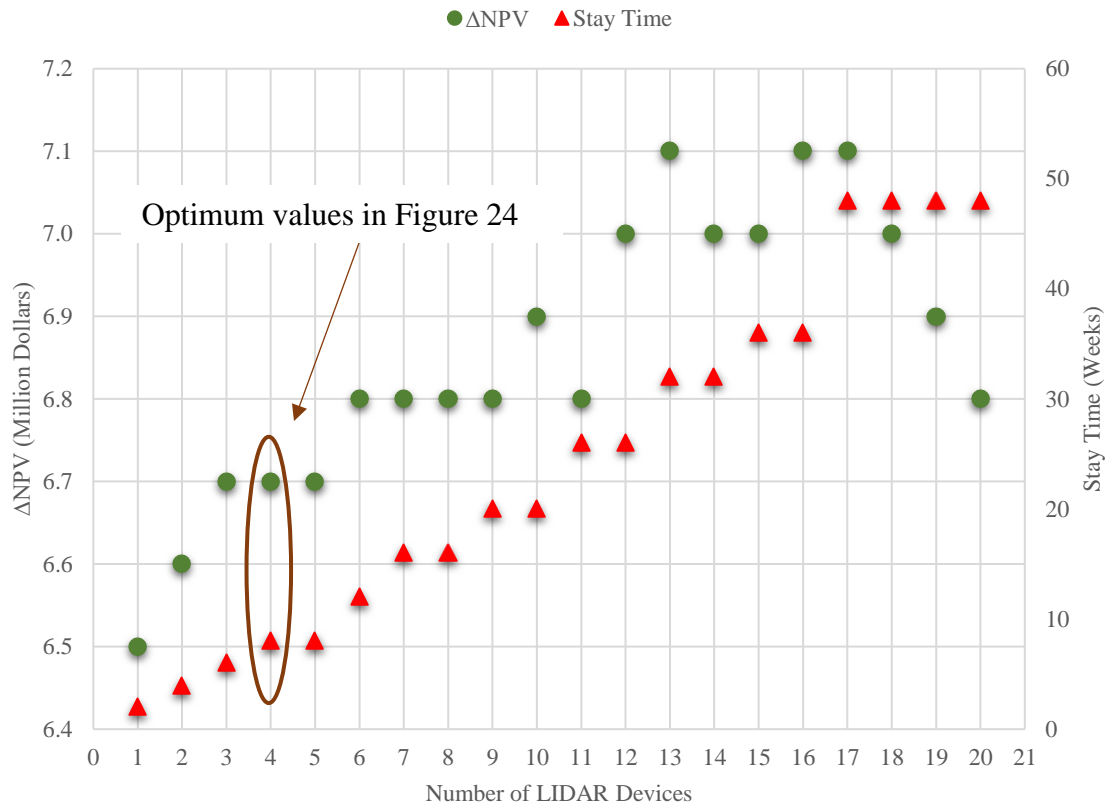


Figure 25- Number of LIDAR devices and their corresponding optimal stay times for a wind farm with 50 turbines of 4 MW size. These are the cases where ΔNPV is maximized

An observation from Figure 25 is that as the number of LIDAR devices in the farm increases, it is better to circulate them between the wind turbines less frequently (i.e., longer stay times). This observation seems obvious, but there are several factors associated with this trade-off. Firstly, with less circulation, the costs of circulating the LIDAR devices decrease. There is downtime associated with each installation/uninstallation of a LIDAR device on a turbine, during which the turbine does not produce any energy, therefore less circulation is better. Alternatively, less frequent circulation may result in turbines that operate at larger values of yaw error. Since there are more LIDAR devices in the wind farm servicing the wind turbines,

the chances of having more turbines with large yaw error values decreases. The peak happens where these costs and benefits are balanced. After the peak, the benefits of having more LIDAR devices in the farm decrease.

Another observation from Figure 25 is the presence of multiple optimum points. For example, in this case, 13, 16 and 17 LIDAR devices all have the same value of return (ΔNPV) while the optimum stay times in all of these cases are different. This is because the cost trade-off balance is not a unique point and under several scenarios with different stay times, the benefits of LIDAR devices can pay for the costs.

In Figure 26, the number of turbines in a wind farm are varied to determine the optimum number of LIDAR devices with their associated stay time. In order to construct Figure 26, the number of LIDAR devices for each farm size case that maximizes the return is chosen. Also, in cases where optimum returns were not limited to a single scenario, the second and third scenarios are plotted as well (if they existed). By using this plot, farm owners and operators could determine how many LIDAR devices they would need for their wind farm and the optimal way to circulate the LIDAR devices between the turbines.

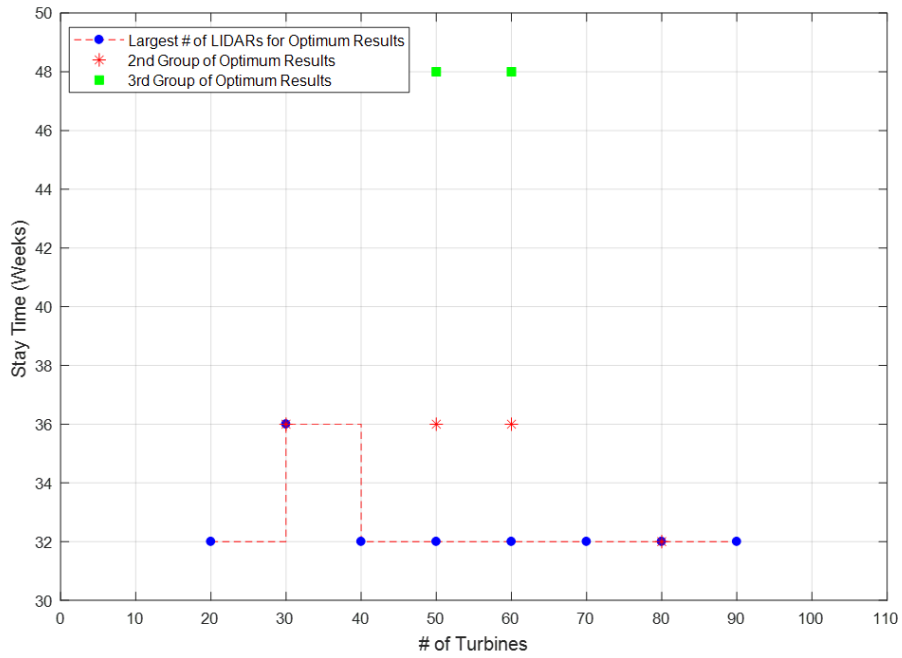
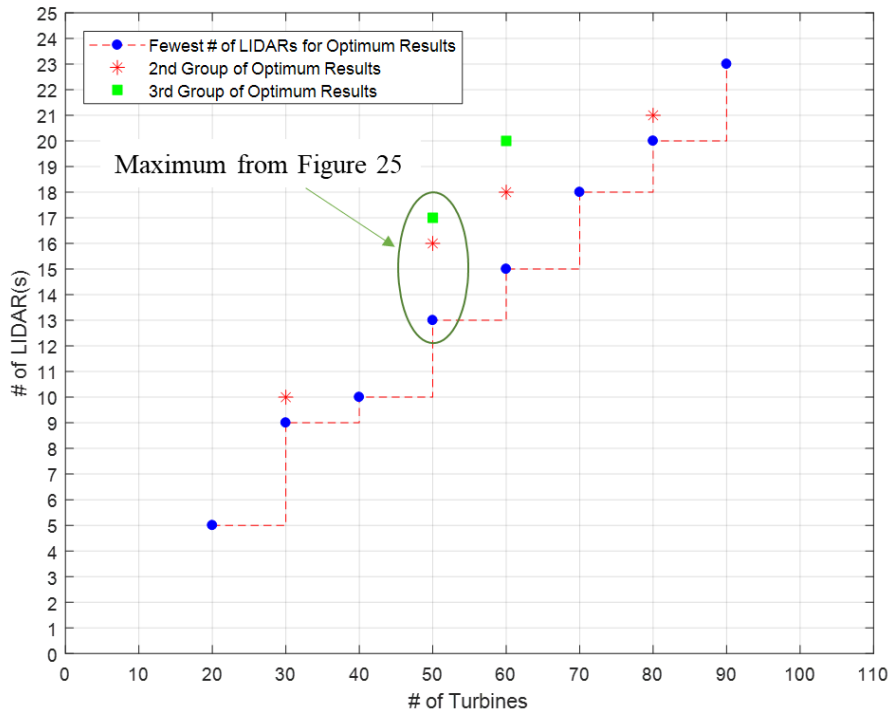


Figure 26- Optimum number of LIDARs for various turbine numbers

To explore the dependence of the results on the assumptions made in the model, a sensitivity analysis was performed to explore how the optimal cases discussed in the previous section change.

5.4. Sensitivity Analysis

5.4.1. Cost of LIDAR Devices

With the advancement of LIDAR technology, it is expected that the price of LIDAR devices could drop substantially in the future. In Figure 27, it is assumed that the cost of LIDAR is \$20,000/unit instead of \$120,000/unit, with maintenance costs of LIDAR lowered proportionally. In Figure 27 the process used to develop Figure 25 is repeated to show how the results change. For all but one case (5 LIDAR devices), the stay time for \$120K LIDAR and \$20K LIDAR are the same.

It can be seen that as the cost of LIDAR is reduced, there is a tendency to deploy more LIDAR devices in the wind farm. At the same time, the returns are higher for a less expensive LIDAR. However, the stay time for the LIDAR does not change. A possible explanation for the behavior of the stay time is that it's the time required to keep the yaw error as low as possible as a function of the LIDAR devices circulating in the wind farm. Similar behavior is observed in the next two cases where the energy price and discount rate are varied.

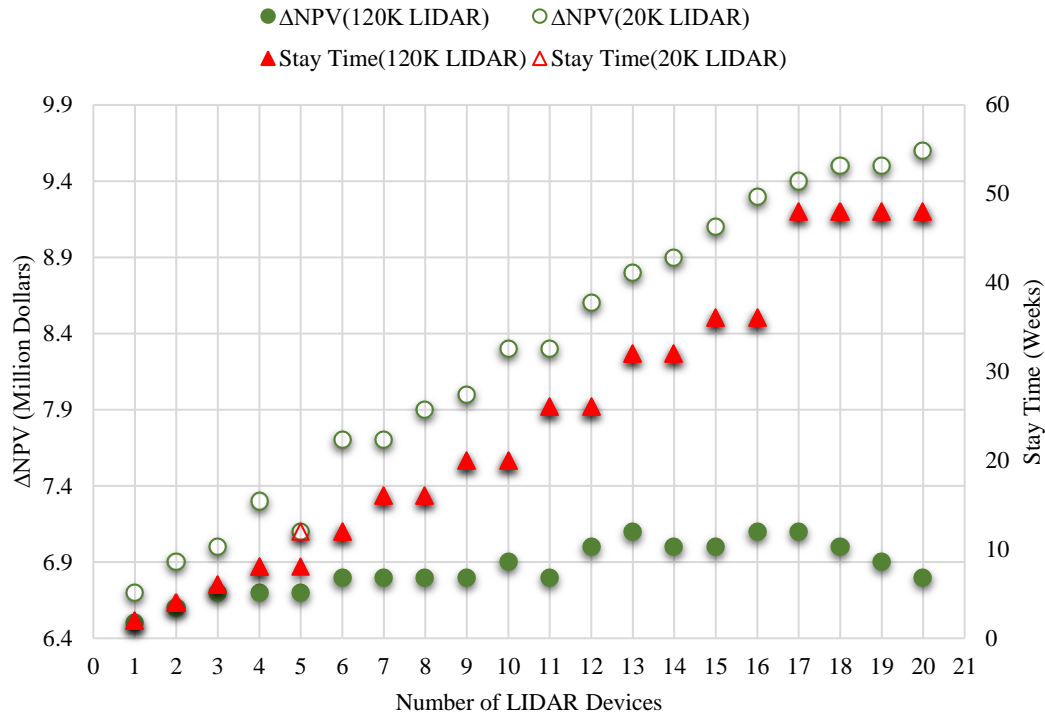


Figure 27- Number of LIDAR devices and their corresponding optimal stay times for a wind farm with 50 turbines of 4MW size where Δ NPV is maximized with LIDAR price lowered to \$20,000

5.4.2. Energy Purchase Price

In the case study, an energy purchase price of \$0.144/kWh was assumed. In this section the outcome of the model for a case where the energy purchase price is reduced to \$0.07/kWh is investigated. Results for a 50-turbine wind farm with 4 LIDAR devices are shown in Figure 28 along with the results for the original assumptions.

It is interesting to see that similar to the previous case in Figure 27, the optimal stay times remained the same. However, as expected the NPV change is less since the wind farm generates less revenue. This also results in having fewer LIDAR devices for optimal cases. One conclusion of these observations is that the model

recommends to the farm owner that they should purchase fewer LIDAR devices and circulate them quicker between the turbines. This is because the owner cannot afford to have their turbines running with large yaw errors for long periods of time when energy prices are low.

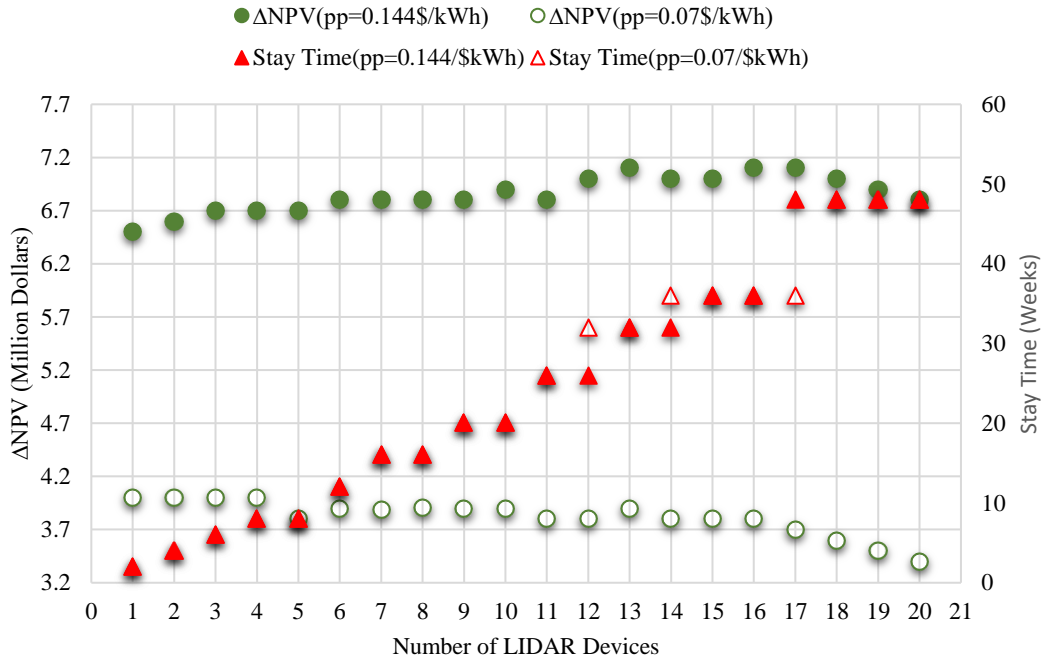


Figure 28- Number of LIDAR devices and their corresponding stay times for a wind farm with 50 turbines of 4MW size where returns are maximized with energy purchase price lowered by 50% to \$0.07/kWh

5.4.3. Discount Rate

The discount rate of wind projects depends on several factors such as interest rates at the time of financing, the risk of wind projects, etc. The assumed 7%/year discount rate in this study is an acceptable average value for wind projects in 2019 [75].

In this case the model is run for a discount rate of 0. The results (Figure 29) did not show a significantly different pattern. The optimums at 16 and 17 LIDAR

devices that were observed in Figure 25 are preserved. However, the optimum at 13 LIDAR devices did not repeat in this case. The values of ΔNPV increased although the pattern remained very similar. This is not a surprising outcome since the cash flow is spread relatively evenly throughout the 20 years of farm life. Therefore, it was expected for the results to ‘shift’ the ΔNPV without changing ‘shape’.

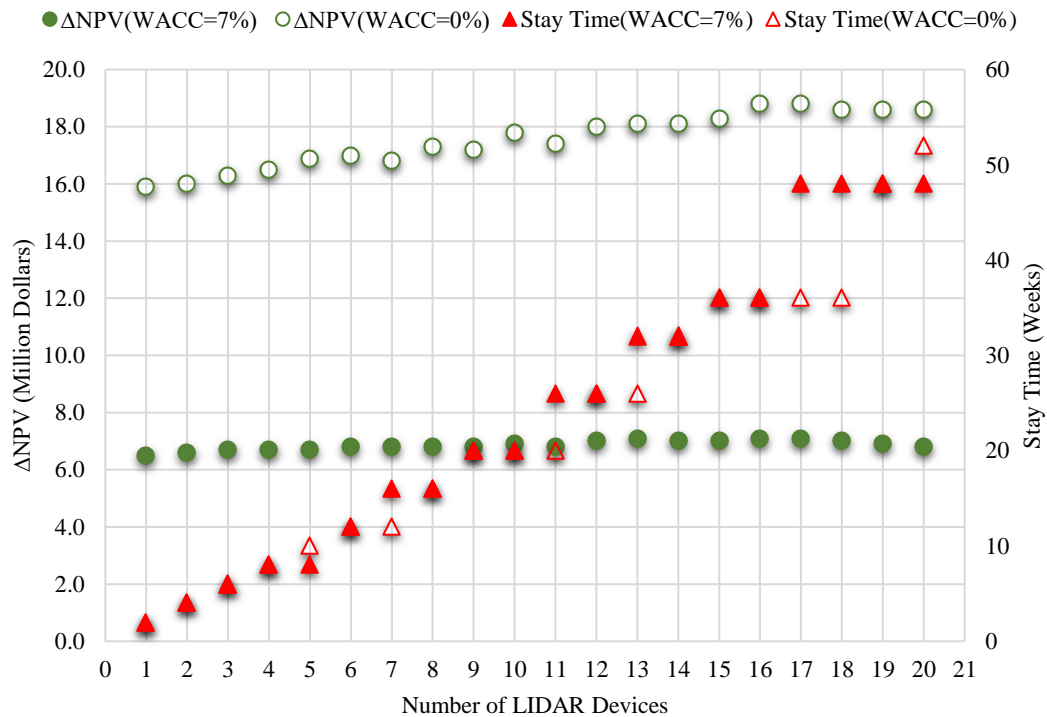


Figure 29- Number of LIDAR devices and their corresponding stay times for a wind farm with 50 turbines of 4MW size where returns are maximized with WACC assumed to be 0%

5.4.4. Yaw Error Regression Profile

Earlier in the case study, it was mentioned that the behavior of yaw error once the LIDAR is removed from a wind turbine is not clear. It is possible that yaw error stays at its minimum values for a period of time and then starts regressing back to uncorrected values.

The assumption in the original analysis was to have a 2-year regression period with no minimized time as shown in Figure 7. In Figure 30, it is assumed that the regression period is 1 year.

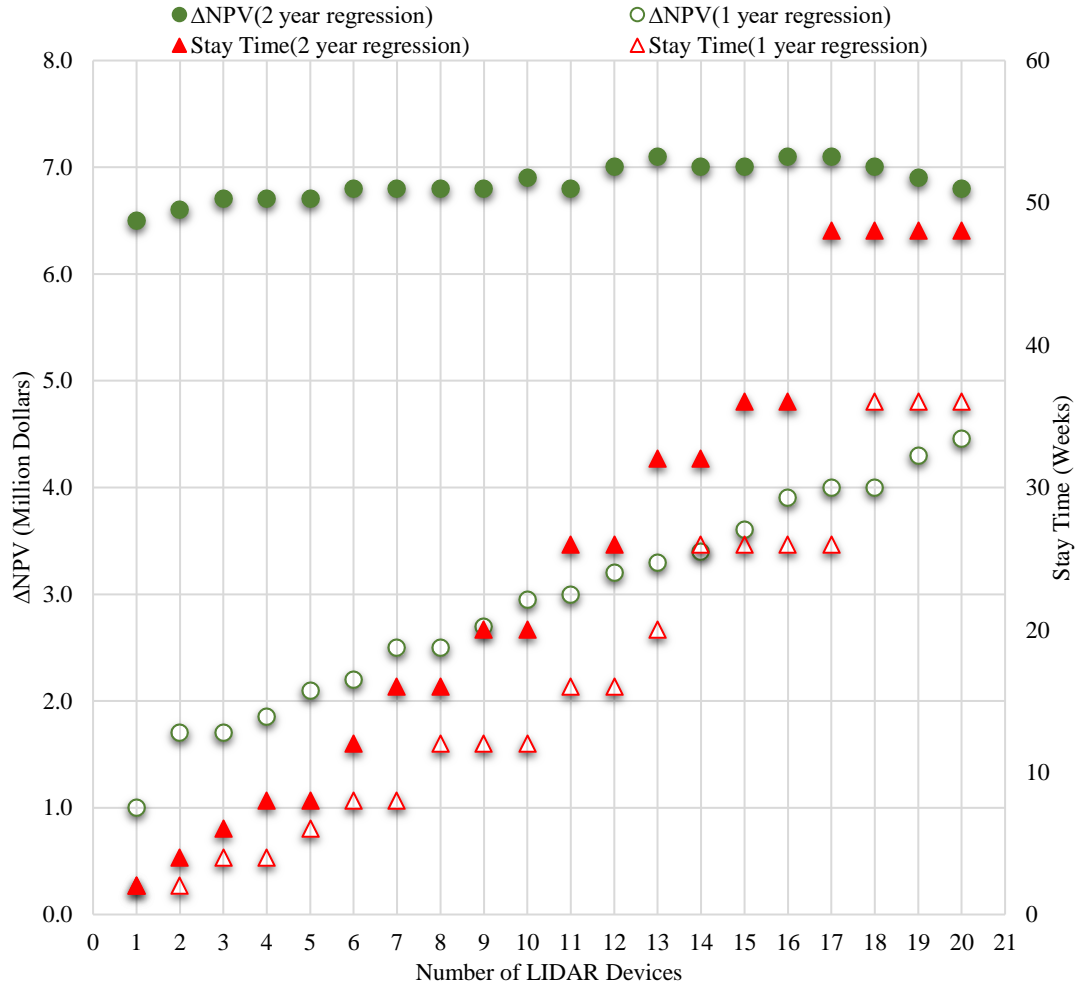


Figure 30- Number of LIDAR devices and their corresponding stay times for a wind farm with 50 turbines of 4 MW size where returns are maximized with yaw error regression profiles of 1 and 2 years

The returns for 1-year regression time are much lower than the 2-year regression time, due to the fact that the yaw error reaches uncorrected values more quickly after the LIDAR departs. Therefore, as it can be seen, the stay time values for 1-year regression are shorter than 2-year cases because LIDAR devices have to be

circulated quicker and correct the yaw error. However, quicker circulation means more circulation costs and more downtime due to installing and uninstalling LIDAR. When the turbines regress more quickly the wind farm requires more LIDAR devices to combat the yaw error problem, which increases the investment costs for LIDAR and lowers the returns. These results are a good way to understand the outcome of other studies such as [18]–[22] discussed earlier where the focus is on optimizing the yaw error control algorithm. A 2-year yaw error regression means the yaw error control algorithm operates better and loses its calibration more slowly.

5.4.5. Turbine Size

Lastly, the effects of turbine size on the results is investigated to see how the optimum values change for 6 MW turbines. In this case, the energy production of the turbines is larger (and so are the maintenance costs since the model scales the costs). The results are shown in Figure 31.

As expected, the returns are substantially larger for 6 MW turbine considering the extra revenue generation and larger cost avoidances for this turbine size.

The optimum number of LIDAR devices in this case is the same as the 4 MW turbine size with both being 13 LIDAR devices. The stay time for the optimum number of LIDAR devices is slightly longer than the 4 MW (36 weeks here versus 32 weeks for 4 MW). Overall, for 6 MW turbine, it is better to keep the LIDAR longer on the turbines. The 4 MW turbine had multiple peaks at 13, 16 and 17 LIDARs with the same returns while there is only two scenarios here at 13 and 14 LIDAR devices.

For 4 MW turbines the returns started dropping after 17 LIDAR devices while the drop starts after 14 LIDAR devices for the 6 MW turbine size.

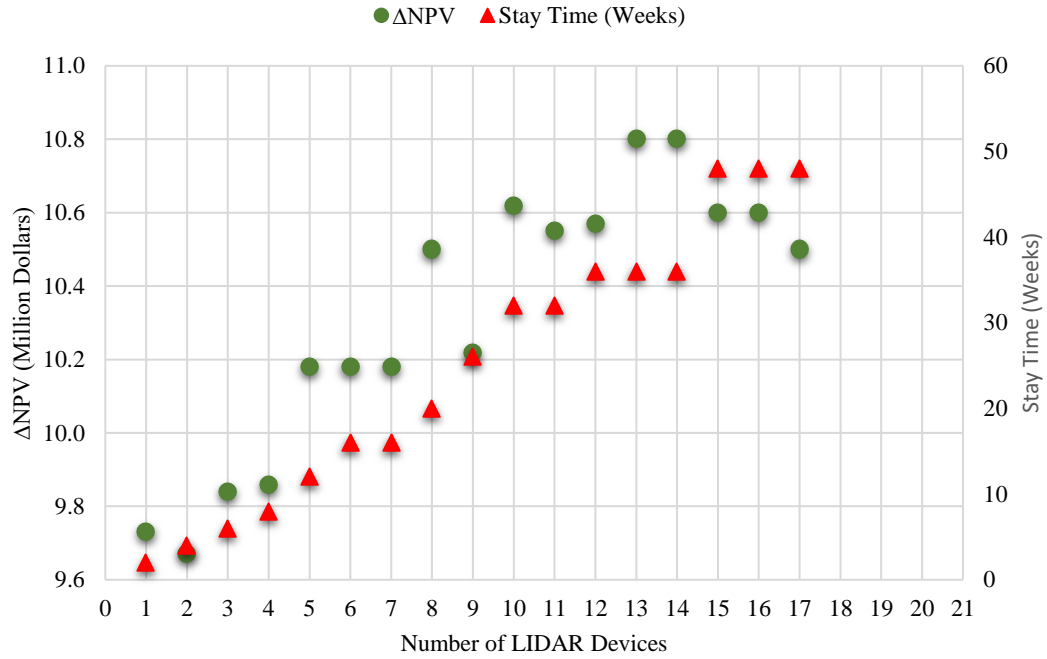


Figure 31- Number of LIDAR devices and their corresponding optimal stay times for a wind farm with 50 turbines of 6 MW size. These are the cases where ΔNPV is maximized

Chapter 6: Conclusions

This dissertation addresses a significant issue in the wind industry - how to best use LIDAR to correct yaw error. Optimizing the use of LIDAR will help to lower the cost of wind energy.

There are several significant uncertainties associated with the model developed in this dissertation, the foremost of which is the behavior of yaw error once the LIDAR device is removed from a wind turbine. Currently, there is no quantitative model of what happens once the LIDAR is removed from a turbine. In this dissertation, after consulting with Avent LIDAR Technologies, a reasonable scenario of what may happen was developed. Then, by performing a sensitivity analysis, an investigation how the model outcome could change was presented. The results show that a 2-year regression time for yaw error will yield significantly more benefits for wind farm owners than a 1-year regression time. Therefore, it would be beneficial to focus on methods that optimize the yaw calculation algorithms in the turbine controller in order to slow down the regression period of yaw error.

While many parameters that impact the optimal use of LIDAR on wind turbines have been considered in this dissertation, some factors have not been treated. For example, wake effects are not considered in the model. Under real wind farm conditions, wake effect have an impact on the energy generation of wind turbines. This model did not make any assumption about the wind farm layout and consequently the wake effect between the turbines. However, in a case where there are downstream turbines, under identical timeline conditions, the wake on the

downstream turbines are a function of the same wind speed for both cases with and without LIDAR. But, the alignment of the turbines with wind flow may affect the direction of the wake. Further analysis of these changes are out of the scope of the current work and can be explored in the future work. Note, there's been research on using yaw error to steer the wake from the turbines in the downstream, hence reducing the wake effect [76]. However, there is also discussion that the presence of yaw error and wake at the same time, together reduces the overall performance of the wind farm [77]. At the time of writing this dissertation, this topic is in early stages and there is significant potential for further work.

In this dissertation, the focus was on one of the applications of LIDAR to correct yaw error. However, farm owners and operators use LIDAR for other applications as well such as measuring the power curve of turbines and energy production as well as calculating structural loads and for collective pitch control purposes. These applications (and the value derived from them) are out of the scope of this work however, they may play a role in the decision making process of wind farm owners. Specifically, the stay time of a LIDAR on a turbine could be longer if the operators decide to collect additional data.

There are several aspects of this work that can be improved. The relationship between yaw error and reliability can be investigated further by performing a finite element analysis on the turbine blades. Subsequently, the model would become a function of yaw error and wind speed. This can be expanded to other components in wind turbine that are affected by yaw error such as the gearbox and yaw mechanism.

In this dissertation, energy purchase price was assumed to be a fixed value over time, however this is not generally the case in practice. Today, industry is using complex power purchase agreements where price of energy could be a function of date, time and grid load. There are also penalties imposed on wind farms in cases where minimum required production levels are missed.

Overall, there is been an uptick in wind industry's interest in LIDAR devices and by providing a model with which wind farm owners can maximize their returns, LIDAR devices could become more mainstream. At the same time, advancements in LIDAR technology and the economics of scale will lower the price of LIDAR and enable the more widespread use of the technology, which could make LIDAR standard equipment in every wind farm. Another application of LIDAR, which is collective pitch control to reduce structural loads, requires permanent integration of a LIDAR on a wind turbine. This application may result in lower LIDAR prices (economics of scale) while at the same time avoiding the cost and logistics overhead of LIDAR circulation.

6.1. Dissertation Contributions

- Development of a parallel dependent Monte Carlo methodology satisfying identical timeline conditions for modeling stochastically-determined discrete time-based events.
- Development of a net present value model-based approach applicable to the insertion of new technologies in sustainment-dominated systems.

- The first known optimization of the utilization of LIDAR devices in wind farms (i.e., determination of the optimum number of LIDAR devices and their stay times).

6.2. Publications to Date

1. R. Bakhshi, P. Sandborn, ‘*Maximizing the Returns of LIDAR Systems in Wind Farms for Yaw Error Correction Applications*’, Wind Energy, 2019, Under Review
2. R. Bakhshi, P. Sandborn, ‘*A Return on Investment Model for the Implementation of New Technologies on Wind Turbines*’, IEEE Transactions on Sustainable Energy, Vol. 9, No. 1, pp. 284-292, 2017
3. R. Bakhshi, P. Sandborn, ‘*Optimizing the Use of LIDAR in Wind Farms: Minimizing Life-Cycle Cost Impact of Yaw Error*’, IOP Science Journal of Physics: Conference Series, Proceedings of the North American Wind Energy Academy (NAWEA) 2019, Amherst, MA, 2019
4. R. Bakhshi, P. Sandborn, E. Lillie, “*Assessing the Value of Corrosion Mitigation Using Cost-Based FMEA*,” to be published Corrosion Processes: Sensing, Monitoring, Data Analytics, Prevention/Protection, Diagnosis/Prognosis and Maintenance Strategies, G. Vachtsevanos, Springer, 2019
5. R. Bakhshi, P. Sandborn, ‘*Using LIDAR on Wind Turbines for Yaw Error Correction: A Financial Prospective*’, Proceedings of 2018 ASME Power conference, Orlando, FL, 2018
6. R. Bakhshi, P. Sandborn, ‘*Overview of Wind Turbine Field Failure Databases: A Discussion of the Requirements for an Analysis*’, Proceedings of 2018 ASME Power conference, Orlando, FL, 2018
7. R. Bakhshi, P. Sandborn, ‘*Analysis of Wind Turbine Capacity Factor Improvement by Correcting Yaw Error Using LIDAR*’, Proceedings of ASME 2017 International Mechanical Engineering Congress and Exposition, Tampa, FL, 2017
8. R. Bakhshi, P. Sandborn, ‘*The Effect of Yaw Error on Reliability of Wind Turbine Blades*’ Proceedings of ASME Power and Energy Conference, North Carolina, June 2016
9. R. Bakhshi, P. Sandborn, ‘*Return on Investment Modeling of Offshore Wind Farm O&M to Support Strategic Technology Insertion*’ Proceedings of AWEA Offshore 2015, Maryland, September 2015
10. R. Bakhshi, P. Sandborn, X. Lei, A. Kashani, ‘*Return on Investment Modeling to Support Cost Avoidance Business Cases for Wind Farm O&M*’ Proceedings of EWEA Offshore, Denmark, March 2015
11. P. Sandborn, C. Wilkinson, K.L. Sharon, T. Jazouli, R. Bakhshi, ‘*PHM Cost and Return on Investment*’, Prognostics and Health Management of Electronics:

- Fundamentals, Machine Learning, and the Internet of Things, Wiley and Sons, pp. 221-260, 2018
12. J. Carroll, A. McMillan, M. O'Barrera, D. McMillan, R. Bakhshi, '*Offshore Wind Turbine Sub-Assembly Failure Rates Through Time*' Proceedings of EWEA 2015, France, December 2015
 13. X. Lei, P. Sandborn, R. Bakhshi, A. Kashani, N. Goudarzi, '*PHM Based Predictive Maintenance Optimization for Offshore Wind Farms*', Proceedings of IEEE Conference on Prognostics and Health Management, p:1-8, 2015
 14. X. Lei, P. Sandborn, R. Bakhshi, A. Kashani, '*Development of a Maintenance Option Model to Optimize Offshore Wind Farm O&M*' Proceedings of EWEA Offshore, Denmark, March 2015

Appendices

Appendix I: Overview of Wind Turbine Field Failure Databases

All O&M models use wind turbine failure parameters as their inputs. These parameters are component specific and they can take the form of failure rates or probability distributions representing failures of components. Failure rates are used in deterministic O&M models where the goal is to estimate the number of failures in a fixed interval of time. Probability distributions are used in stochastic models where the probability of occurrence of failures is considered and the goal is to generate a distribution of O&M costs. However, a model is only as good as its inputs.

The failure parameters (rates or probability distributions) are generated from historical field failure data. Therefore, the accuracy of the parameters will depend on how accurate the failure data was and the underlying assumptions. In this appendix, databases that report the field failure data of wind turbines and the literature that analyzes that data are reviewed. Then, the underlying assumptions of these databases and their analyses will be discussed. Finally, there will be a discussion on what information a database must provide in order to perform a meaningful analysis and what the researcher who uses the information, must consider before implementing the failure parameters in their work.

1.1. Wind Turbine Failure Databases

Pfaffel et al. [78] performed a review of the wind failure databases available in the literature. They mention 29 databases that report failure of wind turbines in different parts of the world for various data collection periods. The authors did not

discuss the underlying assumptions of the databases and the analyses that were performed on the data in the literature they reviewed. Their focus was on comparing the results of the analyses on the databases.

It is important to point out that none of the databases are in the public domain and the actual failure times and any information that is indicative of failures is not accessible publicly. One failure database that includes failure data and can be accessed through subscription is a quarterly report published by Haymarket Group called the Windstats Newsletter [72]. Most of the data from other databases are either propriety to farm owners and turbine manufacturers or collected by government agencies and made available only to researches in their country.

In the literature, there are several studies by researchers who were given access to a particular database by the data owners. These researchers performed various types of statistical analysis on the data and published their results.

In this appendix, only databases with turbines operating in Europe and data collection periods that include years after 2000 are considered. Since the technology of wind turbines has changed significantly in the past 20 years, considering the failure data of turbines that were designed decades ago and using that data to predict and manage the O&M of turbines that are state-of-the-art technology is meaningless. *Table 5* describes seven databases found in the literature that will be discussed.

Table 5- Summary of information provided from various databases. Information collected from [33], [71], [72], [79]–[84]

	Failure Definition	Power Rating	Number of Turbines	Onshore or Offshore	Location of Turbines	Age of Turbines	Period of Data Collection
LWK	Unknown	225kW-1.8 MW	158-643	Unknown	Germany	Unknown	Annually (1993-2004)
Windstats	Corrective maintenance was needed	300kW-8MW	16,000-24,000	Mainly onshore	Germany	Unknown	Quarterly (1989-present)
Strathclyde	Database organized based on maintenance action not failures	2MW-4MW	350	Offshore	Europe	3-10 years	Annual (years unknown)
Sweden	A component that can no longer perform its required function	Contains data for >500kW to <1 MW	More than 700	unknown	Sweden	1-19 years	Annual (1997-2004)
Finnish	Any malfunction that resulted in either repair or replacement	200kW-2.3MW	72	Onshore	Finland	Available in database	1996-2008
WMEP	Any malfunction that resulted in either repair or replacement	Mostly less than 1MW, about 100 turbines above 1 MW	1500	Unknown	Germany	Available in database	1989-2006
CIRCE	Any event resulted in a turbine stop and subsequent repair or replacement	300kW-3MW	Average of 4300	Onshore	Mostly Europe	Around 10 years	3 years (years unknown)

LWK:

LWK (Landwirtschaftskammer Schleswig-Holstein) is a German database that covered the failure data of wind turbines in Germany between 1993 to 2006. There has been no update to the database since then. The number of turbines in database varies between 158 to 650 during different periods of time. Spinato et al. [71] performed reliability analysis on this database.

Windstats Newsletter:

Windstats Newsletter [72] is a quarterly newsletter that's been publishing wind turbine failure data and energy production of wind farms in Europe since 80s. The authors have access to majority of the issues from 2005 to 2016. The report only covers the failure data of turbines in Germany however, for the energy production, during different periods of publications, the newsletter covered the data for wind farms in countries such as Germany, Denmark, Sweden, Finland, Belgium and New Zealand. The number of German turbines that reported their failure and production in 2005 issues is about 16,000 turbines. This number increases to 24,000 turbines for the last issue of 2016. The report provides a failure data table with total number of stops and total number of stop hours for a particular component of wind turbines. Table 6 is an example of some of such data provided by Windstats. The failure data reported are aggregated values for the whole population of German turbines over a three-month period. There is no information on turbine power ratings or age of the turbines in this table.

Table 6- An example of data provided in Windstats Newsletter [72]

	Service		Wear		Failure		Not Reported	
	No.	Hours	No.	Hours	No.	Hours	No.	Hours
Rotor	10	62	4	426	4	221	60	480
Gearbox	4	18	0	0	2	105	4	10
Yaw System	1	1	13	170	2	72	14	12
Hydraulics	1	4	8	76	4	182	1	20

The second part of the report, which covers the energy production of turbines, gives more details about the wind turbines. This information includes, site, manufacturer, power rating and installation date of individual turbines. It is the understanding of the author that these are the turbines corresponding to the failure data table. Turbine sizes vary from hundreds of kilowatts to multi-megawatt turbines. As expected, in the most recent issues, the majority of turbines are multi-megawatt turbines. Age of the turbines vary significantly, however, interestingly in 2016 issues, there are very few turbines with installation dates that go back to 1990s although the lifetime of a turbine is usually 20 years. For the German population, there is no mention whether the turbines' data include offshore installations or not.

Spinato et al. [33], [71] used the data provided by Windstats between 1994 to 2004 and performed reliability analysis to calculate the failure rates and the probability distributions for the various components of wind turbines.

Strathclyde:

Works published by Carroll et al. [79], [80] focus on a database of about 350 offshore turbines across Europe. The turbine sizes vary between 2 to 4 MW and the age of turbines is between 3 to 10 years. The turbines are located in 5 to 10 different wind farms across Europe. The significance of this database is the focus on offshore

installation, which is absent in other databases and the relative young age of the turbines at the time of publication. The authors calculated the failure rate of various turbine components. A major difference between the study of this database and studies covering other databases is that here, the data are classified based on the maintenance events (their costs) rather than the failure of components. The four main categories that the data are classified into are: Major Replacement, Major Repair, Minor Repaired and No Cost Data. This approach is useful to distinguish between total breakdown failures (replacements) and failures that only required repair.

Sweden:

The analysis on this database was published by Ribrant et al. [81] and it covers failures of turbines in Sweden between 1997-2004. The number of turbines varied between 500 to more than 700 over the timespan of data collection. No further study from this database has been published since 2007. The wind turbine components that are discussed in this database are similar to Windstats Newsletter.

Finnish (VTT):

This database covers the failure and production of 72 turbines from 1996-2008 installed in Finland. The analysis on this database was discussed by Stenberg and Holttinen [82]. The turbine sizes vary from 0.2 MW to 2.3 MW and they are all onshore.

WMEP:

This database was a part of German '250MW Wind' program that covered failure and production of more than 1500 wind turbines in Germany. Data collection started in 1989 and by the end of 2006, when Echavarria et al. [83] published their

analysis, more than 63,000 reports concerning maintenance and repair of turbines were submitted to the database. The database contain information about the type of maintenance performed and the components that were affected along with information about downtime and date of maintenance. The majority of the data in this database covers wind turbines with rated powers less than a megawatt.

CIRCE:

This is a database used by CIRCE researchers in Spain [84]. This database covers failures of turbines installed in Europe over 3 years. However, the exact years of data collection are unknown. The average number of turbines in the report is about 4,300 turbines with rated powers ranging from 300kW to 3MW. The analysis of the database investigates the failure rates of more than 20 components in the wind turbine, far more than what databases such as Windstats or Strathclyde report.

1.2. Requirements for Analyzing the Databases

Analysis of failure data have several applications. As mentioned earlier, the results can be used in O&M models to predict O&M costs of wind farms. Other examples of applications are to compare different turbine designs (or their components), finding out what components are more susceptible to failures, understanding what failures were result of infant mortality, random occurrence or wearout, and several other applications.

Overall, in order to have a perfect analysis, the reports in database have to contain data pertaining to each turbine for its lifetime. For example, the failures of an individual turbine should be determined and reported in the database over its lifetime.

This is not the case in many of the databases that mentioned in the previous section, instead they report the total number of failures for the whole population of turbines without any mention of the turbine's age (e.g., Windstats).

A fundamental question for each database is the definition of failure. It turns out, different analyses have different definitions. Some define failure as an event that requires a component replacement while some other define it as an event that requires a maintenance action. In some cases, failures could be resolved with remote resets.

Another parameter that is important in failure data reporting is the failure cause and in particular, distinguishing between failures that occurs due to overstress and the wearout failure mechanisms, e.g., whether a blade failure was due to fatigue, icing or a lightning strike. Overall most databases do not contain any information about failure causes and failure modes. This is understandable since the databases come from log book reports that were filled out by workers who do not necessary possess the reliability engineering knowledge to distinguish and identify failure modes and failure causes.

It is important to know whether the data represents onshore or offshore installation. The offshore environmental conditions are significantly different and possibly harsher than onshore installation. The failure mechanisms for offshore installations could be completely different than onshore ones (e.g., corrosion in offshore), which makes the results of a data analysis of one inaccurate for the other.

Here, seven questions are formulated that evaluate the data in each of the aforementioned databases are:

- What is the definition of failure?

- What is the power rating of the turbines in the population?
- How many turbines are in the reported population?
- Are the turbines onshore or offshore?
- What is the geographic location of the turbines in the population?
- What is the age of the population at the report time?
- What is the period of data collection?

The answers to these questions for the databases considered in this paper are shown in Table 5.

1.3. Discussion

As it can be seen from Table 5, all but one database (Strathclyde) organize their databases based on failure events while Strathclyde organizes based on maintenance events. The definition of failure differs in all the databases. Some refer to failure as an event that needs component replacement, and some refer to it as an event that needs either repair or replacement. Sometimes, it is even possible that the failure event needed an inspection without any repair or replacement. Some failures of components could be secondary failures, meaning the malfunction of a component is the result of failure of another component (collateral damage). One important missing piece of information in all the data analysis in the literature is information on failures of the replaced components. There is no data indicating whether a failure corresponded to the component that originally came with the turbine, or it was associated with a component that was a replacement. Knowing this piece of information provides insight about mean time to failures of components and whether

replacements are as good as new. If the component failures of individual turbines over their lifetime were tracked, it would be possible to distinguish between failures of original and replacement components.

The power rating of turbines in databases vary significantly. Considering there are significant design differences between turbines of different sizes, analyses should categorize the data for each turbine size in the database or at least divided into ranges of turbines sizes (e.g., less than 500kW, between 500kW and 1MW, etc.). Using failure data for a multi-kilowatt turbine to predict the failures and O&M costs of multi-megawatt turbines, may yield inaccurate results. Some of the analyses in the literature do split their analysis results in multiple categories of power rating ranges.

Age of the turbines plays a significant role in the failure occurrence. Lots of the aforementioned data analysis articles (e.g., Carroll et al. [79], [80]) report their analysis based on the age of the turbine. This helps with understanding of the failures rates (or other calculated statistical parameters) as a function of turbine age.

It is evident that there is no consistent definition of failure among different databases, however, most of the analyses that were performed on the data, mention how a failure was defined. Many databases report their failure data as a single value for the whole population, a few databases provide more detailed information regarding the power rating and/or age of the turbines.

Overall, there is no mention of failure modes and causes in the databases and it is not clear whether a failure was due to extreme causes (e.g., lightning strike) or wearout of a component. There is also no information on failure of replacement components.

Appendix II: Model Verification and Validation

In this appendix, the process of developing the return on investment model for implementation of LIDAR devices on wind turbines for the purpose of yaw error correction is explained. As explained in Chapter 2, the NPV model is built upon the ROI formulation, therefore, the verification process in this appendix constitutes verifying for NPV.

The purpose of this appendix is to validate and verify the model. To start off, simple cases are considered (i.e. two turbines here). LIDAR stay time on the turbines is varied (referred to as LIDAR circulation cycles), and the energy production of the whole farm (2 turbines together) along with O&M costs, investment costs and ROI are calculated.

Several simulation assumptions are varied and their effect on the outcome measured. One of the most important features of these tests is the ability to turn off the Monte Carlo (MC). There are 3 sets of MC calculations for 3 different input parameters: yaw error, wind speed and component failure time. For different scenarios MC for these parameters is turned on or off. For cases where MC is off for reliability, a constant value of 0.5 is used instead of using a randomly generated uniform number to sample the reliability distributions. This way, the failure time values will be the same every time the distribution is sampled. In cases where the MC is off for the wind speed, either a value above rated speed is selected (which means LIDAR will have no effect on performance) or a value between cut-in and rated speed is used. These two values are 15 and 10 m/s respectively. In cases where MC is off

for the yaw error, depending on the case study, a constant value of either 7 or 15 degrees of error is used. Two yaw regression scenarios are investigated, the first scenario is that there is no yaw degradation, meaning in the case of no LIDAR, the turbines are running on 7° error constantly and in the case of with LIDAR, the turbines run on 1-degree yaw all the time. In the second scenario where there is degradation, the yaw starts to regress back to values of 7° (or 15°) after the LIDAR is moved to the other turbine.

There are two sets of downtimes in the model, one set is the reliability downtimes, which is the downtime of the turbine due to maintenance events. Another set is downtime due to circulation of the LIDAR between the turbines. The downtimes are turned on and off frequently for different cases and their effects are investigated.

Finally, the last parameter that is investigated is the discount rate (WACC). WACC has been turned on and off frequently, in cases that it's on, the value is assumed to be 7%.

More than two dozen of cases were studied, however, here only 3 cases, which best illustrate the process and purpose of these case studies, are summarized. These cases are simplified versions of the wind farm simulation and help to understand what the details of the simulation are and how it works.

II.1. Case Studies

II.1.1. Case 1

In the first case, the effects of investment variation on the ROI will be studied while the cost benefits are kept constant. The simplest case is having a deterministic

model where all the Monte Carlo is disabled. As a result, the failure of components occur at fixed intervals of time, the yaw error values have no uncertainty, the corrected yaw is 1° while the uncorrected yaw is 7° . There is no yaw regression, meaning after the LIDAR is moved away from the turbine, the yaw values remain the same. Wind blows at constant speeds at all times with the speed assumed to be 10 m/s, below the rated speed of 13 m/s of wind turbine, therefore the LIDAR affects the performance of the turbine. For this case, it is assumed that there is no downtime associated with LIDAR circulation or any downtime for maintenance. Circulating the LIDAR between the turbines costs money, this money is part of the investment costs.

To summarize, here are the assumptions:

- Deterministic model
- $V=10$ m/s, $V_{in} < V < V_{rated}$
- $Y_{aw \text{ LIDAR}}=1^\circ$, $Y_{aw \text{ No-LIDAR}}=7^\circ$
- No yaw regression
- No downtime for LIDAR circulation
- No downtime for maintenance
- Circulation costs are included

Having the aforementioned assumptions, means that the investment costs here are the costs of buying, maintaining, and circulating LIDAR between the two turbines. As the LIDAR stay time increases, the total costs of the LIDAR circulation between the turbines reduces. The effects of LIDAR on turbine performance do not change when the LIDAR stay time on the turbine varies (there is no yaw regression in this case, so the corrected yaw always remain at 1°) and since there are no downtimes, the expectations is to have a constant energy production regardless of the LIDAR circulation policy. As for maintenance costs, two scenarios will be considered here, the first scenario assumes that there is no part replacement costs, which

subsequently means there will be no O&M costs. The second scenario assumed there is maintenance costs for turbine blades so there will be some O&M costs.

Considering the deterministic nature of the case, values for shape and scale parameters and the random number value selected for this case, the first and second blade failures occur at 8 and 16 years of operations for the case of no LIDAR. With the case of LIDAR and the correction of yaw error and its subsequent reliability improvements, these failures move to 9 and 18 years of operation, still within the 20 years of support time.

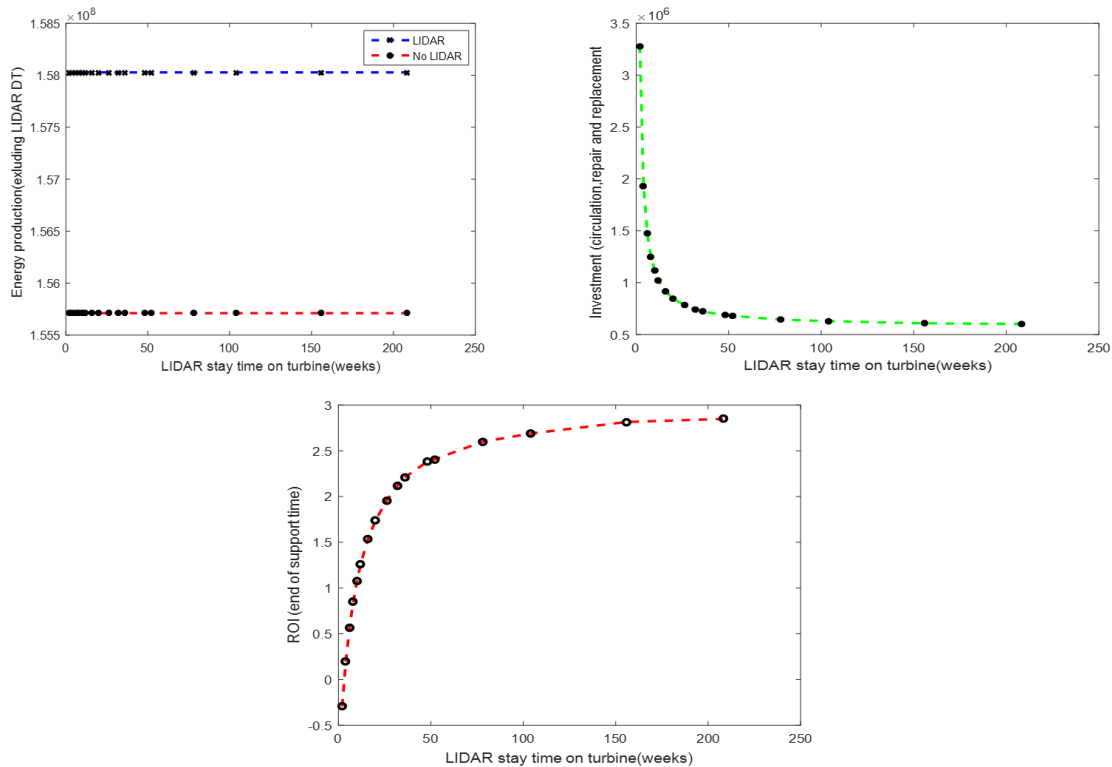


Figure 32- Case 1 simulation outputs. Top left: Energy Production. Top right: Investment costs. Bottom: ROI

Figure 32 shows the behavior of several simulation outputs. Discount rate is assumed to be zero. As expected, since there is no yaw degradation and downtime, the energy production of the farm stays the same for different LIDAR circulation

policies. The investment costs decrease with longer cycles, LIDAR purchase and maintenance costs remain the same for all the policies while the circulation costs decrease.

As a result, the ROI increases with longer cycles. Repeating the same scenario with discount rate set to 7% results in similar results. However, because of cost of money, the farm will produce less revenue over time although the energy production is the same. The revenue production for the cases with and without WACC are shown in *Figure 33*.

Now for scenario 2 of this case, turning on the maintenance costs for only the blades will result in an O&M costs for the whole farm. The failure time of the blade is a function of yaw error. Since the yaw error is constant regardless of the circulation policy, the failure times remain the same. The maintenance costs should not be affected by the LIDAR circulation policy. As mentioned earlier, the correction in the yaw error due to LIDAR will shift the blades' failure time, however, the delayed failures still occur within the 20-year support time of the turbines. In cases where WACC is assumed to be zero, the total O&M costs will be the same for both LIDAR and no-LIDAR cases (each case has 4 blade failures in 20 years). However, when the effects of cost of money is included, due to the shift in the timing of the maintenance, the O&M cost for the LIDAR case will be less than the no-LIDAR case even though the same number of maintenance events performed. The results are shown in *Figure 34*.

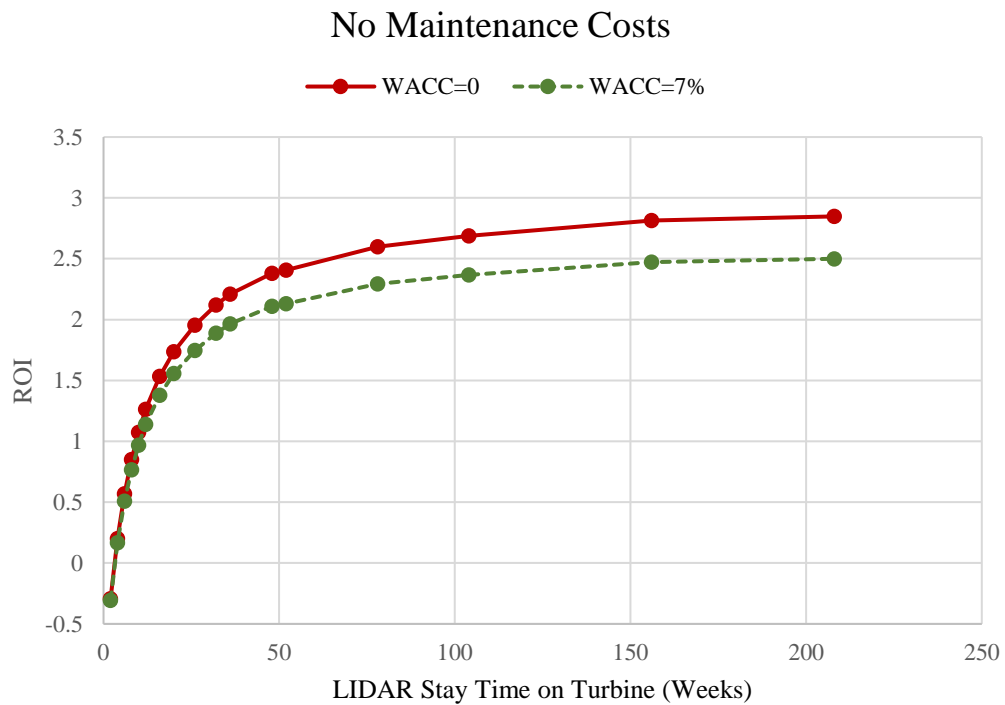
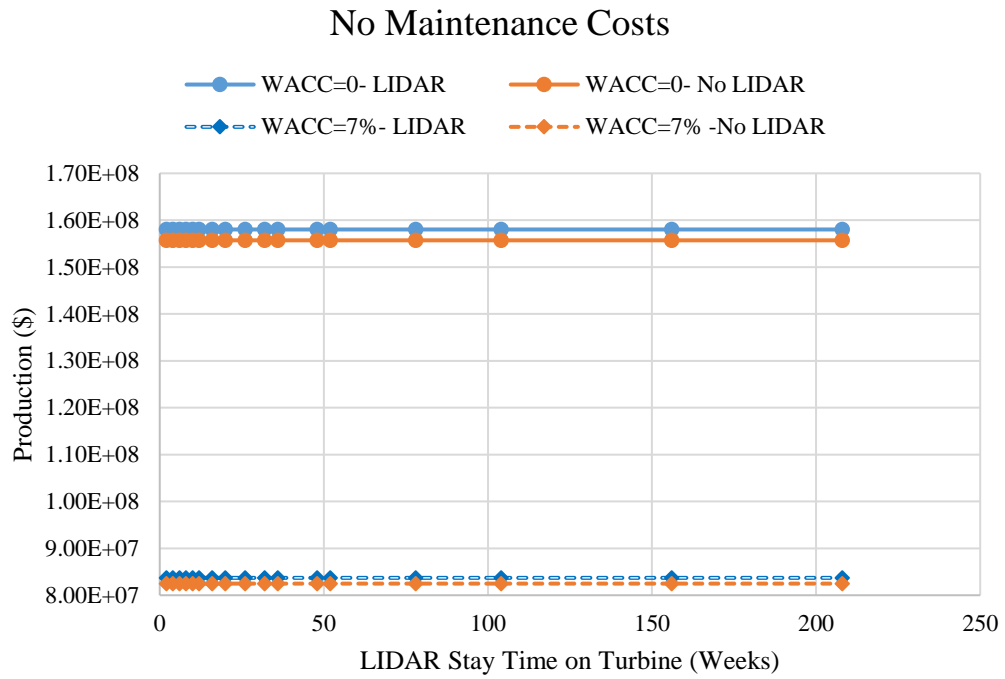
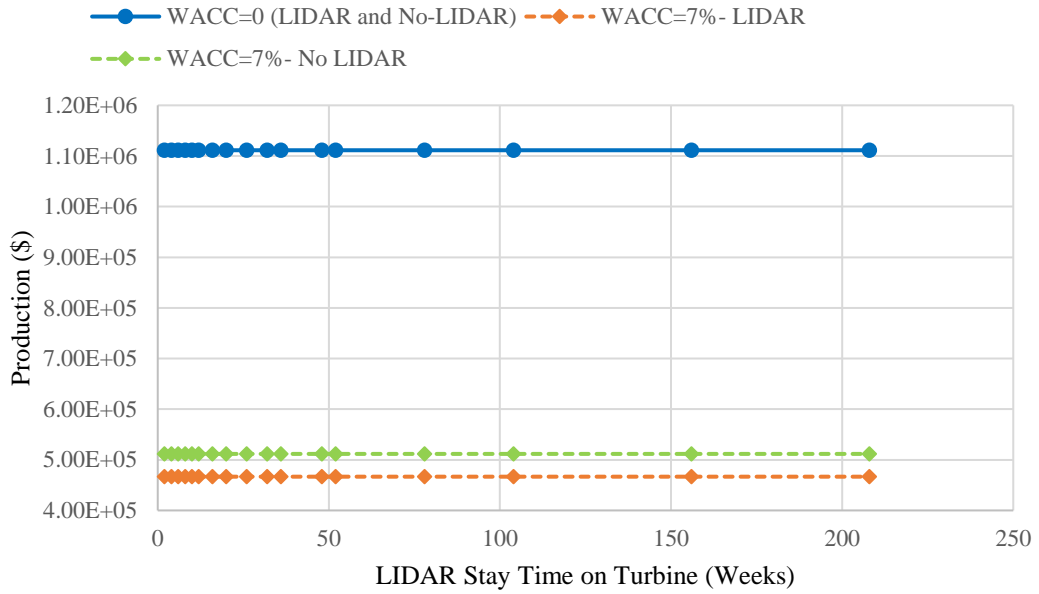


Figure 33- Effects of WACC on revenue and ROI with no maintenance cost. Top: Revenue. Bottom: ROI

O&M Only Including Blade Maintenance Costs



O&M Only Including Blade Maintenance Costs

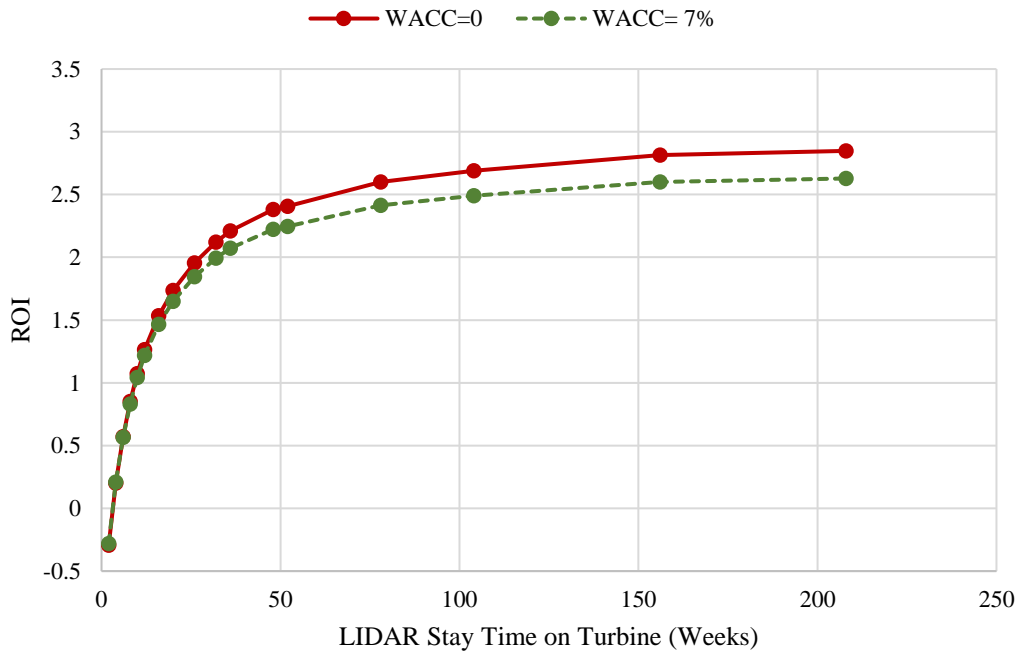


Figure 34- Effects of WACC on revenue and ROI with Blade maintenance costs. Top: Revenue. Bottom: ROI

II.1.2. Case 2

In case 2, the goal is to keep the investment costs constant over different circulation policies and investigate the changes in ROI with variations in cost benefits. In order to do so, the circulation costs of LIDAR are assumed to be zero. As a result, the investment costs are only the costs of purchasing LIDAR and maintaining it. The downtimes due to maintenance and LIDAR circulation are assumed to be zero. All the components have maintenance costs and their reliability is affected by yaw error. The yaw error is 1° for the turbine with corrected yaw and a constant value of 15° error for uncorrected yaw. This value is selected to highlight the effects of circulation periods on the performance and reliability. In this case study, the yaw regression is considered in the calculations, meaning that after the LIDAR is removed from the turbine, the yaw error will gradually regress back to the uncorrected value of 15° over time. Two scenarios will be investigated here, in first scenario, Monte Carlo is turned on for the components reliability while the wind speed is kept constant at 10 m/s. In the second scenario, the failure times will be deterministic similar to Case 1 while the Monte Carlo is used to generate wind speeds. To summarize, here are the assumptions:

- No LIDAR circulation costs
- No downtime due to maintenance or LIDAR circulation
- Yaw error is deterministic, 1 and 15 degrees for corrected and uncorrected cases
- There is yaw regression
- MC on for wind speed and off for reliability or MC on for reliability and off for wind speed

II.1.2.1. MC on for Wind Speed and Off for Reliability

The expected result here is to see a production that stays relatively constant during the scenarios where LIDAR quickly circulates between the two turbines. The reason is that the yaw regression takes a period of approximately 6 months to show a significant regression to uncorrected values so if the window between the LIDAR visits to a turbine is less than 6 months, the yaw error remains close to 1 degree. For periods longer than 6 month, the yaw error becomes larger than 1 degree, which will hurt the energy production of the turbine and eventually decreasing the production. For the cases of no-LIDAR, the expectation is a relatively constant energy production over different circulation policies. There might be possible fluctuations due to uncertainties in wind speed.

As for the O&M, since the system is deterministic, the expectation is to have a flat O&M costs for the no-LIDAR case. Yaw error remains constant for all the circulation scenarios so the exact same failures occur for all the scenarios. For the case of LIDAR, the lower yaw could result in fewer failures and subsequently lower O&M costs than the no-LIDAR case. The number of failures could change for different circulation scenarios, however, it is still possible that the total number of failures over 20 years remain the same. If this is the case, when discount rate is assumed zero, the O&M costs for LIDAR case will be a flat line (Figure 35).

Since the investment costs remain constant for all the different circulation scenarios, the trend in the ROI should be similar to the performance.

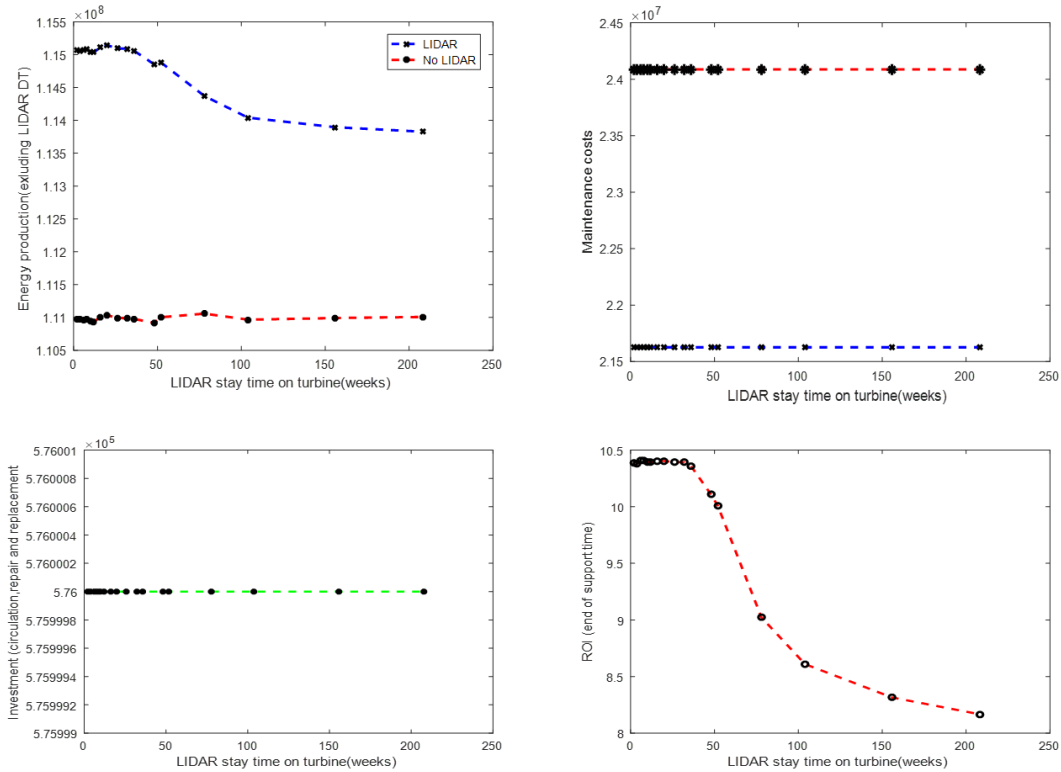


Figure 35- Effects of uncertainties in wind speed with WACC=0. Top left: Revenue, Top right: O&M costs. Bottom left: investment costs. Bottom right: ROI

II.1.2.2. MC on for Reliability and off for wind speed

In this case, uncertainties in wind speeds are removed and a constant value will be used. In the case of no-LIDAR energy production will be a constant value over all the scenarios. As for the case of LIDAR, the expectations is to see a flat line at the beginning that will start trending down as the circulation cycles increases because the turbines experience larger values of yaw error.

For O&M costs, the no-LIDAR case should have a higher maintenance costs than the LIDAR case. The behavior of the costs for different circulation scenarios is not predictable since the events are stochastic but the graph should be bounded by a

maximum and minimum. This should be true for both cases of LIDAR and no-LIDAR.

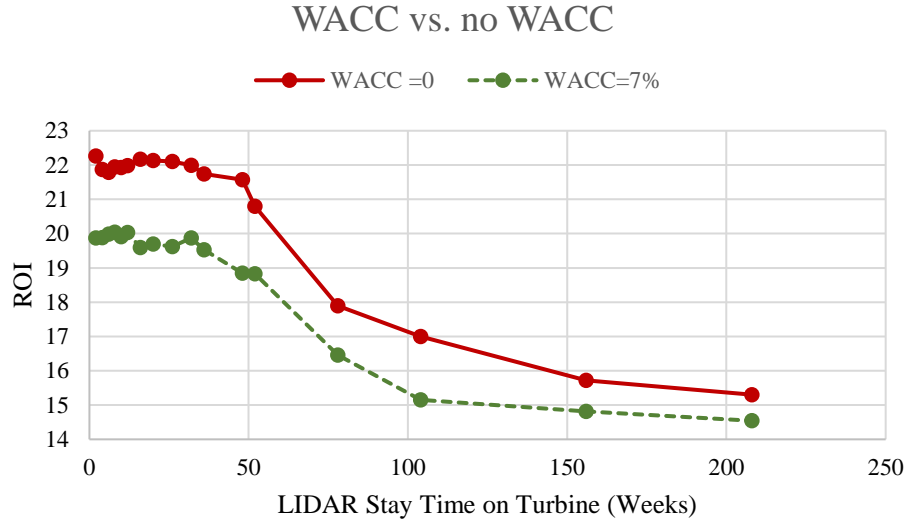


Figure 36- Effects of uncertainties in failure times on ROI

The fluctuations of the O&M costs may or may not have an effect on the ROI. It depends on the magnitude of the O&M values and the energy production at each point. If performance values are much higher than the O&M costs, then ROI plots will look like the performance plot, and if it is the opposite, where the magnitude of O&M costs are higher than performance costs, then ROI will take shape like the O&M. If performance and O&M costs are in the same order of magnitude, then the beginning part of the ROI plot should behave like O&M plot then, it will move like performance plot with some fluctuations. Here the results are for the case where discount rate is zero. Including the discount rate did not result in a significant change to the shape of the ROI plot, it is just shifted. This can be seen in Figure 36.

II.1.3. Case 3

In this case the model inputs are closer to realistic assumptions. The Monte Carlo is turned on for wind speed, failures and the yaw error.

After LIDAR leaves the turbine, the yaw error gradually starts regressing back to uncorrected values that are randomly generated. There are costs of circulating the LIDAR similar to Case 1 and the investment costs will look like that case too.

With regards to downtime, four scenarios can be assumed, one without any downtime (neither failures, nor circulation), one with only failure downtime, one with only LIDAR circulation downtime and finally one with all the downtimes considered. In order to avoid confusion in the case comparisons, a 'guidance table' is produced for all the cases and included in all figures where the corresponding boxes that show the particular cases are marked. In the guidance table, "L" refers to cases where there is LIDAR, "NL" is for cases without LIDAR. "No" means there is no downtime considered at all. "R" means only downtime for reliability.

The expectation is that the failure downtimes affect the performance of the farm by making a shift in the production compared to the no-downtime case (however, not necessarily shifting the curve by a constant value). This can be seen more clearly in a no-LIDAR case where all the turbines run on higher yaw values (these values are generated randomly as well). These are shown in Figure 37.

When the LIDAR circulation downtime comes into play, the behavior will be different. As the circulation cycles increase, the reliability downtime decreases, since the production is relatively constant for the shorter cycles as we have seen in the previous cases, a decrease in downtime in these periods will show itself as an increase

in production. As the circulation cycles increase, the yaw error will be lower and the production increases but there will be more downtime due to circulation. The behavior of the trend depends on the trade-off between the production reduction due to yaw error increase and the production loss reduction due to fewer failure downtime hours.

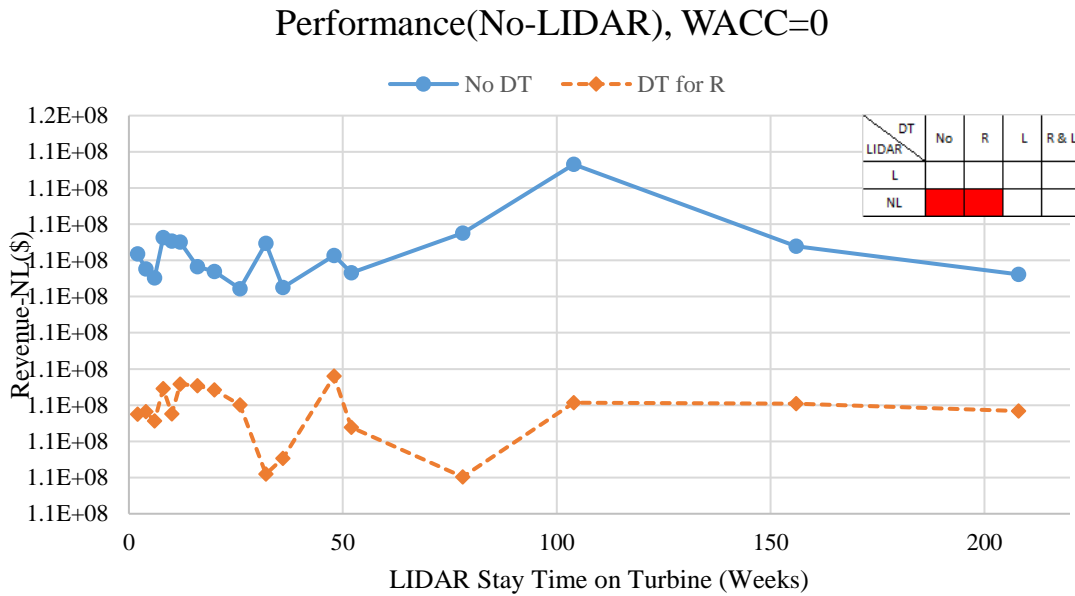


Figure 37- Effects of downtime on revenue: No LIDAR devices.

Per event, LIDAR circulation downtime is shorter than the maintenance downtime. However, it is the frequency of circulation downtime that affects the revenue generation, and when the frequency is high there is a significant production loss. Overall, maintenance downtime affects the revenue with its magnitude while the LIDAR downtime affects the revenue with its frequency.

In Figure 38, as it can be seen the red line that represents no-LIDAR case has no LIDAR downtime in it, however, since turbines are operating on higher yaw error,

which lowers the reliability, the maintenance downtime will be higher than the LIDAR case. As a result, once the LDAIR circulation downtime effect on production becomes less in higher circulation cycles, the maintenance downtime magnitude shows its real effects on the overall performance of the system.

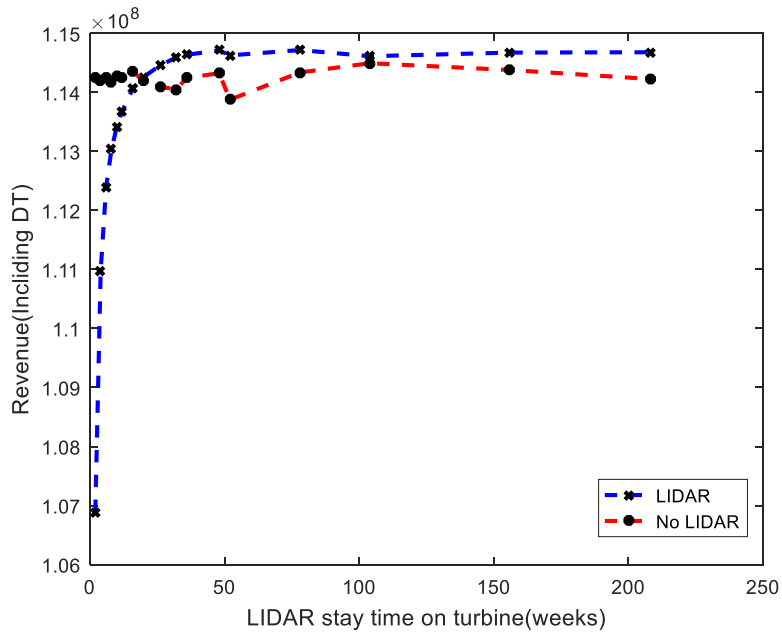


Figure 38- Effects of downtime on revenue

Figure 39 shows the performance of the two turbines for all the 4 scenarios and the individual and collective effects that the downtimes have on energy production.

Performance(LIDAR), WACC=0

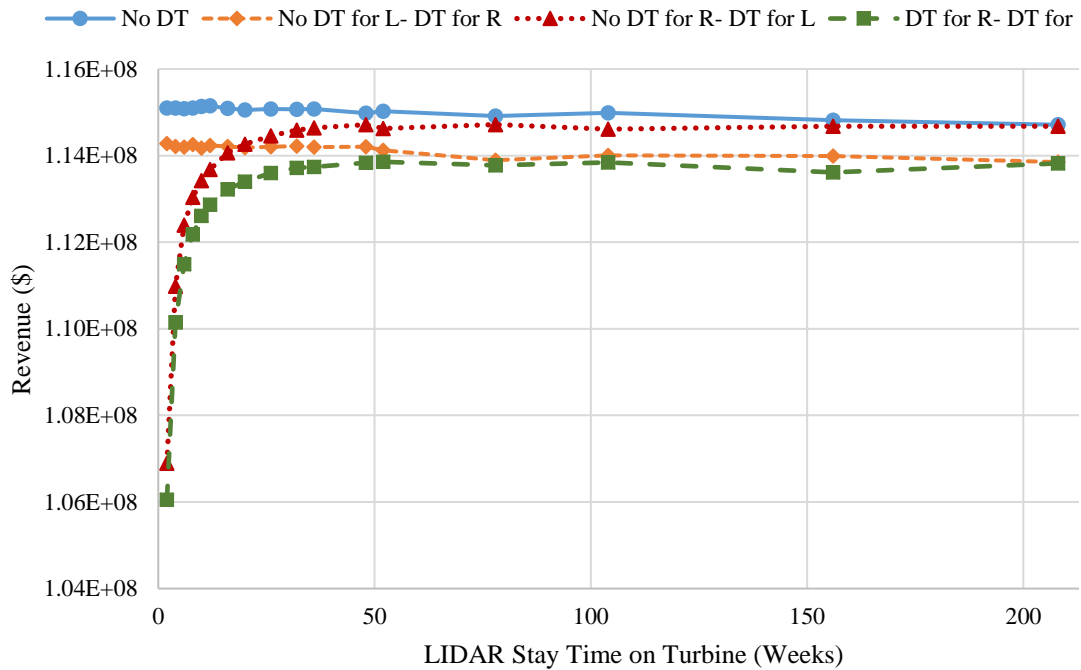


Figure 39- Effects of downtime on revenue generation

Several observations can be made from Figure 39. The no downtime production is the highest as it was expected. The cases where there is LIDAR circulation downtime, there is significant power loss for the shorter circulation cycles and as LIDAR downtime dwindles with the higher cycles, the production goes up. For higher cycles, as expected, there is a trade-off between lower production due to higher yaw error and lower production loss due to less circulation. This causes some fluctuations in the chart. This can be seen in the third case where no maintenance downtime is taken into account. For the longer cycles for this case, the production almost matches the no downtime scenario since the effects of circulation downtime almost disappear. However, this is not the true for the fourth case where reliability

downtime is included. As it can be seen, although the reliability downtime is not frequent, but its magnitude is high enough to significantly affect the production.

Lastly, the ROI of these four cases has to be compared. The expectation is to see a lower ROI for the cases with LIDAR circulation downtime especially for the shorter circulation cycles. This is demonstrated in Figure 40.

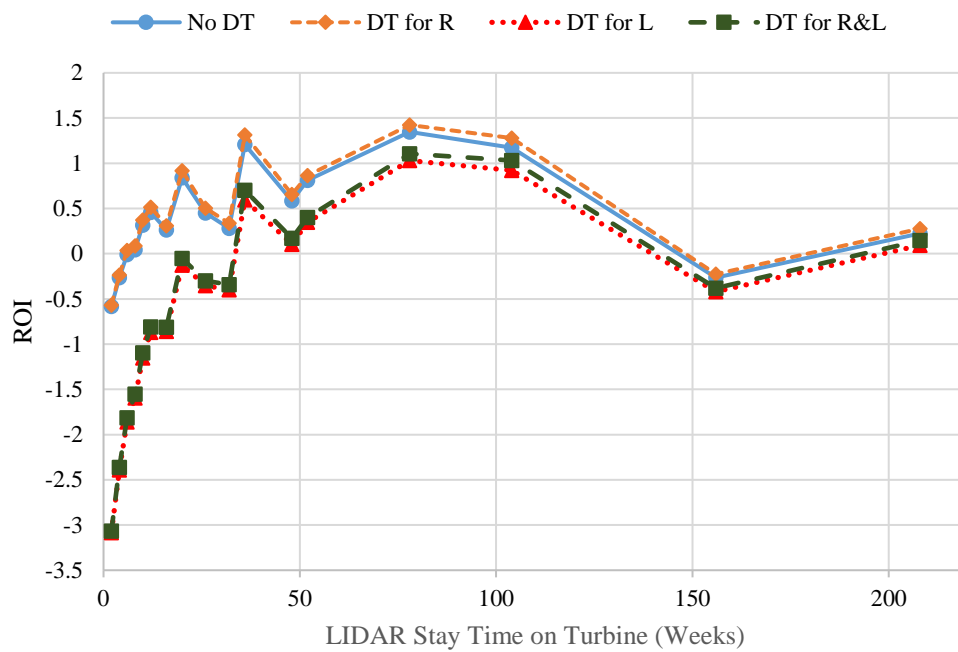


Figure 40- Effects of downtime on ROI

Overall, it can be seen that the inclusion of the downtimes makes a shift in the ROI plots as it was expected. The interesting observation is the move of the second scenario (downtime for reliability) above the no downtime case, which shows that inclusion of the maintenance downtime into calculations demonstrates the value of LIDAR addition better.

The maintenance downtime effects, show up in the production for both LIDAR and no-LIDAR cases and their subsequent revenue generation terms in the ROI formula whereas the LIDAR circulation downtime only shows up in the LIDAR revenue terms in the ROI formula. This and the frequency of the LIDAR downtime result in lower ROI values for the cases where LIDAR downtime is included compared to the cases where it's not included.

Bibliography

- [1] Energy Information Administration (EIA), “United States Carbon Dioxide Emission Production,” 2019.
- [2] B. Snyder and M. J. Kaiser, “Ecological and Economic Cost-Benefit Analysis of Offshore Wind Energy,” *Renewable Energy*, vol. 34, no. 6, pp. 1567–1578, 2009
- [3] A. Lopez, B. Roberts, D. Heimiller, N. Blair, and G. Porro, “U.S. Renewable Energy Technical Potentials: A GIS-Based Analysis.” *National Renewable Energy Laboratory*, July 2012.
- [4] American Wind Energy Association (AWEA), “Wind Energy in the United States.” Accessed: July 2019.
- [5] Energy Information Administration (EIA), “United States Energy Production,” 2016.
- [6] American Wind Energy Association (AWEA), “US Offshore Wind Farms Projections Infographic Map,” 2016..
- [7] Wikipedia, “List of Offshore Wind Farms in The United States,” *Wikipedia*, Accessed: October 2019.
- [8] B. Hamilton, “Offshore Wind O&M: Costs, Trends, and Strategies for the Coming Decade,” *Proceedings of AWEA Offshore Windpower Conference & Exhibition*, 2011.
- [9] “Wind Turbine Schematic.” [Online]. Available: wind.energy.gov. Accessed: May 2016.
- [10] J. Serrano-González and R. Lacal-Aránategui, “Technological Evolution of Onshore Wind Turbines—A Market Based Analysis,” *Wind Energy*, vol 19, no. 12, pp. 2171-2184, 2016.
- [11] A. Myhr, C. Bjerkseter, A. Ågotnes, and T. A. Nygaard, “Levelized Cost of Energy for Offshore Floating Wind Turbines in a Life Cycle Perspective,” *Renewable Energy*, vol. 66, pp. 714–728, 2014.
- [12] J. F. Manwell, J. G. McGowan, and A. L. Rogers, *Wind Energy Explained*, 2nd ed. *John Wiley and Sons*.
- [13] T. Mikkelsen N. Angelou K. Hansen M. Sjöholm M. Harris C. Slinger P. Hadley R. Scullion G. Ellis G. Vives, “A Spinner-Integrated Wind LIDAR for Enhanced Wind Turbine Control,” *Wind Energy*, vol. 16, no. 4, pp. 625–643, 2013.
- [14] E. Marin and H. Pedersen, “Pointing to The Right Direction,” *presented at EWEA*, Malmo, Sweden, Dec-2014.
- [15] J. Dai, X. Yang, W. Hu, L. Wen, and Y. Tan, “Effect Investigation of Yaw on Wind Turbine Performance Based on SCADA Data,” *Energy*, vol. 149, pp. 684–696, 2018.
- [16] N. Marathe, A. Swift, B. Hirth, R. Walker, and J. Schroeder, “Characterizing Power Performance and Wake of a Wind Turbine Under Yaw and Blade Pitch,” *Wind Energy*, vol. 19, no. 5, pp. 963–978, 2016.
- [17] M. Smith, M. Harris, J. Medley, and C. Slinger, “Necessity is the Mother of Invention: Nacelle-Mounted LIDAR for Measurement of Turbine Performance,” *Energy Procedia*, vol. 53, pp. 13–22, 2014.

- [18] N. Mittelmeier and M. Kühn, “Determination of Optimal Wind Turbine Alignment into The Wind and Detection of Alignment Changes with SCADA Data,” *Wind Energy Science*, vol. 3, no. 1, pp. 395–408, 2018.
- [19] D. Choi, W. Shin, K. Ko, and W. Rhee, “Static and Dynamic Yaw Misalignments of Wind Turbines and Machine Learning Based Correction Methods Using LIDAR Data,” *IEEE Transactions on Sustainable Energy*, vol. 10, no. 2, pp. 971-982, 2019.
- [20] D. Song, L. Qingan, Z. Cai, L. Li, J. Yang, M. Su, Y. Hoon Joo “Model Predictive Control Using Multi-Step Prediction Model for Electrical Yaw System of Horizontal-Axis Wind Turbines,” *IEEE Transactions on Sustainable Energy*, vol. 10, no. 4, pp. 2084-2093, 2019.
- [21] T. Ouyang, A. Kusiak, and Y. He, “Predictive Model of Yaw Error in A Wind Turbine,” *Energy*, vol. 123, pp. 119–130, 2017.
- [22] Y. Pei, Z. Qian, B. Jing, D. Kang, and L. Zhang, “Data-Driven Method for Wind Turbine Yaw Angle Sensor Zero-Point Shifting Fault Detection,” *Energies*, vol. 11, no. 3, p. 553, 2018.
- [23] K. A. Kragh, M. H. Hansen, and T. Mikkelsen, “Precision and Shortcomings of Yaw Error Estimation Using Spinner-Based Light Detection And Ranging,” *Wind Energy*, vol. 16, no. 3, pp. 353–366, 2013.
- [24] M. Courtney, R. Wagner, and P. Lindelöw, “Commercial LIDAR Profilers for Wind Energy: A Comparative Guide,” in *Proceedings of the 2008 European Wind Energy Conference*, Brussels, Belgium, 2008.
- [25] P. A. Fleming, A. K. Scholbrock, A. Jehu, S. Davoust, E. Osler, A. D. Wright, A. Clifton “Field-Test Results Using a Nacelle-Mounted LIDAR for Improving Wind Turbine Power Capture by Reducing Yaw Misalignment,” *Journal of Physics: Conference Series*, vol. 524, no. 1, 2014.
- [26] F. Rebeyrat, “Turbine-mounted LIDAR for Performance Optimization,” *presented at the Wind Energy Update: 6th International Wind O&M Forum*, Hamburg, Germany, January 2014.
- [27] R. Wagner, M. S. Courtney, T. F. Pedersen, and S. Davoust, “Uncertainty of Power Curve Measurement With A Two-Beam Nacelle-Mounted LIDAR,” *Wind Energy*, vol. 19, no. 7, pp. 1269-1287, 2016
- [28] L. Huang, A. Cordle, and G. McCann, “Fatigue Load Calculations for ROMO Wind to Assess Sensitivity to Changes in 10-min Mean Yaw Error.” *GL-Garrad Hassan*, 2012.
- [29] R. Damiani, S. Dana, J. Annoni, P. Fleming, J. Roadman, J. van Dam, and K. Dykes “Assessment of Wind Turbine Component Loads Under Yaw-Offset Conditions,” *Wind Energy Sciences*, vol. 3, no. 1, pp. 173–189, 2018.
- [30] F. Castellani, D. Astolfi, F. Natili, and F. Mari, “The Yawing Behavior of Horizontal-Axis Wind Turbines: A Numerical and Experimental Analysis,” *Machines*, vol. 7, no. 1, p. 15, 2019.
- [31] L. Castro-Santos and V. Dias-Casas, “Life-Cycle Cost Analysis of Floating Offshore Wind Farms,” *Renewable Energy*, vol. 66, pp. 41–48, 2014.
- [32] F. Ding, Z. Tian, and T. Jin, “Maintenance Modeling and Optimization for Wind Turbine Systems: A Review,” *2013 International Conference on Quality*,

- Reliability, Risk, Maintenance, and Safety Engineering (QR2MSE)*, pp. 569–575, 2013.
- [33] P. J. Tavner, J. Xiang, and F. Spinato, “Reliability Analysis for Wind Turbines,” *Wind Energy*, vol. 10, no. 1, pp. 1–18, 2007
- [34] F. Besnard, M. Patriksson, A.-B. Stromberg, A. Wojciechowski, and L. Bertling, “An Optimization Framework for Opportunistic Maintenance of Offshore Wind Power System,” *PowerTech, 2009 IEEE Bucharest*, 2009, pp. 1–7.
- [35] Zhu and M. Fouladirad, “A Reactive Multi-Component Maintenance Policy for Offshore Wind Turbines”, *23rd European Safety and Reliability Conference (ESREL 2013)*, Amsterdam, Netherlands. pp.811-817, Sep 2013.
- [36] B. Kerres, K. Fischer, and R. Madlener, “Economic Evaluation Of Maintenance Strategies For Wind Turbines: A Stochastic Analysis,” *IET Renewable Power Generation.*, vol. 9, no. 7, pp. 766–774, 2015.
- [37] J. Nilsson and L. Bertling, “Maintenance Management of Wind Power Systems Using Condition Monitoring Systems -Life Cycle Cost Analysis for Two Case Studies,” *IEEE Transactions on Energy Conversion*, vol. 22, no. 1, pp. 223–229, 2007.
- [38] K. Fischer, F. Besnard, and L. Bertling, “Reliability-Centered Maintenance for Wind Turbines Based on Statistical Analysis and Practical Experience,” *IEEE Transactions on Energy Conversion*, vol. 27, no. 1, pp. 184–195, 2012.
- [39] F. Besnard, K. Fischer, and L. B. Tjernberg, “A Model for the Optimization of the Maintenance Support Organization for Offshore Wind Farms,” *IEEE Transactions on Sustainable Energy*, vol. 4, no. 2, pp. 443–450, 2013.
- [40] G. Puglia, P. Bangalore, and L. B. Tjernberg, “Cost Efficient Maintenance Strategies for Wind Power Systems Using LCC,” in *2014 International Conference on Probabilistic Methods Applied to Power Systems (PMAPS)*, pp. 1–6, 2014.
- [41] G. Van Bussel and C. Schöntag, “Operation and Maintenance Aspects of Large Offshore Windfarms,” *Proceedings of the European Wind Energy Conference*, 1997.
- [42] J. J. Nielsen and J. D. Sørensen, “On Risk-Based Operation and Maintenance of Offshore Wind Turbine Components,” *Reliability Engineering Systems and Safety*, vol. 96, no. 1, pp. 218–229, 2011.
- [43] T. Jazouli and P. S. and A. Kashani-Pour, “A Direct Method for Determining Design and Support Parameters to Meet an Availability Requirement,” *International Journal of Performability Engineering*, vol. 10, no. 2, p. 211, 2014.
- [44] E. Brigham and P. Daves, "Intermediate Financial Management", 10th ed. *Cengage Learning*", 2010
- [45] P. Fernandez, "Valuation Methods and Shareholder Value Creation", 1st ed. *Academic Press*, 2002.
- [46] J. A. Miles and J. R. Ezzell, “The Weighted Average Cost of Capital, Perfect Capital Markets, and Project Life: A Clarification,” *Journal of Financial and Quantitative Analysis*, vol. 15, no. 03, pp. 719–730, Sep. 1980.

- [47] K. Cory and P. Schwabe, "Wind Levelized Cost of Energy: A Comparison of Technical and Financing Input Variables", *National Renewable Energy Laboratory*, 2009.
- [48] A. C. Levitt, W. Kempton, A. P. Smith, W. Musial, and J. Firestone, "Pricing Offshore Wind Power," *Energy Policy*, vol. 39, no. 10, pp. 6408–6421, 2011.
- [49] J. B. Welch and A. Venkateswaran, "The Dual Sustainability of Wind Energy," *Renewable and Sustainable Energy Reviews*, vol. 13, no. 5, pp. 1121–1126, 2009.
- [50] C. M. Wyman and C. J. Jablonowski, "A Workflow and Estimate for the Economic Viability of Offshore Wind Projects," *Wind Engineering*, vol. 39, no. 5, pp. 579–594, 2015.
- [51] T. Jin and Z. Tian, "Uncertainty Analysis for Wind Energy Production With Dynamic Power Curves," in *2010 IEEE 11th International Conference on Probabilistic Methods Applied to Power Systems (PMAPS)*, 2010, pp. 745–750.
- [52] M. Lydia, S. S. Kumar, A. I. Selvakumar, and G. E. Prem Kumar, "A Comprehensive Review on Wind Turbine Power Curve Modeling Techniques," *Renewable and Sustainable Energy Reviews*, vol. 30, pp. 452–460, 2014.
- [53] R. Wagner, M. Courtney, J. Gottschall, and P. Lindelöw-Marsden, "Accounting for the Speed Shear in Wind Turbine Power Performance Measurement," *Wind Energy*, vol. 14, no. 8, pp. 993–1004, 2011.
- [54] D. L. Elliott and J. B. Cadogan "Effects of Wind Shear and Turbulence on Wind Turbine Power Curves," Pacific Northwest Lab., Richland, WA (USA), PNL-SA-18354; 1990.
- [55] J. Sumner and C. Masson, "Influence of Atmospheric Stability on Wind Turbine Power Performance Curves," *Journal of Solar Energy Engineering*, vol. 128, no. 4, pp. 531–538, 2006.
- [56] T.-J. Chang and Y.-L. Tu, "Evaluation of Monthly Capacity Factor of WECS Using Chronological and Probabilistic Wind Speed Data: A Case Study of Taiwan," *Renewable Energy*, vol. 32, no. 12, pp. 1999–2010, 2007.
- [57] C. Nemes and F. Munteanu, "The Wind Energy System Performance Overview: Capacity Factor vs. Technical Efficiency," *International Journal of Mathematical Models Methods in Applied Sciences*, vol. 5, no. 1, pp. 159–166, 2011.
- [58] C. G. Justus, *Winds and Wind System Performance*. 1978.
- [59] S. Wan, L. Cheng, and X. Sheng, "Effects of Yaw Error on Wind Turbine Running Characteristics Based on the Equivalent Wind Speed Model," *Energies*, vol. 8, no. 7, pp. 6286–6301, 2015.
- [60] K. E. Johnson, L. J. Fingersh, M. J. Balas, and L. Y. Pao, "Methods for Increasing Region 2 Power Capture On A Variable Speed HAWT," *presented at the 42nd AIAA Aerospace Sciences Meeting and Exhibit*, Reno, Nevada, USA, 2004.
- [61] G. Cortina, V. Sharma, and M. Calaf, "Investigation of The Incoming Wind Vector for Improved Wind Turbine Yaw-Adjustment Under Different Atmospheric And Wind Farm Conditions," *Renewable Energy*, vol. 101, pp. 376–386, 2017.
- [62]"Enercon Wind Turbines Product Overview."

- [63] B. Sorensen, E. Jorgensen, C. Debel, F. Jensen, and H. Jensen, “Improved Design of Large Wind Turbine Blade of Fibre Composites Based on Studies of Scale Effects (Phase 1) - Summary Report,” *Riso National Laboratory*.
- [64] K. O. Ronold, J. Wedel-Heinen, and C. J. Christensen, “Calibration of Partial Safety Factors for Design of Wind Turbine Rotor Blades Against Fatigue Failure in Flapwise Bending,” *1996 European Union Wind Energy Conference*, Sweden, 1996.
- [65] Y. J. Jang, C. W. Choi, J. H. Lee, and K. W. Kang, “Development of Fatigue Life Prediction Method and Effect of 10-Minute Mean Wind Speed Distribution on Fatigue Life Of Small Wind Turbine Composite Blade,” *Renewable Energy*, vol. 79, pp. 187–198, 2015.
- [66] H. Li, Z. Hu, K. Chandrashekhara, X. Du, and R. Mishra, “Reliability-Based Fatigue Life Investigation for A Medium-Scale Composite Hydrokinetic Turbine Blade,” *Ocean Energy*, vol. 89, pp. 230–242, 2014.
- [67] C. Kong, T. Kim, D. Han, and Y. Sugiyama, “Investigation of Fatigue Life for A Medium Scale Composite Wind Turbine Blade,” *International Journal of Fatigue*, vol. 28, no. 10, pp. 1382–1388, 2006.
- [68] National Data Buoy Center, “Station 44009 (LLNR 168) - DELAWARE BAY 26 NM Southeast of Cape May, NJ.” [Online]. Available: http://www.ndbc.noaa.gov/station_page.php?station=44009. Accessed: November 2014.
- [69] C. C. Ciang, J.-R. Lee, and H.-J. Bang, “Structural Health Monitoring for A Wind Turbine System: A Review Of Damage Detection Methods,” *Measurements and Science Technology*, vol. 19, no. 12, 2008.
- [70] X. Shen, X. Zhu, and Z. Du, “Wind Turbine Aerodynamics and Loads Control in Wind Shear Flow,” *Energy*, vol. 36, no. 3, pp. 1424–1434, 2011.
- [71] F. Spinato, P. J. Tavner, G. J. W. van Bussel, and E. Koutoulakos, “Reliability of Wind Turbine Subassemblies,” *IET Renewable Power Generation*, vol. 3, no. 4, pp. 387–401, 2009.
- [72] “Windstats Newsletter.” Haymarket Media Group.
- [73] L. Fingersh, M. Hand, and A. Laxson, “Wind Turbine Design Cost and Scaling Model,” NREL/TP-500-40566, 2006.
- [74] M. Boquet, “LIDAR Costs and Yaw Error Information,” December 2015.
- [75] T. Freyman, T. Tran, “Renewable Energy Discount Rate Survey Results,” *Grant Thornton*, 2018.
- [76] M. F. Howland, S. K. Lele, and J. O. Dabiri, “Wind Farm Power Optimization Through Wake Steering,” *Proceedings of the National Academy of Sciences*, vol. 116, no. 29, pp. 14495–14500, 2019.
- [77] A. M. Urbán, J. Liew, E. Dellwik, and G. C. Larsen, “The Effect of Wake Position and Yaw Misalignment on Power Loss in Wind Turbines,” *Journal of Physics: Conference Series*, vol. 1222, p. 012002, 2019.
- [78] S. Pfaffel, S. Faulstich, and K. Rohrig, “Performance and Reliability of Wind Turbines: A Review,” *Energies*, vol. 10, no. 11, p. 1904, 2017.

- [79] J. Carroll, A. McDonald, and D. McMillan, "Failure Rate, Repair Time and Unscheduled O&M Cost Analysis Of Offshore Wind Turbines," *Wind Energy*, vol. 19, no. 6, pp. 1107-1119, 2015
- [80] J. Carroll, A. McDonald, O. Barrera Martin, D. McMillan, and R. Bakhshi, "Offshore Wind Turbine Sub-Assembly Failure Rates Through Time," in *Scientific Proceedings: EWEA Annual Conference and Exhibition 2015*, Paris, France, 2015, pp. 112–116.
- [81] J. Ribrant and L. M. Bertling, "Survey of Failures in Wind Power Systems with Focus on Swedish Wind Power Plants During 199 -2005," *IEEE Transactions on Energy Conversions*, vol. 22, no. 1, pp. 167–173, 2007.
- [82] A. Stenberg and H. Holttinen, "Analyzing Failure Statistics of Wind Turbines in Finland," *presented at the European Wind Energy Conference*, 2010.
- [83] E. Echavarria, B. Hahn, G. J. van Bussel, and T. Tomiyama, "Reliability of Wind Turbine Technology Through Time," *Journal of Solar Energy Engineering*, vol. 130, no. 3, pp. 031005-031005–8, 2008.
- [84] M. D. Reder, E. Gonzalez, and J. J. Melero, "Wind Turbine Failures - Tackling Current Problems in Failure Data Analysis," *Journal of Physics: Conference Series*, vol. 753, no. 7, p. 072027, 2016.